Investigating Vasomotion and Neurovascular Function in Pre-Clinical Models of Alzheimer's Disease & Hypertension

Shannon M. O'Connor

A thesis submitted for the degree of Doctor of Philosophy (PhD)

July 2025

Acknowledgements

First and foremost, I would like to express my sincere gratitude to my supervisor, Chris Martin, for his unwavering support, guidance, and encouragement throughout my PhD journey. His expertise, patience, and insightful feedback have been instrumental in shaping this research and in my development as a scholar.

I am also very grateful to Jason Berwick and Clare Howarth for being incredible supervisors and providing valuable input and support at every stage of this project. Their insightful guidance, practical assistance with experiments, and consistent encouragement have greatly enhanced both the quality of this work and my PhD experience.

A special thanks to Osman Shabir for his friendship and for training me on *almost* all experimental techniques that I've done throughout this PhD, and also to Beth Eyre for her expertise and training on awake imaging experiments! I'd also like to thank all my colleagues *and* close friends in the Sheffield Neurovascular Lab (in no particular order) - Rahul, Llywelyn, Kira, Naomi, Tom, Ali, Dirk, and Runchong - for their kindness, advice, and friendship, and for the many moments of laughter and support we shared.

Finally, this thesis is dedicated to my family and friends, whose endless love, patience, and encouragement have been a constant source of strength throughout the ups and downs of this journey.

Abstract

Background: Vascular risk factors, particularly hypertension (HTN), are key contributors to the development of Alzheimer's disease (AD). Both conditions are linked to cerebral vascular dysfunction, potentially disrupting processes such as vasomotion and neurovascular coupling (NVC). Vasomotion, a low-frequency (~0.1 Hz) oscillation in vascular diameter, is thought to support tissue oxygenation, perfusion, and solute clearance from the brain. NVC is a critical process for brain health, and its impairment is believed to play a central role in AD pathophysiology.

Aims: This project aimed to (I) characterise vasomotion in vivo and explore its potential as an early biomarker of vascular dysfunction in AD and HTN; (II) examine the relationship between vasomotion and neuronal activity; and (III) assess how HTN affects brain vascular function.

Methods: Low-frequency oscillations (LFOs; 0.06–0.2 Hz) in cerebral arteries of AD (J20-AD), HTN (angiotensin-II-induced), and healthy control mice were measured using 2D-optical imaging spectroscopy and compared between groups. Simultaneously gathered multi-unit neuronal activity data were used to assess whether LFOs were independent of neural activity. In HTN mice, neurovascular function, cognition, and cellular changes were also evaluated through in vivo imaging, electrophysiology, behavioural paradigms, and immunohistochemistry.

Results: LFO power was unchanged in AD mice but significantly reduced in male HTN mice versus controls. This reduction preceded detectable changes in NVC, cognition, and histology, suggesting LFO deficits as early indicators of HTN-related dysfunction. LFOs were also coupled to neuronal activity, providing important insights into the interpretation of vasomotion signals in-vivo. While NVC was largely preserved in HTN mice, a faster onset of haemodynamic responses were observed in HTN mice compared to controls, suggesting that temporal features of NVC may offer a more sensitive index of early vascular dysfunction. Sex significantly influenced both haemodynamic responses and LFOs, emphasising the importance of sex-aware approaches in neurovascular research.

Table of Contents

List of Tables

List of Figures

Abbreviations

SMCs	Smooth Muscle Cells
NVU	Neurovascular Unit
CBF	Cerebral Blood Flow
NO	Nitric Oxide
ECs	Endothelial Cells
BBB	Blood Brain Barrier
AA	Arachidonic Acid
CNS	Central Nervous System
GFAP	Glial Fibrillary Acidic Protein
IBA1	Ionised Calcium-binding Adapter Molecule 1
NVC	Neurovascular Coupling
NMDA	N-methyl-D-aspartate
nNOS	Neuronal NO Synthase
mGluR	Metabotropic Glutamate Receptors
PLA_2	Phospholipase A_2
EET	Epoxyeicosatrienoic Acid
PGE_2	Prostaglandin E_2
Aβ	Amyloid-beta
AD	Alzheimer's Disease
APP	Amyloid Precursor Protein
HTN	Hypertension
CVDs	Cardiovascular Diseases
BP	Blood Pressure

SBP	Systolic Blood Pressure
DBP	Diastolic Blood Pressure
RAAS	Renin-Angiotensin-Aldosterone-System
ACE	Angiotensin-converting Enzyme
Ang-II	Angiotensin-II
AT_1	Angiotensin Type 1 Receptor
AT_2	Angiotensin Type 2 Receptor
SHR	Spontaneously Hypertensive Rat
IPAD	Intramural Periarterial Drainage
DSS	Dahl Salt-Sensitive
ISF	Interstitial Fluid
BM	Basement Membrane
L-NAME	Nω-Nitro-l-arginine methyl ester hydrochloride
fMRI	Functional Magnetic Resonance Imaging
BOLD	Blood Oxygen Level Dependent
2D-OIS	2-Dimensional Optical Imaging Spectroscopy
HbT	Total Haemoglobin
HbO	Oxyhaemoglobin
HbR	Deoxyhaemoglobin
LFO	Low-frequency Oscillation
MUA	Multi-Unit Activity
FFT	Fast Fourier Transform
α-SMA	Alpha Smooth Muscle Actin

Declaration

I, Shannon O'Connor, confirm that this thesis is my own work. I am aware of the University's Guidance on the Use of Unfair Means *(https://www.sheffield.ac.uk/study-skills/assessment/academic-integrity/academic-integrity)*. This work has not previously been presented for an award at this, or any other, University.

This thesis is in a publication format and is comprised of a literature review and two manuscripts:

1. Chapter 1 - Literature Review (Not published)
2. Chapter 2 - O'Connor et al., 2025 (published). Hemodynamic and neuronal contributions to low-frequency vascular oscillations in a preclinical model of Alzheimer's disease. *Neurophotonics,* 12(S1), S14615. https://doi.org/10.1117/1.NPh.12.S1.S14615
3. Chapter 3 - O'Connor et al., 2025 (in preparation). Effects of angiotensin-II on cerebral haemodynamics and low-frequency vascular oscillations in awake mice.
4. Chapter 4 - Discussion and conclusion

A full acknowledgement and reference to the paper is made at the start of each publication-based chapter, in addition to a statement regarding my contribution as well as that of each of my co-authors to the paper.

Chapter 1 - Introduction

Chapter Summary

The aim of this thesis is to explore vasomotion and neurovascular function in preclinical models of Alzheimer's disease and hypertension. This chapter begins with an overview of the neurovascular unit, a critical component in the regulation of cerebral blood flow and neurovascular coupling. It then introduces the pathophysiological features of Alzheimer's disease and hypertension, with a focus on their known effects on the brain vasculature. Given the potential of vasomotion as an early indicator of vascular dysfunction, the chapter also examines the mechanisms underlying vasomotion and its proposed physiological roles. Finally, relevant methodological background is provided to contextualise the experimental approaches used in the subsequent studies.

1.1 The Neurovascular Unit and Brain Vascular Function

Complex interactions between neurons, endothelial cells, mural cells [pericytes, vascular smooth muscle cells (SMCs)], and glia make up what is referred to as the neurovascular unit (NVU) (Lecrux & Hamel, 2011; Zlokovic, 2011). The dynamic communication between these components of the NVU contribute to processes such as the regulation of blood flow, delivery of energy substrates to neurons, and clearance of waste metabolites from the brain (Presa et al., 2020). These processes are crucial for ensuring that optimal brain function can occur, and thus, the function of the NVU and its constituent cells is of utmost importance.

1.1.1 Vascular Cells

The endothelium consists of a monolayer of endothelial cells which line the inside of blood vessels (arteries, veins, and capillaries) and is a major player in the regulation of vascular tone, cellular adhesion, smooth muscle cell proliferation and vessel wall inflammation (Deanfield et al., 2007; Félétou, 2011). The endothelium regulates vascular tone, and thus, cerebral blood flow (CBF) via the release of vasoactive signaling molecules that relax or constrict blood vessels (Deanfield et al., 2007), including nitric oxide (NO), prostacyclin, endothelin, and endothelial-derived hyperpolarizing factor (Galley & Webster, 2004).

Endothelial cells (ECs) and mural cells are the two main cell types that make up blood vessels (Siekmann, 2023). ECs form the vessel walls, and positioned on the abluminal surface of the EC layer are mural cells (Daneman & Prat, 2015). Mural cells can be divided into SMCs and pericytes, which vary in subtype along the vascular network (Grant et al., 2019; Muhl et al., 2022) and enable control of vessel diameter and subsequent blood flow via their contractile properties (Kisler et al., 2017). Vascular SMCs reside in the medial layer of major blood vessels and regulate arterial and arteriolar vessel diameter, thereby maintaining vascular tone and regulating both blood circulation and blood pressure (Grootaert & Bennett, 2021; Shen et al., 2021). Pericytes line the walls of capillaries and support angiogenesis, maintenance of the blood-

brain barrier (BBB), and regulation of immune cell entry to the central nervous system (CNS) (Attwell et al., 2016; Dalkara et al., 2011). Additionally, pericytes are important in the control of brain blood flow (Attwell et al., 2016) via the ability to control/constrict capillary diameter (Peppiatt et al., 2006).

1.1.2 Glia

Astrocytes play an important role in the neurovascular system by providing energy substrates, supporting synaptic plasticity and function, and regulating regional CBF by inducing local vasodilation or vasoconstriction responses (Volterra & Meldolesi, 2005). Astrocytes produce and release various signaling molecules such as NO, prostaglandins, and arachidonic acid (AA) that can modulate blood vessel diameter and thereby blood flow in the CNS (Sofroniew & Vinters, 2010). Astrocytes also adjust blood flow in response to synaptic activity via astrocytic processes that are in contact with both blood vessels and synapses (Sofroniew & Vinters, 2010). Astrocytes respond to pathologies in a process known as reactive astrogliosis, associated with an upregulation of glial fibrillary acidic protein (GFAP) and morphological changes such as hypertrophy, altered ramification, and outgrowth of long processes (Escartin et al., 2021; Schiweck et al., 2018).

Microglia are considered to be the principal immune cells of the brain, involved in both homeostasis and in the defense against pathogens and CNS dysfunction or damage (Hickman et al., 2018; Kettenmann et al., 2011). In a homeostatic state, microglia survey the microenvironment using their ramified processes, clearing cellular debris and responding to injury or infection (Gao et al., 2023). Microglia secrete several soluble factors (e.g., cytokines and neurotropic factors) that contribute to immune responses in the CNS as well as tissue repair (Colonna & Butovsky, 2017). Injury or an inflammatory stimulus can induce a change in resting microglia from a ramified to amoeboid morphological appearance (enlarged cell body and shorter processes), which is reflective of a highly activated state associated with phagocytosis

and proinflammatory function (Colonna & Butovsky, 2017) and is also associated with an increased expression of ionised calcium-binding adapter molecule 1 (Ito et al., 1998).

1.2 The Blood-Brain Barrier

The BBB is a cellular membrane composed of a monolayer of endothelial cells linked by complex, tight junctions that create a continuous barrier (Jagtiani et al., 2022; Knox et al., 2022), astrocytes, and a basement membrane (BM) (Roberts et al., 2012). Cerebrovascular integrity is maintained by the BBB through constant crosstalk between the cells of the NVU (endothelium, mural cells, astrocytes, and neurons) (Sweeney et al., 2018). The BBB plays an essential role in maintaining brain homeostasis by controlling the environment of the central nervous system (CNS) via tightly regulating the movement of ions, molecules, and cells between the blood and brain parenchyma (Daneman & Prat, 2015; Knox et al., 2022). The BBB controls both the delivery of energy metabolites and nutrients into the central nervous system as well as preventing the entry of neurotoxic molecules and pathogens (Scheffer et al., 2021; Zlokovic, 2011). Thus, providing the brain with adequate nutrients to achieve optimal neuronal and synaptic function (Zlokovic, 2011), while also protecting the CNS from pathogens, toxins, inflammation, injury, and disease, which would otherwise lead to impairments in neuronal function and neurodegeneration (Daneman & Prat, 2015; Knox et al., 2022).

1.3 Neurovascular Coupling

To ensure proper functioning of neurons in the brain, an adequate supply of blood is required, which is delivered via a vast vascular network of veins, arteries, venules, arterioles and capillaries (Sweeney et al., 2018). Neurovascular coupling (NVC) refers to the mechanism by which changes in regional neural activity drive increases in CBF that are specific to the active area. It has been postulated that increases in CBF in response to brain activity likely reflect the need for oxygen and glucose delivery to areas of activation, as the brain lacks its own energy reserves despite having a significantly high energy demand. This rapid redirection of blood flow

to areas of neuronal activation (i.e., NVC) ensures a targeted and uninterrupted flow of blood that is essential for brain viability (Presa et al., 2020), as disruption of NVC may result in the energy needs of neurons being unmet, which in the long term can lead to neuronal dysfunction and cognitive impairment (Iadecola, 2013; Sweeney et al., 2018). Increases in blood flow in response to neuronal activation depend on the collaborative actions of neurons, astrocytes, and vascular cells through various types of molecular signalling (Iadecola, 2013).

Neurons and astrocytes respond to increases in extracellular glutamate to transmit vasoactive signals to regulate CBF appropriately (Phillips et al., 2016). Glutamate is a neurotransmitter that is released when the presynaptic neuron depolarises (Hübel et al., 2017). The release of glutamate from the synapse activates neuronal *N*-methyl-D-aspartate (NMDA) receptors, which results in Ca^{2+} entry into neurons and activation of neuronal NO synthase (nNOS), leading to NO release and vessel dilation (Attwell et al., 2010). Additionally, synaptic glutamate release activates metabotropic glutamate receptors (mGluR) on astrocytes, which also increases cytosolic calcium concentrations (Phillips et al., 2016). Ca^{2+} increases within astrocytes activates phospholipase A_2 (PLA_2), generating AA and thus epoxyeicosatrienoic acid (EET) and prostaglandin E_2 (PGE_2), which also lead to vessel dilation (Phillips et al., 2016). Though Ca^{2+} elevation in astrocytes can drive arteriole dilation to increase CBF, it is relatively unclear how essential the role of astrocytes are in the NVC process. While it has been shown that direct stimulation of astrocytes in rat brain slices has resulted in vasodilation, providing evidence that astrocytes may play a role in activity-dependent increases in blood flow (Zonta et al., 2003), others have determined that astrocytic signalling does not initiate neurovascular coupling (Bonder & McCarthy, 2014; Nizar et al., 2013), at least via calcium-dependent mechanisms. However, Institoris et al., (2022), found that clamping astrocyte Ca^{2+} signalling in vivo reduces sustained, but not brief, vascular responses to sensory stimulation (Institoris et al., 2022). Further, antagonising NMDA-receptors or EET production reduced only the late component of the NVC response but not initial increases in CBF to sensory stimulation (Institoris et al., 2022). These findings suggest that a role of astrocytes in this context may be to amplify NVC responses when neuronal activation is prolonged. Interestingly, Lind et al., (2024) found that astrocytic contributions to NVC responses may be dependent on brain state; NVC responses to self-

directed sensory processing in this study were confirmed to depend on noradrenaline and astrocyte activity (Lind et al., 2024).

1.4 Alzheimer's Disease

1.4.1 Introduction to Alzheimer's disease

Alzheimer's disease is the most common form of dementia, accounting for around 60-80% of cases (Crous-Bou et al., 2017), followed by vascular dementia, dementia with Lewy bodies, and frontotemporal lobe dementia (Uchida, 2022). Increased levels of amyloid-beta (Aβ), which aggregate and form into extracellular senile plaques, and hyperphosphorylated tau, which form intracellular neurofibrillary tangles (NFTs), are histopathological hallmarks of AD (Cheignon et al., 2018; Dubois et al., 2014; Hardy & Selkoe, 2002). A clinical onset of AD which occurs before the age of 65 years is referred to as early-onset, or familial, AD (Mendez, 2019). Mutations in APP and presenilin PS1 and PS2 are known to cause early onset AD and facilitate Aβ deposition through increased production resulting in an elevated extracellular concentration of Aβ (Scheuner et al., 1996). Late-onset AD occurs in individuals aged 65 or above and progresses continuously from the preclinical stage in which there are no clinical symptoms to pre-dementia, mild cognitive impairment and AD, in which the clinical symptoms impact daily life (Uchida, 2022). In late onset AD, the elevated levels of Aβ are thought to be promoted by faulty Aβ clearance, rather than increased production of Aβ (Nelson et al., 2016).

1.4.2 Amyloid Cascade Hypothesis

The amyloid cascade hypothesis centralises abnormal Aβ production and deposition in the brain as the key trigger in AD pathogenesis (Hardy & Selkoe, 2002). According to this hypothesis, disturbances in amyloid precursor protein (APP) metabolism can result in the overproduction and faulty clearance of Aβ, causing Aβ build-up to occur in the CNS in the form of plaques,

monomers, oligomers, or insoluble fibrils (Mawuenyega et al., 2010; Volianskis et al., 2010) in addition to contributing to tau tangle formation (Fang et al., 2021). This aggregation of Aβ is thought to trigger a cascade of pathological events which eventually lead to AD-linked neurodegeneration (Chavez-Gutierrez & Szaruga, 2020; Hardy & Selkoe, 2002), such as activation of glia, inflammation, synapse dysfunction, loss of neurons and eventual cognitive decline (Hardy & Selkoe, 2002; Zhang et al., 2019). There has been a great deal of findings over the years that support this theory (Coomans et al., 2023; Goate et al., 1991; Rogaev et al., 1995; Sherrington et al., 1995), yet, therapeutics targeted at inhibiting Aβ production or removing Aβ from the brain have demonstrated limited clinical efficacy (Karran & De Strooper, 2022). Although, recently, Aβ-based therapies are receiving encouraging results, such as monoclonal antibodies (i.e., donanemab and lecanemab), in aiding in clearance of Aβ from the brain and moderately improving cognitive decline (Kim et al., 2025; van Dyck et al., 2022; Zhang et al., 2023). Despite being present in most patients with AD (90% of cases), Aβ plaque pathology alone may not fully account for AD development, as studies have found that Aβ load is not always correlated with dementia severity (Berlau et al., 2009; Hsia et al., 1999; Swerdlow et al., 2014). Indeed, a large proportion of AD dementia patients exhibit a mixed pathology at autopsy, in that AD pathology is observed alongside other pathologies, such as age-related cerebrovascular disease and vascular pathologies (Fu et al., 2024; Jack & Holtzman, 2013).

1.4.3 Vascular Cascade Hypothesis

In addition to AD pathology, studies have observed vascular pathology in a large proportion of individuals with AD (Launer et al., 2008; Schneider et al., 2009), suggesting the existence of a vascular component to AD pathophysiology. In some cases, alterations in vascular function have been observed decades before the onset of the disease, suggesting the earliest marker of AD progression may be vascular dysregulation (Iturria-Medina et al., 2016). In addition, despite decades of research based on the amyloid-hypothesis of AD, there has been a lack of success in finding an effective treatment for AD using Aβ-based drugs. Thus, more interest has been given to alternative theories of AD development, such as those that focus on the vascular contributions to AD and AD progression. Vascular degeneration has been suggested to be associated with the

onset or progression of AD and has been of interest in recent years. The two-hit vascular hypothesis of AD, proposed by Zlokovic, postulates that initial damage to the microcirculation (considered to be "hit one"), initiates neuronal dysfunction and injury leading to BBB dysfunction and impairments in Aβ clearance, causing the promotion/accumulation of Aβ in the brain (considered to be "hit two") (Zlokovic, 2011). The two processes interact and can independently or synergistically lead to the onset or worsening of AD dementia (Nelson et al., 2016).

The vascular-driven theory of AD suggests that a functional deficit within the cells of the neurovascular unit would provide inadequate oxygen and glucose to neurons, which may trigger the onset of the disease or aid in its progression. Aβ peptides contribute to the dysregulation of vascular tone and weakening of the BBB as well as inducing vascular inflammation due to their vasculotoxic effects (Govindpani et al., 2019). Aβ may therefore be implicated in disease onset and/or progression, as its overaccumulation has been found to be detrimental to the vascular system. Lower resting CBF and impairments in vascular responses have been shown to be associated with elevated levels of Aβ and Aβ deposits in rodent models (Kimbrough et al., 2015; Niwa et al., 2001). In mouse models, tau has also been found to cause reductions in CBF (Ahmad et al., 2021; Park et al., 2020) and cerebrovascular dysfunction (Park et al., 2020). Impairments in neurovascular coupling have also been observed in AD, in both human patients and animal models of the disease (Hock et al., 1997; Lacoste et al., 2013; Li et al., 2021; Park et al., 2020; Royea et al., 2017; van Dijk et al., 2024). Although, interestingly, neurovascular uncoupling and diminished haemodynamic responses have not been universal findings in AD research. Studies have found intact neurovascular function (Munting et al., 2021; Sharp et al., 2020), or even augmented haemodynamic responses (Kim & Jeong, 2013; Shabir et al., 2020) in mouse models of AD. As vascular dysregulation is associated with AD development and progression (Iturria-Medina et al., 2016), vascular risk factors, specifically hypertension (HTN), have emerged as key pathogenic factors in vascular cognitive impairment and AD (Iadecola & Gottesman, 2019). HTN may lead to cognitive decline or impairment through its detrimental impacts on brain blood flow, neurovascular function, and AD pathology (Iadecola & Gottesman,

2019), specifically, through the promotion of Aβ accumulation and tau phosphorylation (Faraco et al., 2015; Iadecola & Gottesman, 2019; Schreiber et al., 2014).

1.5 Hypertension

Diseases involving the heart and blood vessels constitute what is referred to as cardiovascular diseases (CVDs), such as stroke, heart failure, coronary artery disease, and cardiac arrest (Donato et al., 2018). There are several major modifiable risk factors for CVD including cigarette smoking, diabetes mellitus, lipid abnormalities and high blood pressure (Fuchs & Whelton, 2020). Among these risk factors, high blood pressure is associated with the strongest evidence for causation of CVD and early death (Mills et al., 2020), greatly increasing the risk of detrimental renal, cardiovascular, and cerebrovascular events (Bolivar, 2013). HTN is a rise in blood pressure (BP), more specifically, a systolic blood pressure (SBP) of ≥140 mmHg and/or a diastolic pressure (DBP) ≥90 mmHg (Bolivar, 2013). Primary HTN accounts for 95% of cases of HTN, and cannot be determined by a specific cause (Weber et al., 2014). Secondary HTN accounts for the remaining 5% of HTN cases in which the underlying cause can be identified, and can be attributed to factors such as chronic kidney disease, excessive aldosterone secretion, renal artery stenosis, pheochromocytoma, and sleep apnoea (Weber et al., 2014). Primary HTN is currently considered a multifactorial disease influenced by a combination of genetic, environmental, and behavioural factors (Bolivar, 2013). Although the cause of primary HTN is unknown, it is often associated with lifestyle risk factors such as obesity and diet, specifically, a high dietary salt intake (Delacroix & Chokka, 2014). There is also a relationship to family history, suggesting that some individuals may have a genetic predisposition to developing HTN (Weber et al., 2014). Genetic factors may include abnormally high activity of the Renin-Angiotensin-Aldosterone System (RAAS) and sympathetic nervous system, and a predisposition to the effects of dietary salt on BP (Weber et al., 2014). HTN is becoming more prevalent globally due to factors such as aging (Presa et al., 2020) and increases in lifestyle risk factors such as high sodium intake/unhealthy diet, physical inactivity, obesity, and alcohol consumption (Mills et al., 2020). Complications of high BP can result in both short-term and long-term consequences, consisting of stroke, coronary heart disease, heart failure, atrial fibrillation,

valvular heart disease, aortic syndromes, peripheral arterial disease, hypertensive cardiomyopathy, and now recognised, dementia (Fuchs & Whelton, 2020).

1.5.1 The Renin-Angiotensin-Aldosterone System

The RAAS is an endocrine pathway that plays an integral role in regulating BP, extracellular fluid volume, sodium balance and cardiovascular function (Ferrario & Strawn, 2006; Hussain & Awan, 2018). Overactivation of the RAAS is associated with hypertension and ultimately, the development of CVD (Hussain & Awan, 2018). The protein angiotensinogen, which is primarily produced in the liver, is a key precursor molecule of the RAAS, and is cleaved to angiotensin-I by renin, an enzyme produced in the kidney via the juxtaglomerular apparatus (Fournier et al., 2012). Renin is involved in the regulation of cardiovascular homeostasis, and is secreted by the kidneys in response to reduced arterial BP, ionic imbalance, or reduced glomerulus filtration rate (Hussain & Awan, 2018). Angiotensin-converting enzyme (ACE) from the lungs cleaves angiotensin-I to the active peptide angiotensin-II (ang-II) (Fournier et al., 2012; Scott et al., 2023). Ang-II is the central effector peptide of the RAAS, and regulates both renal function and BP (Zain & Awan, 2014). Ang-II acts on the adrenal cortex to release the mineralocorticoid hormone aldosterone, which influences water and salt regulation in the body (Scott et al., 2023). When BP is low, ang-II plays an integral role in raising BP via promoting vasoconstriction, decreasing NO production, and stimulating aldosterone production (Hussain & Awan, 2018). Ang-II diffuses to tissues to bind to its receptors (ang-II type 1 receptor, AT_1, and ang-II type 2 receptor, AT_2) to exert effects (Te Riet et al., 2015). Activation of AT_1 receptors induce vasoconstriction, aldosterone release, salt retention and stimulation of the sympathetic nervous system (Bader & Ganten, 2008), while activation of AT_2 receptors is thought to counteract these effects, for instance, by promoting NO release and vasodilation (Hussain & Awan, 2018). However, some studies have observed AT_2 receptor-mediated vasoconstriction in spontaneously hypertensive rats (SHR) (Moltzer et al., 2010; You et al., 2005). The RAAS is implicated in the pathogenesis of HTN (Ma et al., 2010), thus, medications that target and inhibit the RAAS are frequently used to treat HTN, for instance, ACE inhibitors and angiotensin receptor blockers (ARBs), which reduce the effects of ang-II and lower BP (Pacurari et al., 2014).

1.6 Hypertension and Cognitive Impairment

High BP is a well-established risk factor for age-related cognitive decline (Pacholko & Iadecola, 2024). Studies employing neuropsychological tests have shown that hypertensive BP levels negatively affect cognitive function, as hypertensive patients have repeatedly shown mild deficits in cognitive domains such as perceptual motor speed and executive function compared to normotensive controls (Jennings et al., 2020). The *Atherosclerosis Risk in Communities Study* evaluated the association between mid-life HTN and changes in cognitive performance over 20 years, finding that mid-life HTN and elevated mid-life systolic BP were associated with higher levels of cognitive decline in the duration of the study, as determined by the *Delayed Word Recall Test, Digit Symbol Substitution Test* and *Word Fluency Test* (Gottesman et al., 2014). This decline in cognition was the case for elevated systolic BP in mid-life but not for elevations in BP that occur in late-life (Gottesman et al., 2014). The *Honolulu-Asia Aging Study* investigated the association between mid-life BP and late-life cognitive performance, finding that an increased level of mid-life BP was related to poorer cognitive performance in later-life (Launer et al., 1995). However, results indicated that mid-life diastolic BP was not associated with later-life cognitive function (Launer et al., 1995). Similar findings have occurred in another study, showing an association between heightened mid-life BP and cognitive decline in later life, in addition to exhibiting larger volumes of white matter hyperintensities (Swan et al., 1998).

1.7 The Link Between Hypertension and Dementia

HTN is a risk factor for both vascular cognitive impairment and AD, which are the most common causes of dementia, accounting for 85% of cases (Arvanitakis et al., 2019; Canavan & O'Donnell, 2022). Many studies have reported an association between HTN and an increased risk of cognitive decline and dementia (Abell et al., 2018; Gottesman et al., 2017; Skoog et al., 1996). In these cohort studies, the strongest association was found between mid-life HTN and risk of future cognitive decline and dementia. A reduced risk of cognitive impairment in older adults

with HTN was observed following adequate BP control in a longitudinal study (Elahi et al., 2023; Hughes et al., 2020), conversely, other studies have found no differences in the risk of cognitive decline and dementia between patients receiving antihypertensive treatment and the placebo group (Cunningham et al., 2021). Further, there have also been conflicting reports on the effectiveness of antihypertensive treatment on preventing cognitive decline (Ding et al., 2020). Therefore, this may highlight the importance of the identification of early biomarkers of HTN-induced cerebrovascular dysfunction as therapeutic targets for the prevention of cognitive decline and/or dementia. A longitudinal study examining the relationship between late-life BP and cerebrovascular and AD neuropathology found that higher levels of late-life systolic BP and diastolic BP were associated with a greater amount of brain infarcts (Arvanitakis et al., 2018). There was also an association between systolic BP with AD pathology, specifically higher mean systolic BP was associated with a higher number of neurofibrillary tangles (Arvanitakis et al., 2018). However, there was no observed relationship between systolic or diastolic BP and amyloid plaques (Arvanitakis et al., 2018). Conversely, the development of HTN at older ages has been found to have a potential protective effect on the development of dementia (Qiu et al., 2009). In a longitudinal study, participants who had an onset of HTN at age 80 or above exhibited a lower dementia risk compared to those without HTN, this was particularly the case for those with an onset age of 90 years or above (Corrada et al., 2017).

Preclinical models of HTN have found an increased permeability of the BBB in the cortex and hippocampus, in addition to enhanced Aβ deposition (Gentile et al., 2009). The acceleration of AD pathology has also been observed when preclinical models of AD are hypertensive. The induction of chronic HTN in the TgSwDI mouse model of AD resulted in cognitive deficits, microvascular amyloid deposition, vascular inflammation, BBB leakage, and pericyte loss at an earlier age than the normotensive mice (Kruyer et al., 2015). Similar findings were observed in other studies, where APP/PS1 mice with high BP exhibited increased levels of cerebral Aβ accumulation (Cifuentes et al., 2015; de Montgolfier et al., 2019) and cognitive decline (de Montgolfier et al., 2019). The findings of these studies suggest that HTN may contribute to the acceleration of the development of AD-like pathology, potentially through vascular damage (de Montgolfier et al., 2019) and/or reductions in nitric oxide production

(Cifuentes et al., 2015); as reductions in microvessel density and NOS1 and NOS3 were observed in addition to the increased amyloid depositions in hypertensive APP/PS1 mice in this study (Cifuentes et al., 2015). Endothelial NO has been found to play a role in maintaining Aβ levels in the brain, particularly via its ability to inhibit Aβ generation and secretion (Austin et al., 2010). Therefore, reductions in NO bioavailability in hypertensive animal models may result in the exacerbation of AD pathology. The exact mechanisms by which HTN may promote cognitive impairment and enhance AD pathology remain to be fully understood, however, it is known that HTN disrupts the structural and functional integrity of cerebral vessels (Pacholko & Iadecola, 2024), which may contribute to these findings.

1.8 Effects of Hypertension on the Brain and Neurovascular Function

1.8.1 Structural Changes

1.8.1.1 Damage to Cerebral Arteries and Arterioles

HTN has been found to result in changes in both the structure and function of the cerebral vasculature. Changes in the microcirculation, such as decreases in vessel lumen diameter have been found to occur in HTN, which result in increased energy dissipation and resistance to flow in arteries and arterioles (Schiffrin, 2020). Vascular hypertrophy is also associated with HTN, evidenced by patients with primary HTN whom have exhibited a significantly increased media-to-lumen ratio of vessels compared to normotensive subjects (Rizzoni et al., 1996). These changes in vascular morphology can be attributed to vascular remodelling; a process which has also been found to occur in preclinical models of HTN as well, both in transgenic (Baumbach et al., 2003; Halabi et al., 2008) and diet-induced hypertensive mice (Zhang et al., 2021). Vascular remodelling is an active process depending on interactions between local growth factors, vasoactive substances, and hemodynamic stimuli (Renna et al., 2013). This process may occur as a response to chronic changes in haemodynamic conditions, but may also contribute to the

pathophysiology of disorders involving vascular and/or circulatory systems (Renna et al., 2013), such as HTN. In the hypertensive state, the remodelling of the structure of resistance arteries (those of 100-300 μm diameter) may occur, either through eutrophic remodelling or hypertrophic remodelling (Schiffrin, 2020). Hypertrophic remodelling involves hypertrophy or hyperplasia of smooth muscle cells and inward growth, resulting in an increased thickness of the vessel wall and a reduction in lumen diameter (Iadecola & Davisson, 2008). Eutrophic remodelling involves rearrangement of smooth muscle cells resulting in a reduction in lumen diameter without changes to vessel wall thickness or vascular mass (Iadecola & Davisson, 2008). Capillary rarefaction has also been observed in both hypertensive patients (Antonios et al., 1999; Bosch et al., 2017) and animal models of HTN (Tarantini et al., 2016). A loss of capillaries has been found to be associated with ischemia which impedes the delivery of energy substrates to neurons and glial cells, contributing to oxidative stress and neuroinflammation (Presa et al., 2020). Arterial stiffening is another change in the vasculature associated with hypertension, in which collagen content is increased and vessel walls become rigid (Iadecola & Davisson, 2008).

Interestingly, some studies have observed arterial changes that occur prior to the development of HTN. A study in Spontaneously Hypertensive Rats (SHRs) has observed increased vertebrobasilar artery resistance and arterial remodelling (specifically, narrowing) which occurred prior to the onset of HTN (Cates et al., 2011). Arterial stiffness was also found to occur prior to the onset of HTN in a mouse model of diet-induced obesity (Weisbrod et al., 2013). Vascular changes have been found to occur in individuals during ageing, such as increases in large elastic artery stiffness, and are associated with the development of conditions such as HTN and stroke, as well as increased CVD risk (Donato et al., 2018). As these arterial changes often precede the development of CVD, it is suggested that age-related vascular dysfunction may be a precursor to the diagnosis of CVD (Donato et al., 2018).

1.8.2 Functional Changes

1.8.2.1 Endothelial Function

Endothelial dysfunction is associated with several CVD risk factors, including HTN (Gallo et al., 2021; Vanhoutte et al., 2017), and is characterised by a shift towards reduced vasodilation, cell proliferation, platelet adhesion and activation, and a proinflammatory and prothrombotic state (Gallo et al., 2021). Damage to endothelial cells has been found to occur during HTN in various vascular beds and in both small and large arteries (Park et al., 2001; Schiffrin et al., 2000). However interestingly, it has been unclear as to whether HTN is a cause or consequence of this damage. Endothelial dysfunction may manifest before the development of HTN, and may contribute to the development of the disease through mechanisms that lead to increased vasoconstriction and vascular remodeling of resistance arteries, specifically, through factors such as activation of the RAAS, endothelin-1, catecholamines, and growth factors production, which contribute to an increased resistance to blood flow and ultimately to an increased peripheral BP (Gallo et al., 2021). Findings such as the fact that normotensive offspring of individuals with HTN have displayed endothelial dysfunction (Zizek et al., 2001) supports the notion that endothelial dysfunction may be a cause of HTN. Further, Panza et al., (1993) found that HTN treatment did not restore endothelial function, suggesting that endothelial dysfunction is either primary or possibly non-reversible after HTN occurs (Panza et al., 1993). On the other hand, several studies have found that increases in blood pressure were associated with increases in impairment of endothelial function (Benjamin et al., 2004; Dohi et al., 1990; Hermann et al., 2006; Higashi et al., 2012).

1.8.2.2 BBB Dysfunction

HTN has been found to result in dysfunction of the BBB. Preclinical studies have shown that oxidative stress in hypertensive mice resulted in increased inflammation in the cerebral microvasculature and significantly higher BBB permeability than that of control mice (Zhang et al., 2010). Similar to other studies, inducing HTN in mice has been found to result in disruptions of BBB function in addition to neuroinflammation and cognitive impairment (de Montgolfier et al., 2019; Kruyer et al., 2015; Toth et al., 2013). Gentile et al., (2009) found that chronic HTN in

mice lead to an increase in Aβ deposition in addition to increased BBB permeability (Gentile et al., 2009). Thus, suggesting BBB disruption may play a key role in the development of cognitive decline and dementia. Indeed, breakdown of the BBB has been observed in human HTN (Iadecola et al., 2016; Rosenberg, 2012), and AD (Montagne et al., 2017; Nelson et al., 2016; Rosenberg, 2012), confirmed by post-mortem studies of human patients with AD (Nelson et al., 2016). Additionally, BBB impairment has been found to be an early biomarker in the development of cognitive dysfunction, however, BBB breakdown may also occur in the absence of AD pathology (Nation et al., 2019).

1.8.2.3 Neurovascular Uncoupling

Cells within the neurovascular unit work in concert to ensure that brain homeostasis is maintained, and that adequate energy and nutrients are available when required. In an altered state, such as during disease or dysfunction, neurovascular coupling can become uncoupled. This results in impaired delivery of oxygen and energy substrates in addition to impaired clearance of metabolic by-products (Ungvari et al., 2021). Preclinical studies have demonstrated that disruptions in NVC are associated with impairments in both cognitive and sensorimotor function (Tarantini et al., 2015). HTN interferes with NVC through disturbances in vascular function, for instance, through structural alterations of vessels (i.e., vascular hypertrophy and remodelling) that facilitate vascular occlusions and compromise cerebral perfusion (Girouard & Iadecola, 2006). In addition, HTN impairs endothelium-dependent relaxation of vessels (Faraci & Heistad, 1998) and has been found to alter cerebrovascular regulation (Strandgaard & Paulson, 1989). However interestingly, Machado et al., (2020), have found that hypertensive patients under treatment, regardless of their BP control, exhibit intact cerebral autoregulation (Machado et al., 2020). Neurovascular uncoupling has also been observed after administration of ang-II in mice, attenuating sensory-evoked CBF increases to whisker stimulation without reducing resting CBF (rCBF) (Kazama et al., 2003). It has been suggested that ang-II, a peptide involved in human HTN, activates ang-II type 1 (AT_1) receptors on blood vessels inducing production of ROS through the enzyme NADPH oxidase (Kazama et al., 2004). Subsequently, ROS-mediated production of vasopressin occurs, acting on blood vessels to trigger endothelin-1 production,

which alongside circulating ang-II induces oxidative stress (Iadecola & Gottesman, 2019). Vascular oxidative stress produced by ang-II and endothelin-1 suppresses NVC and endothelium-dependent responses, ultimately resulting in cerebrovascular dysfunction (Capone et al., 2012). However, exactly how oxidative stress alters cerebrovascular function remains unclear (Iadecola & Gottesman, 2019).

1.8.2.4 Reductions in CBF

In addition to detrimental effects on NVC and endothelium-dependent responses, HTN also reduces resting cerebral blood flow (rCBF) (Iadecola & Gottesman, 2019), and is one of the major risk factors of chronic cerebral hypoperfusion (Zhao & Gong, 2015). Several studies have reported focal or global reductions in rCBF in patients with HTN (Dai et al., 2008; Fujishima et al., 1995; Wang et al., 2024). Further, larger declines in parenchymal CBF have been observed in patients with high BP or with untreated or poorly controlled HTN compared to nonhypertensive patients (Muller et al., 2012). A study examining the regional CBF (rCBF) rates of cognitively normal subjects with HTN using arterial spin-labeled MRI found that the hypertensive subjects had lower rates of rCBF compared to normotensive controls in several brain regions, including subcortical regions in addition to limbic and paralimbic structures of the brain (Dai et al., 2008). Similar decreases in rCBF have been observed in other studies examining the rate of CBF in older hypertensive patients (Beason-Held et al., 2007), in which greater rCBF decreases were observed in prefrontal, anterior cingulate, and occipital areas (Beason-Held et al., 2007). Interestingly, Wang et al., (2024) found a CBF decrease in the basal ganglia in patients with high-risk HTN, while the moderate-risk group exhibited an increase in CBF in some regions such as the white matter, putamen, globus pallidus, lentiform nucleus, and amygdala (Wang et al., 2024). Although, CBF values in both the midbrain and cerebellum were still lower in the moderate-risk group compared to the control group (Wang et al., 2024).

1.8.2.4.1 Implications of Hypoperfusion. Clinical symptoms from hypoperfusion arise when the level of hypoperfusion exceeds the ability of the cerebral vasculature to autoregulate

and meet the metabolic demands of neurons (Rajeev et al., 2022). Chronic cerebral hypoperfusion activates and prolongs mechanisms in the brain such as inflammation, oxidative stress, endoplasmic reticulum stress and mitochondrial dysfunction, leading to extensive and accumulating damage in addition to downstream structural changes (Rajeev et al., 2022). Chronic cerebral hypoperfusion has been found to play an important role in the development of vascular dementia, AD, and subcortical arteriosclerotic encephalopathy (Zhao & Gong, 2015). In rodent models, inducing chronic hypoperfusion has been found to cause atrophy in the hippocampus and enlargement of lateral ventricles, resulting in AD-like deficits in cognitive function (Zuloaga et al., 2015), and impairments in short-term memory (Zhao et al., 2014; Zuloaga et al., 2015) and long-term spatial memory (Zhao et al., 2014). Hypoperfusion also induces the dysregulation of synaptic proteins and insulin signalling (Zhao et al., 2014), selective neurodegeneration (Zhao et al., 2014), and white matter lesions (Nakaji et al., 2006; Shibata et al., 2004; Yoshizaki et al., 2008), which contribute to impairments in cognition and motor dysfunction (Nakaji et al., 2006). In addition to functional deficits caused by reductions in CBF, evidence has shown that hypoxia is closely involved in promotion and or worsening of AD pathology (Tao et al., 2024), encouraging the accumulation of Aβ (Zhang & Le, 2010), and hyperphosphorylation of tau (Zhang & Le, 2010; Zhao et al., 2014).

1.8.2.5 Impairments in Waste Clearance

It may be possible that HTN can reduce the clearance of proteins, as HTN has been found to be associated with amyloid and tau pathology (Iadecola & Gottesman, 2019). Enlargement and distortion of perivascular spaces has been observed in HTN, which may negatively affect waste clearance (Brown et al., 2018). This widening of the perivascular space may indicate obstruction by waste products and reductions in fluid clearance (Brown et al., 2018). This can have detrimental effects on the brain, as it has a very high metabolic rate, yet lacks conventional lymphatic vessels to assist in the clearance of interstitial metabolic waste products (Jessen et al., 2015; Plog & Nedergaard, 2018). In order to maintain brain homeostasis, and thus, optimal brain and cerebrovascular function, the removal of waste products from the brain is essential (Kaur et al., 2021), therefore, adaptations have been developed to allow for the regulation of fluid balance

and removal of excess products. The CSF and vascular systems are two distinct systems involved in this regulation, helping the transport of waste products from the parenchyma to outside of the cranium (Kaur et al., 2021).

Waste products are removed through CSF pathways via perivascular and periaxonal/perineural routes or through the vascular pathway via the BBB (Kaur et al., 2021). While there is an agreement among researchers regarding the use of periaxonal or perineural routes of CSF-driven clearance, there is some debate regarding which perivascular route is undertaken in this process; two of the most supported pathways are intramural periarterial drainage (IPAD) and the glymphatic system. Disruption of these pathways can have adverse effects on brain health. The glymphatic system has been found to be impaired or dysfunctional in several neurological conditions, including hypertension and diabetes (Benveniste & Nedergaard, 2022), small vessel disease (Mestre et al., 2017; Xue et al., 2020), stroke (Mestre et al., 2020; Toh & Siow, 2021), and AD (Harrison et al., 2020; Reeves et al., 2020). Impairment or dysfunction of either the glymphatic system or IPAD results in the inability to clear soluble metabolites (Aldea et al., 2019), which can account for vascular depositions of Aβ. Thus, this faulty clearance has the potential to induce and/or advance AD pathology. Interestingly, a study by van Veluw et al. (2020), found that vasomotion (a low-frequency arteriolar oscillation) may aid in paravascular clearance of Aβ from the brain, as increasing amplitudes of vasomotion using visually evoked vascular responses were found to increase paravascular clearance of fluorescent dextran from the visual cortex of awake mice (van Veluw et al., 2020). Further, in mice with cerebral amyloid angiopathy, and thus impaired vascular reactivity, clearance rates were slower (van Veluw et al., 2020).

1.9 Vasomotion

Vasomotion is a phenomenon that can be described as a spontaneous oscillation or rhythmic constriction and dilation of small vessels that can be observed in several microvascular beds (Pradhan & Chakravarthy, 2011; Rivadulla et al., 2011). The rhythm of vasomotion oscillations

can vary both temporally and spatially, ranging from almost sinusoidal to chaotic or irregular in rhythm (Griffith & Edwards, 1994). This oscillation has been thought to characteristically peak around 0.1 Hz or 6 cycles per minute (Mayhew et al., 1996). Flow motion recorded from laser Doppler flowmetry has also shown the existence of "slow wave" and "fast wave" vasomotion, with oscillations of 1-3 cycles per minute and 10-25 cycles per minute, respectively (Pradhan & Chakravarthy, 2011). Slow wave vasomotion arises from large arterioles (50-100μm), while fast wave vasomotion arises from terminal arterioles (Intaglietta, 1990).

1.9.1 Vasomotion as a Biomarker for Disease

The underlying mechanisms and functional implications of vasomotion remain relatively unclear, despite decades of research. It has been suggested that vasomotion does not occur in healthy, normal physiological conditions (Schmidt-Lucke et al., 2002), and that it seems instead to be a mechanism most prominent under conditions of metabolic stress (Pradhan & Chakravarthy, 2011). A higher incidence and magnitude of vasomotion has been observed in conditions associated with compromised oxygen delivery, for example, low blood pressure and hypoperfusion (Intaglietta, 1991; Nilsson & Aalkjaer, 2003), suggesting that the role of vasomotion may be of a protective nature (Di Marco et al., 2015). Theories regarding the purpose of vasomotion have suggested that better tissue oxygenation may be achieved via the oscillatory flow produced by vasomotion than what is obtained from steady blood flow (Nilsson & Aalkjaer, 2003). A study by Salvi et al., found that prolonged hypobaric-hypoxia exposure resulted in an increase in slow-wave vasomotion, and that the amplitude of vasomotion increased even further after the induction of ischemia (Salvi et al., 2018). Thus, as vasomotion often appears to be most prevalent under abnormal or compromised oxygen conditions, it seems that vasomotion may be a reaction of the vascular system to improve blood circulation and oxygen delivery to hypoxic areas of tissue.

Impairments in vasomotion, specifically reductions, have been observed relatively early in the disease course of diabetes, preceding parasympathetic neuropathy (Meyer et al., 2003).

These reductions in vasomotion may be an early indicator of sympathetic dysfunction, as these reductions were found more often in diabetic patients whom displayed disturbances in cardiac autonomic tests (Meyer et al., 2003). Alterations in vasomotion have also been observed in HTN. An increased amplitude of vasomotion has been observed in patients with primary HTN compared to normotensive individuals (Hollenberg & Sandor, 1984). Further, enhanced vasomotion has been observed in isolated arteries from women with preeclampsia, a hypertensive disorder which may occur in pregnancy, compared to the arteries of normotensive pregnant women (Pascoal et al., 1998). Enhanced vasomotion has been observed in spontaneously hypertensive rats (SHR) (Boonen & De Mey, 1990; Holloway & Bohr, 1973; Lefer et al., 1990; Liu et al., 2017), DOCA-salt hypertensive rats (Holloway & Bohr, 1973), renal sensitive rats (Holloway & Bohr, 1973), and Dahl salt-sensitive (DSS) rats (Boegehold, 1993) compared to normotensive controls. The amplitude of vasomotion in hypertensive animals can vary considerably from normotensive controls, in the latter aforementioned study, the average amplitude of vasomotion was 93% greater in hypertensive DSS rats than normotensive DSS rats (Boegehold, 1993).

Although, interestingly, in a study by Fujii et al., 1990, moderate HTN (evoked by phenylephrine) or vasoconstriction in the anaesthetised rat increased the frequency of vasomotion whilst more severe HTN, hypotension, or vasodilation was observed to completely abolish the presence of vasomotion (Fujii et al., 1990). In hypertensive rats treated with ACE inhibitors, the prevalence of vasomotion was decreased (Sada et al., 1990; Watts et al., 1994). Thus, an elevated BP appears to be able to promote or induce vasomotion oscillations. Studies investigating vasomotion in the context of AD have been relatively limited, however interestingly, both enhancements (Kotliar et al., 2022; van Beek et al., 2012) and impairments (Rivera-Rivera et al., 2020) in vasomotion have been reported in humans, and in mice possessing the APOE4 allele, considered to be a significant risk factor for AD, impaired vasomotion has also been observed (Bonnar et al., 2022).

1.9.2 Vasomotion as a Clearance Mechanism

A concept of recent interest is the idea that vasomotion could be a potential driver of perivascular clearance. Arterial pulsation was thought to be the major driving force behind clearance from the brain (Hadaczek et al., 2006; Iliff et al., 2013); however, it has been postulated that it alone is not sufficient to drive perivascular clearance (Diem et al., 2017). Further, as reported by van Veluw et al. (2020), inducing vasomotion oscillations through a visual stimulus resulted in increased clearance of fluorescent dextran from the visual cortex of mice, suggesting that this process may be a major driving force of paravascular clearance (van Veluw et al., 2020). Another study has found that the clearance of fluid and soluble metabolites from the brain via IPAD could be a potential role of vasomotion (Aldea et al., 2019). The IPAD pathway is postulated to conduct interstitial fluid (ISF) and solutes along the basement membranes (BM) of capillaries, arterioles and arteries towards the cervical lymph nodes in the neck via the BM cerebral arteries (Diem et al., 2017; Gouveia-Freitas & Bastos-Leite, 2021). The vasomotion-driven IPAD hypothesis suggests that IPAD is driven by contractile vascular SMCs of cerebral arteries which induce BM deformations, thus inducing net intramural fluid flows which occur in the same direction of the vasomotion wave (Aldea et al., 2019). These studies taken together suggest that vasomotion may play a key role in the clearance of solutes from the brain via perivascular clearance along blood vessels. Other studies have confirmed that vasomotion appears to play a role in enhancing tissue perfusion. By evoking vasomotion in rabbit ear skin through electrical stimulation, it was found that the clearance rate of a tracer injected into the ear tissue was significantly greater with vasomotion present than in tissue without vasomotion (Sakurai & Terui, 2006).

1.9.3 Mechanisms Underlying Vasomotion

There are three types of cellular oscillations that have been suggested to be responsible for vasomotion: the cytosolic oscillator model, the membrane oscillator model, and the metabolic oscillator model (Aalkjaer & Nilsson, 2005). Based on the cytosolic oscillator model, vasomotion is thought to be initiated when asynchronous oscillations in intracellular Ca^{2+} ($[Ca^{2+}]_i$) concentration become synchronised within vascular SMCs (Aalkjaer et al., 2011).

Global oscillations in $[Ca^{2+}]_i$ then occur, as a uniform $[Ca^{2+}]_i$ increase has occurred throughout the entirety of the cell (Aalkjaer et al., 2011). This increase in $[Ca^{2+}]_i$ opens intermediate conductance potassium channels, leading to hyperpolarisation of the membrane, and then closing of voltage-dependent $[Ca^{2+}]_i$ channels and vasodilation follows (Di Marco et al., 2015). The cytosolic oscillator is responsible for "slow wave" vasomotion oscillations (Pradhan & Chakravarthy, 2011). The membrane oscillator model suggests that vasomotion is initiated by an oscillation originating in the sarcolemma (Aalkjaer & Nilsson, 2005). The membrane oscillator is responsible for "fast wave" vasomotion (Pradhan & Chakravarthy, 2011). The metabolic oscillator model suggests that oscillations in membrane voltage may occur due to oscillations in glycolysis and subsequently, ATP concentrations, which may then cause oscillations in the electrogenic sodium-potassium pump (Pradhan & Chakravarthy, 2011).

1.9.4 Investigating Vasomotion In-Vivo and In-Vitro

Methods used to study vasomotion have included use of vital microscopy, pressure measurements, blood-cell velocity measurements, Laser-Doppler flow measurement, and the study of isolated vessels (Nilsson & Aalkjaer, 2003). Differences in vasomotion in vivo have been observed, seemingly dependent on differences in study methodology, for instance, in the use of anaesthesia. Vasomotion has been observed under awake conditions in animals, but has been found to become depressed or even disappear completely with the use of anaesthesia (Colantuoni et al., 1984; Hundley et al., 1988). Yet, some studies have reported the presence of vasomotion under anaesthetised conditions (Dirnagl et al., 1989; Fujii et al., 1990), or even observed that vasomotion is inducible by anaesthetic use (Rivadulla et al., 2011). Inspired oxygen content has also been found to alter patterns of vasomotion. Arteriolar vasomotion was observed to increase in frequency under conditions of hypoxia, whilst hyperoxia (100% O2) resulted in a reduction in the frequency of vasomotion (Bertuglia et al., 1991). To study the cellular mechanisms underlying vasomotion, isolated vessels have been used, however, these studies have typically used large, isolated arteries, and thus it has been debated whether the observed oscillations in vitro have the same origin as vasomotion seen in the microcirculation (Nilsson & Aalkjaer, 2003). Yet, oscillations have been observed in vitro in several preparations,

such as rabbit mesenteric artery (Omote et al., 1993) and small arteries in the ear (Griffith & Edwards, 1993), rat tail (Lamb et al., 1985) and mesenteric small arteries (Gustafsson et al., 1993), in addition to human pial (Gokina et al., 1996) and coronary arteries (Kawasaki et al., 1981).

1.10 Investigating Brain Vascular Function in Animal Models

1.10.1 Hypertension Models

Animal models enable experimental strategies that would otherwise not be possible in human studies, making these models vital in the investigation of disease pathogenesis (Lerman et al., 2019). HTN models exist in several species; however, rodent models offer significant advantages such as readily available techniques for genetic manipulation, in addition to a shorter gestation period and greater cost-effectiveness than larger animal models (Lerman et al., 2019). Inducing HTN in animal models can be carried out via methods such as dietary manipulation, surgical procedures, or use of pharmacological agents (Jama et al., 2022). The manipulation of the diet to include high salt or fat has been used to induce HTN (Carlson et al., 2002; Gros et al., 2002; Yu et al., 2004; Zhang et al., 2021), however, the onset of HTN after diet manipulation has been found to vary (Mills et al., 1993; Yu et al., 2004; Zhang et al., 2021), or not occur at all (Monassier et al., 2006), while others have observed increased oxidative stress and changes in cognition independent of SBP and DBP (Liu et al., 2014). Surgically induced HTN includes procedures such as constriction of the aorta by extravascular banding, implantable occluders in the suprarenal aorta or renal arteries, or intravascular devices in the renal arteries (Lerman et al., 2019). Others have used chronic administration of Nω-Nitro-l-arginine methyl ester hydrochloride (L-NAME) (Chen et al., 2019; Kruyer et al., 2015; Ribeiro et al., 1992) which can be dissolved in drinking water to obtain a NO-deficient HTN, which has been associated with marked endothelial dysfunction and smooth muscle dysfunction of large conduit arteries (Küng et al., 1995).

1.10.2 Angiotensin-II Model of Experimental Hypertension

A widely used method for inducing HTN in animal models is through the administration of ang-II infused via a subcutaneously implanted osmotic minipump (Capone et al., 2012; Duchemin et al., 2013; Foulquier et al., 2018; Gomolak & Didion, 2014; Gonzalez-Villalobos et al., 2008; Kawada et al., 2002; Ling et al., 2018). HTN can be induced at different severities using exogenous ang-II infusion, thus various doses have been used based on the experimental needs. The ang-II model resembles some forms of human HTN, as the RAAS is broadly activated in human HTN; and the doses of ang-II commonly used in mice achieve BP elevations that are on par with those seen in uncontrolled stage 2 HTN (Lerman et al., 2019). Kawada et al. (2002) investigated BP responses of mice to graded ang-II doses, finding that SBP increased at day 3 with a high dose of ang-II (1000/ng/kg/min), while a lower dose of ang-II (400 ng/kg/min) resulted in a slow-pressor response, showing a delayed rise in BP by days 9-13 (Kawada et al., 2002). A dose of 600 ng/kg/min of ang-II is a commonly used "slow pressor" dose used to investigate the development of HTN and its effects on the cerebrovasculature (Cao et al., 2012; Capone et al., 2011; Youwakim et al., 2023).

1.10.2.1 Angiotensin-II and Cognition

Ang-II infusion has been found to impair cognitive function, however, conflicting findings have been reported on how and when memory deficits manifest. A study by Meissner et al. (2017) found that ang-II infusion along with L-NAME administration resulted in short term memory deficits after 4 weeks, and in mice treated with an additional daily ang-II bolus (0.5 µg/kg BW s.c.) from week 2 onward displayed both short and long term deficits at the 4 week point (Meissner et al., 2017). Effects of ang-II on cognition may be age-related, as some studies have found learning (Toth et al., 2013) and spatial memory (Csiszar et al., 2013) deficits in aged (24 month old) but not young (3 month old) mice after 4 weeks of ang-II infusion. Conversely, Duchemin et al. (2013) have found learning and spatial memory impairments in young (eight week old) mice after 21 days of ang-II infusion at a rate of 1900 ng/kg/min (Duchemin et al.,

2013), which was higher than the 1000 ng/kg/min dosage used by the aforementioned studies. Short-term memory impairments have also been observed in young (3-4 mo) mice after 3 months of ang-II infusion, however, no deficits in working memory were observed (Foulquier et al., 2018). Using an ang-II daily injection (1mg/kg/day), Gao et al., (2021) have found cognitive deficits in mice after just 14 days (Gao et al., 2021).

1.10.2.2 Angiotensin-II and Cerebral Blood Flow

In 10 month old mice, ang-II infusion for 2 months increased SBP in both WT and AD mice, but resulted in a greater increase in SBP for AD mice in addition to decreased hippocampal and thalamic CBF (Wiesmann et al., 2015). Antihypertensive treatment after the first month of ang-II infusion was less effective on AD mice in reducing the ang-II-induced HTN than it was on their WT counterparts (Wiesmann et al., 2015). Both acute and sustained ang-II administration has been found to impair the neurovascular coupling response to whisker stimulation without reducing resting CBF (Capone et al., 2011; Kazama et al., 2003). An attenuated CBF response to whisker stimulation and acetylcholine has also been observed in Girouard et al.'s (2008) study which included both male and female mice, and interestingly, this attenuated response was observed in male mice only (Girouard et al., 2008). However, in female mice, after ovariectomy, protection against the cerebrovascular effects of ang-II were no longer present, yet, the administration of estrogen was found to reinstate this protection (Girouard et al., 2008). The administration of estrogen to male mice was also found to prevent ang-II from affecting CBF responses (Girouard et al., 2008). Some studies have indicated that ang-II administration may impact neurovascular coupling independent of its effects on BP. Ang-II infusion with the prevention of increased arterial pressure has still resulted in NVC impairments (Kazama et al., 2003).

1.11 Two-Dimensional Optical Imaging Spectroscopy

Functional magnetic resonance imaging (fMRI) is a method that has been used to map neural activity in the human brain by measuring changes in the Blood Oxygen Level Dependent (BOLD) response that are associated with changes in neural activity. Two-dimensional optical imaging spectroscopy (2D-OIS) is a method that can be used to investigate the haemodynamic basis of the fMRI signal in more detail, through the measurement of changes in remitted light from cortical tissue, which then can be used to estimate aspects of the haemodynamic response (Berwick et al., 2005). Thus, 2D-OIS can provide concurrent measures of changes in oxyhaemoglobin (HbO), deoxyhaemoglobin (Hbr), and total haemoglobin (HbT) concentrations, that are akin to changes in cerebral blood volume and oxygenation (Kennerley et al., 2005). Using this method, several different vascular compartments can be assessed in terms of their contribution to the overall haemodynamic response, specifically, the whisker barrel cortex (WBC), artery, vein, and parenchyma. Our laboratory amongst others has used OIS to investigate haemodynamic responses to sensory stimulation (Berwick et al., 2005; Eyre et al., 2022; Malonek & Grinvald, 1996; Nemoto et al., 1997; Shabir et al., 2020; Sharp et al., 2020). The thinned skull preparation used for 2D-OIS is the preferred method for imaging experiments, as it is minimally invasive to parenchymal tissue compared to other methods (Helm et al., 2009; Klohs et al., 2014). In this preparation, the skull is thinned to translucency using a dental drill over the somatosensory cortex, allowing for the animal to undergo in-vivo imaging with 2D-OIS. The somatosensory pathway from the whisker to the topographically organised barrel cortex is well-defined, making it a commonly used pathway of study in neurovascular research (Lecrux & Hamel, 2011; Sharp et al., 2015). With the installation of a thinned cranial window, chronic 2D-OIS imaging can be used to obtain measures of blood volume and oxygenation in both the anaesthetised and awake mouse over multiple imaging sessions with high temporal and spatial resolution (Kennerley et al., 2012). This measure can also be combined with multi-channel electrophysiology, which can be difficult with other methods such as fMRI, to gain a detailed understanding of neurovascular function in the animal model (Kennerley et al., 2012).

1.12 Thesis Aims and Hypotheses

The overarching objective of this thesis is to elucidate the impact of preclinical disease on cerebrovascular function. This work will first investigate alterations in vasomotion within preclinical models, aiming to better characterise this process in vivo and assess its potential as a biomarker for early vascular function in disease. In addition, the influence of HTN on brain vascular function will be examined, to better understand the impact of HTN on the pathogenesis of AD. Although the association between HTN, vascular dysfunction, and dementia is increasingly recognised, the underlying mechanisms remain poorly defined. Advancing knowledge in this domain may facilitate the identification of novel therapeutic targets for the prevention or treatment of dementia.

H1: Vasomotion will differ in a mouse model of AD compared to healthy control mice.

H2: Vasomotion will differ in a mouse model of ang-II-induced HTN compared to healthy control mice.

H3: Vascular function will differ in a mouse model of ang-II-induced HTN compared to healthy control mice.

Chapter 2 - Haemodynamic and neuronal contributions to low-frequency vascular oscillations in a preclinical model of Alzheimer's disease

This chapter is a published research paper (O'Connor et al., 2025. Neurophotonics, 12(S1), S14615).

Chapter Summary

This chapter investigates vasomotion as a potential early biomarker for Alzheimer's disease. The study involved analysis of haemodynamic and neural data collected from a preclinical model of Alzheimer's disease (J20-AD mice) and healthy wild-type controls using 2D-OIS and electrophysiology. The primary aim was to characterise vasomotion in vivo and assess its potential to differentiate between Alzheimer's disease and healthy control mice. In addition, the study examined the relationship between vasomotion and neuronal activity.

2.1 - Paper Title and Authors

Haemodynamic and neuronal contributions to low-frequency vascular oscillations in a preclinical model of Alzheimer's disease

Shannon M O'Connor[a]*, Runchong Wang[a]*, Paul S Sharp[b], Osman Shabir[c,d], Kira Shaw[a], Michael Okun[e,a], Clare Howarth[a,d,f], Chris Martin[a,d], Jason Berwick[a,d,f]

*These authors contributed equally to this work

[a]University of Sheffield, Faculty of Science, School of Psychology, Sheffield, UK

[b]Medicines Discovery Catapult, Macclesfield, UK

[c]University of Sheffield, Division of Clinical Medicine, School of Medicine and Population Health, Sheffield, UK

[d]University of Sheffield, Neuroscience Institute, Sheffield, UK

[e]University of Nottingham, School of Life Sciences, Nottingham, UK

[f]University of Sheffield, Healthy Lifespan Institute, Sheffield, UK

Corresponding Author Shannon M. O'Connor, smoconnor1@sheffield.ac.uk; Jason Berwick, j.berwick@sheffield.ac.uk

⁎These authors contributed equally to this work.

I, Shannon O'Connor, performed analyses and wrote the majority of the manuscript. Runchong Wang also perfomed analyses and contributed to the writing of the manuscript. Experiments were performed by Paul Sharp and Osman Shabir. Kira Shaw helped with statistical analysis. Chris Martin and Jason Berwick helped with MATLAB data analysis and figure generation. Michael Okun, Clare Howarth, Chris Martin, and Jason Berwick supervised the research, proofread and helped edit the manuscript.

2.2 Introduction

Vascular dysfunction is a commonly observed occurrence in both Alzheimer's disease (AD)[1] and aging[2]. In some cases, alterations in vascular function have been observed decades before the onset of AD, suggesting the earliest marker of AD progression may be vascular dysregulation[3]. The neurovascular degeneration hypothesis of AD postulates that neurovascular dysfunction can lead to the onset or worsening of AD dementia through factors such as blood-brain barrier dysfunction and impaired cerebral blood flow (CBF), which can result in the development of tau-related pathology and a build-up of amyloid-beta peptide (Aβ)[4,5], considered to be neuropathological hallmarks of AD[6].

To ensure proper functioning of neurons in the brain, an adequate supply of blood is required, which is delivered via a vast vascular network of veins, arteries, venules, arterioles and capillaries. Neurovascular coupling (NVC), or functional hyperaemia, refers to the relationship between neuronal activity and cerebral blood flow (CBF), whereby increases in neuronal activity drive an increase in CBF to the active area. This rapid redirection of blood flow to areas of neuronal activation ensures a targeted and uninterrupted flow of blood that is essential for brain viability[7]. Despite a need for a continuous supply of glucose and oxygen, the brain lacks fuel stores[8] and therefore relies on the concerted action of the cells within the neurovascular unit to maintain brain homeostasis and ensure that adequate energy and nutrients are available when required. It has been reported that deficits in NVC are present in AD, in both human patients and preclinical models of the disease[9,10,11,12,13], but there remains some uncertainty over whether NVC deficits are present in mouse models used in the study of AD[14,15,16].

Another aspect of vascular function that may be altered in disease and aging is vasomotion. This is a rhythmic oscillation in vascular diameter which peaks around 0.1 Hz[17,18,19]. The physiological importance of vasomotion remains somewhat unclear, however, higher amplitudes and prevalence of vasomotion have been reported in conditions associated with compromised oxygen delivery[20,21,22,23], suggesting that the role of vasomotion may be of a

protective nature[24]. It has been postulated that the oscillatory blood flow produced by vasomotion may achieve better tissue oxygenation than that obtained from a steady flow of blood[25]. Further, it has been reported that hypoxic conditions have resulted in an increase in arteriolar vasomotion in an un-anaesthetised hamster skinfold preparation, while inducing hyperoxia (using 100% O_2) resulted in a reduced frequency of vasomotion[26]. Studies investigating vasomotion in the context of AD have been relatively limited, however, both enhancements[27,28] and reductions[29] in vasomotion have been reported in human patients, as well as impairments observed in mice expressing APOE4, a genetic risk factor for AD[30]. Vasomotion has also been theorised to contribute to the driving force of solute clearance from the brain[31,32], and thus, impairments in this process might contribute to or aggravate progression of pathology in AD by hindering the removal of Aβ. Thus, a better understanding and characterization of vasomotion in AD is of significant importance. Classically defined vasomotion (i.e., of a purely vascular origin) can occur in any tissue of the body[20,23,26,27], and Hudetz et al. among others have shown the same oscillation in the brain[33,18]. The term "vasomotion" has been used to describe two separate phenomena, a 0.1 Hz oscillation originating from intrinsic vascular mechanisms, or a mixture of neural-induced and neural-independent mechanisms. For the current study, we refer to vasomotion resulting from vascular-only derived activity as "neural-independent" vasomotion.

To enable the investigation of vasomotion and its physiological basis in health and disease, various in vivo mesoscale imaging studies have converted blood volume changes into the frequency domain and categorised blood volume change occurring around 0.1 Hz as vasomotion (for a review on this issue, see Das et al., 2020[34]). However, this categorization may not be accurate when investigating cerebrovascular vasomotion, as neural activity also occurs at 0.1 Hz. Consequently, the low-frequency vascular oscillation may represent a blend of vasomotion and spontaneous NVC (i.e., neurally-induced blood volume changes that are distinct from vasomotion). Furthermore, the role of neural activity in low-frequency oscillation remains largely unknown. Mateo et al. (2017) found that the pial vessel diameter covaries with slow changes in the amplitude of high-frequency LFP (gamma band: 30-80 Hz) in the vibrissa area, and activation of layer 5b pyramidal neurons at the same frequency leads to pial vessel diameter change at 0.1 Hz[35]. Winder et al. (2017) also found blood volume change correlated with

gamma-band LFPs in the somatosensory cortex[36]. However, when local neural activity was substantially suppressed by muscimol, no significant changes in low-frequency vessel diameter were observed compared to the control group.

Existing studies thus provide evidence for both neural-induced and neural-independent low-frequency blood volume oscillations in wild-type (WT) mice, while the neural basis of low-frequency blood volume oscillations in mouse models of AD remains largely unexplored. The current study uses data collected from the transgenic J20-AD mouse model, a widely used model in preclinical studies of Alzheimer's disease. The J20-AD mouse model overexpresses human APP with familial AD mutations[37] and recapitulates AD-like phenotypes such as synaptic loss[38], impairments in cognition[39], and plaque pathology from 6 months of age onward[40].

As vasomotion could potentially be a biomarker of the vascular dysfunction that may occur in AD, the current study aimed to investigate low-frequency hemodynamic oscillations (LFOs) occurring in anaesthetised J20-AD mice compared to WT C57Bl/6 controls, and to determine whether these oscillations are independent of neural activity. We tested the hypothesis that a respiratory challenge in the form of an inspired gas transition from 100% oxygen to medical air (21% O_2) will be sufficient to drive increases in vasomotion oscillations.

2.3 Materials and Methods

To assess whether LFOs in cerebral blood volume differ between diseased and healthy states, data from experiments in which the hemodynamic responses and neurovascular function of mice were recorded using 2-dimensional optical imaging spectroscopy (2D-OIS) and electrophysiology were analysed. 2D-OIS offers measurements of changes in total haemoglobin (HbT), akin to changes in cerebral blood volume and oxygenation, with high temporal and spatial resolution[41]. When used alongside electrophysiology, this approach offers a concurrent measurement of hemodynamic and neural activity. Previously we developed a chronic mouse

preparation in which a thinned cranial window implant enabled repeated hemodynamic imaging followed by a single acute experiment in which 2D-OIS and electrophysiological silicon-probe recording were performed simultaneously. Data from these experiments have been published previously[15,16] (see Shabir et al., 2022; Sharp et al., 2020), however, no analysis was performed to explore LFOs or vasomotion in data collected from these animals.

2.3.1 Animals and Experimental Paradigm

Changes in the blood volume and oxygenation of anaesthetised 9-12 month-old J20-AD (MMRRC Stock No: 34836-JAX) and WT C57Bl/6 controls [N = 23 mice, (n = 13 J20-AD, n = 10 WT), males] were analysed. Plaque pathology and impairments in long-term memory have been confirmed to be present by 9 months of age in this mouse model using an age-matched sibling cohort[40] to the animals in the current study. All animals were anaesthetised with fentanyl-fluanisone (Hypnorm, Vetapharm Ltd), midazolam (Hypnovel, Roche Ltd), and sterile water (ratio of 1:1:2 by volume; 7mL/kg, i.p.) for surgery and imaging, in addition to 0.3-0.8% isoflurane in 100% oxygen for maintenance[16], as described previously by Sharp et al., 2020. Our established anaesthetic regime has been determined to enable evoked hemodynamic responses resembling those in the awake state[42].

All animals underwent three chronic imaging sessions, beginning approximately one week after thinned cranial window surgery. Each session was separated by ~30 days. The animals then underwent a final acute (4th) imaging session, in which a 16-channel electrode (100 µm spacing, site area 177 µm2, 1.5–2.7 MΩ impedance; Neuronexus Technologies, Ann Arbor, MI, USA) was inserted into the right whisker barrel cortex (WBC) which allowed for simultaneous measurement of neural activity and hemodynamic function. Each 2D-OIS session consisted of 8 experiments performed in the same order.

Exp1: Sensory stimulation while breathing 100% oxygen. Experiment consisted of 30 trials of 25s each, with whisker stimulation administered 5s after the start of each trial. Whiskers were mechanically deflected using a plastic T-shaped stimulator for a 2s duration to evoke a hemodynamic response in the somatosensory cortex of the mouse. 2D-OIS lasted 750s.

Exp2: Repeat of experiment 1 to ensure preparation and recording stability.

Exp3: Mild gas challenge: transition of breathing gas from 100% oxygen to normal air. 2D-OIS lasted 750 seconds with the transition to air occurring after 105 seconds.

Exp4: Sensory stimulation while breathing air. Paradigm is the same as experiment 1, except the animal was breathing air rather than oxygen.

Exp5: Long-duration sensory stimulation while breathing air. Experiment consisted of 15 trials of 70s each, with whisker stimulation administered 10s after the start of each trial. 2D-OIS lasted 1050s.

Exp6: Mild gas challenge: transition of breathing gas from air to 100% oxygen. 2D-OIS lasted 750 seconds with the transition to air occurring after 105 seconds.

Exp7: Long-duration sensory stimulation while breathing oxygen. Paradigm is the same as experiment 5, except the animal was breathing oxygen rather than air.

Exp8: Major gas challenge in the form of hypercapnia. Animal was switched from breathing 100% oxygen to 90% oxygen and 10% carbon dioxide. Duration of challenge was 250s.

The current study analysed data from experiments 3 and 6, in which mice underwent a mild gas challenge in which inspired gas was switched from 100% O_2 to medical air (21% O_2) during the course of the experiment[16] (see Sharp et al., 2020 for more detailed experimental outline). In acute sessions, in which electrophysiology occurred alongside 2D-OIS, imaging experiments started 30 minutes after the electrode had been inserted. All animal procedures were performed with approval from the UK Home Office in accordance with the guidelines and regulations of the Animal (Scientific Procedures) Act 1986 and were approved by the University of Sheffield ethical review and licensing committee.

2.3.2 Measurement of Arterial LFOs

Recordings of changes in HbT were used to obtain a measure of LFOs occurring in four regions of interest (whisker barrel cortex [WBC], artery, vein, and parenchyma, Fig. 1). WBC location was determined based on the HbT activation map from a stimulation experiment in which whiskers were mechanically deflected using a plastic T-shaped stimulator to evoke a hemodynamic response in the somatosensory cortex of the mouse. Data were imported to MATLAB (R2022a; MathWorks[43]) for analysis. HbT data from 375-750s of experiments 3 and 6 were used to assess LFOs in each inspired gas condition. A high-pass filter with a cutoff frequency of 0.01 Hz was applied to remove low-frequency noise. A fast Fourier transform (FFT) was conducted to obtain the data in the frequency domain for analysis. Oscillations within 0.06 - 0.2 Hz, a range typically associated with vasomotion[44,45], were summed for each animal in both the oxygen-breathing condition (Exp 6) and the air-breathing condition (Exp 3). As the strongest response was expected to occur in the artery, the main focus of the current study was on this region.

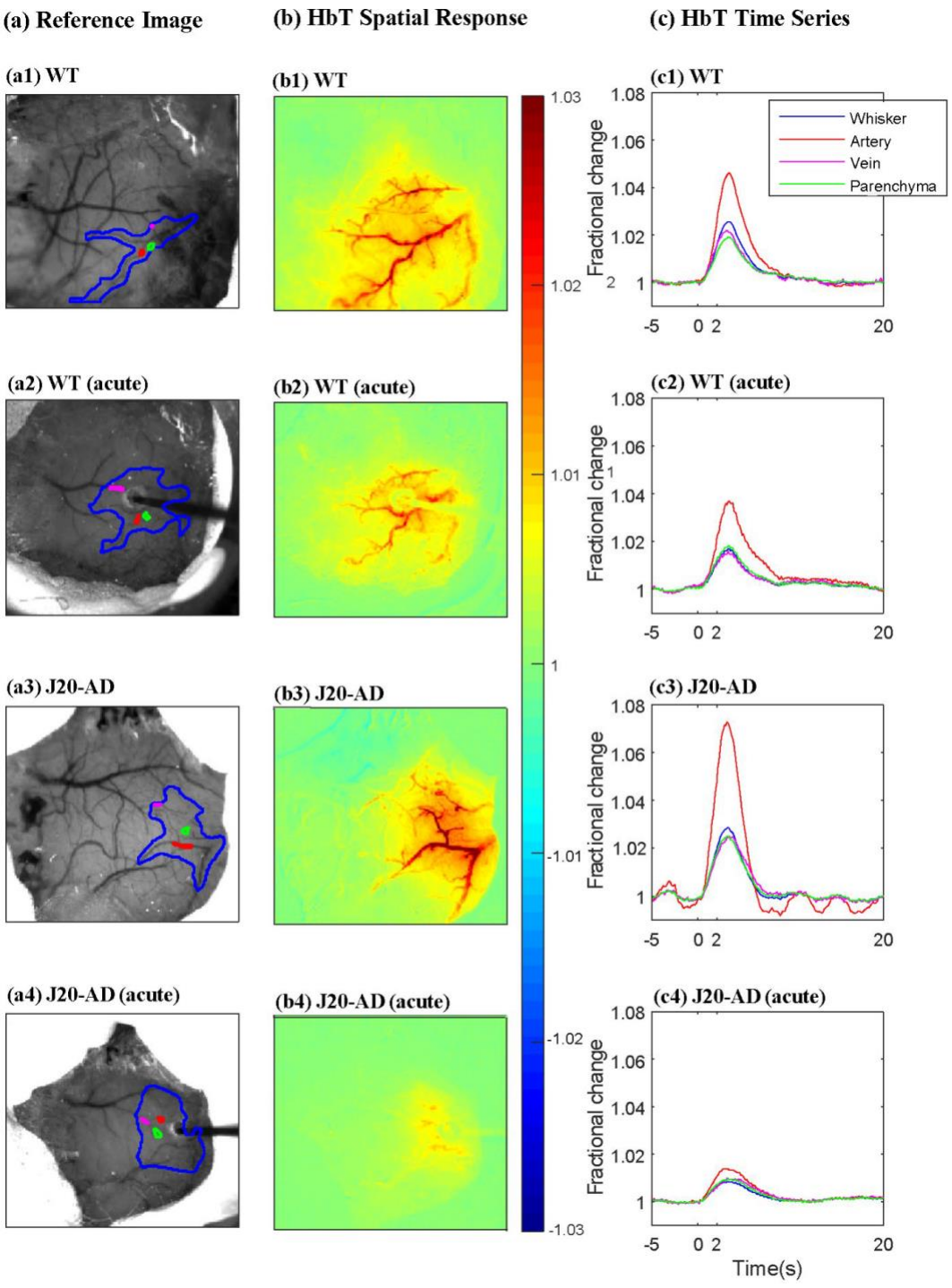

Fig 1. Region of Interest Selection and HbT Response to Whisker Stimulation. A reference image of the thinned cranial window over the somatosensory cortex with four regions of interest (ROIs) selected: whisker region (blue), artery (red), vein (pink), and parenchyma (green) for (a1) WT, (a2) WT in the acute session (i.e., with electrode

present), (a3) J20-AD, and (a4) J20-AD in the acute session (i.e., with electrode present). The corresponding HbT spatial response to a 2-second mechanical whisker stimulation of (b1) WT, (b2) WT in the acute session, (b3) J20-AD, and (b4) J20-AD in the acute session. HbT time series for (c1) WT, (c2) WT in the acute session, (c3) J20-AD, and (c4) J20-AD in the acute session. Whisker stimulation occurred at 0 seconds (after a 5-second baseline) for a 2-second duration. Colour bar represents fractional change.

2.3.3 Downsampling Multi-Unit Activity (MUA)

Neural activity was recorded using a 16-channel electrode implanted in the whisker barrel cortex, concurrently with 2D-OIS HbT measurements. Signals from channels 3–8 were high-pass filtered, and events exceeding 1.5 standard deviations from the mean were identified and counted as spikes. Then, MUA was downsampled to match the 8 Hz sampling frequency of the HbT recordings. Downsampling was achieved by identifying the MUA timestamps that were closest to the HbT timestamps and calculating the total MUA activity within each 0.125-second interval. This approach preserved temporal alignment between MUA and HbT data.

2.3.3.1 Kernel analysis of MUA and HbT

The linear relationship between MUA and HbT, representing NVC, was modelled using a kernel-based approach[46]. The relationship is expressed as:

$$H(t) = K * M(t) \quad (1)$$

where H(t) is the predicted HbT, M(t) is the MUA, $*$ denotes the convolution operator, and K is the kernel.

The correlation between the measured HbT and the predicted HbT was computed to evaluate how effectively MUA explains HbT fluctuations. The kernel was normalised and five key parameters were defined to describe the shape of the kernel (see Fig.2):

Peak: The maximum value of the kernel occurring after time 0s, representing the highest HbT response following neural activity.

Slope to Peak: The best-fit line between time 0s and the peak, reflecting how rapidly HbT changes in response to neural activity.

Slope to Baseline: The best-fit line between the peak and when the kernel intersects with the baseline, representing how quickly HbT returns to baseline after neural activity.

Region Before: The area under the kernel curve before the intersection between kernel and baseline, indicating the amount of HbT decrease preceding neural activity.

Region After: The area under the curve after time 0s, capturing the total HbT increase associated with neural activity.

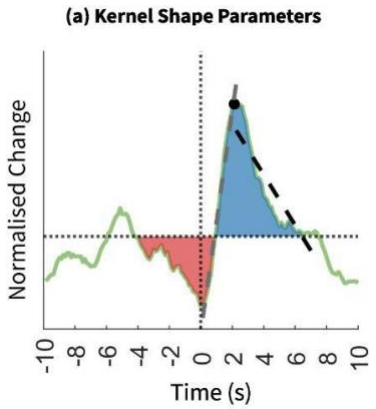

Fig 2. Kernel Shape Parameters. An example of a kernel. The red and blue region highlights the region before and after, respectively. The grey dashed line represents the slope to peak (from time 0s to the peak), while the black dashed line represents the slope to baseline (from the peak to the x-axis). The black dot represents the peak.

2.3.3.2 Peak-triggered analysis

To confirm the kernel analysis result, we conduct an additional analysis. For both WT and AD groups in air and oxygen we manually selected HbT peaks and then extracted the hemodynamic time series [i.e., HbT, oxyhaemoglobin (HbO), and deoxyhaemoglobin (HbR)] 10s prior and 10s post this peak [WT oxy (n=10, average number of peaks = 38±2.9sem), WT air (n=10, average number of peaks 37±2.1sem), AD oxy (n=12, average number of peaks=47±3.5sem), AD air

(n=12, average number of peaks 51±4.5sem)]. All trials were averaged to create a mean hemodynamic time series across animals. To understand if there was a neural component to vasomotion we took all the time points used to create these hemodynamic vasomotion trials to extract time matched neuronal responses from the MUA data.

2.3.4 Statistical Analysis

2.3.4.1 Analysis of HbT data

Analysis was conducted to determine the effect of group (J20-AD or WT C57Bl/6 control) and inspired gas (oxygen or air) on the power of LFOs in HbT in the artery ROI. Analysis of the chronic sessions included $N = 21$ mice ($n = 11$ J20-AD and $n = 10$ C57Bl/6 controls), and each mouse contributed between 1 to 4 sessions to the analysis. To account for multiple measurements taken from the same subject, data were analysed using a linear mixed model (LMM) (R version 2024.04.2+764, lme4 package, Bates et al. 2015[47]) to account for random (animal ID, session ID) and fixed (group) effects on LFO power in the oxygen and air breathing conditions. Where post-hoc tests were performed, Tukey's method for multiple comparisons was applied.

Previous literature has shown that the electrophysiological preparation can affect the cerebral hemodynamic responses due to a cortical spreading depression (CSD) as a result of electrode insertion into the cortex, resulting in a sustained reduction in HbT[15]. Therefore, acute sessions in which an electrode was in place were analysed separately. Two additional mice underwent acute imaging, resulting in $N = 23$ ($n = 13$ J20-AD and $n = 10$ C57Bl/6 control) mice, with each animal contributing one session for each inspired gas condition. However, one acute session was removed from the analysis due to noise which was impacting the quality of HbT and MUA measurements. All other sessions from all animals were included in the analysis. Therefore, $N = 22$ ($n = 12$ J20-AD and $n = 10$ C57Bl/6 control) mice were included in the analysis. A mixed analysis of variance (ANOVA) was conducted to determine the effect of group (J20-AD or WT C57Bl/6 control) and inspired gas (oxygen or air) on the power of LFOs

in HbT in the artery ROI. An α-level of 0.05 was considered to be statistically significant for both analyses.

2.3.4.2 Analysis of HbT and neural data

Analysis was then conducted to explore the relationship between MUA and HbT. An electrode implant was present only in the final terminal experiment for each animal, thus, each animal only contributed one imaging session to the analysis. A mixed model ANOVA was conducted on LFP band power, parameters of kernel shape and kernel prediction across groups and inspired gas conditions (R 2024.04.2+764, rstatix package; Kassambara, 2021[48]). The assumptions of normality and homogeneity of variance were assessed using Q–Q plots, and Levene's test, as implemented in the rstatix package (Kassambara, 2021[48]). The assumption of homogeneity was violated for the increasing slope. Therefore, a robust ANOVA (WSR2 package; Mair & Wilcox, 2020[49]) was used for increasing slope. An α-level of 0.05 was considered to be statistically significant. A simple effects test was conducted for any variables with a significant interaction, and a Bonferroni correction was applied to correct for multiple comparisons for the 5 kernel parameters and 5 LFP power bands.

For both analyses, preliminary screening of the data indicated a skewed distribution of LFO power, and as such a log transformation was performed to improve normality of the distribution to increase the robustness of the applied statistical model and meet required assumptions. Researchers were blinded to animal group information (J20-AD or WT control) while statistical tests were performed. Where possible, the same arterial segment of each animal was used for both chronic and acute analyses.

2.4 Results

2.4.1 Arterial Low-Frequency Oscillations are Unchanged in J20-AD Mice Compared to WT Controls (Chronic Imaging Sessions)

An FFT was conducted on HbT data from WT and J20-AD mice in the oxygen and air-breathing conditions (Fig. 3), after which the power of the signal occurring in the range of 0.06-0.2 Hz was summed and used as a measure of LFOs occurring in the artery. Data were sorted into 4 groups for analysis using linear mixed modelling: J20-AD oxygen, J20-AD air, WT oxygen, and WT air. The LMM analysis revealed a significant difference in LFO power between these groups [$F(3, 30.20) = 9.05$, $p < .001$], specifically, there was a significant difference in LFO power between J20-AD mice in the oxygen condition compared to the air condition, as well as a significant difference in LFO power between WT mice in the oxygen condition compared to the air condition, as determined by pairwise comparison (see Supplementary Materials, Table S1). In both J20-AD and WT mice, LFO power was found to be significantly increased when mice were breathing air compared to breathing oxygen (Fig. 4). However, no significant differences were observed in LFO power between J20-AD and WT mice.

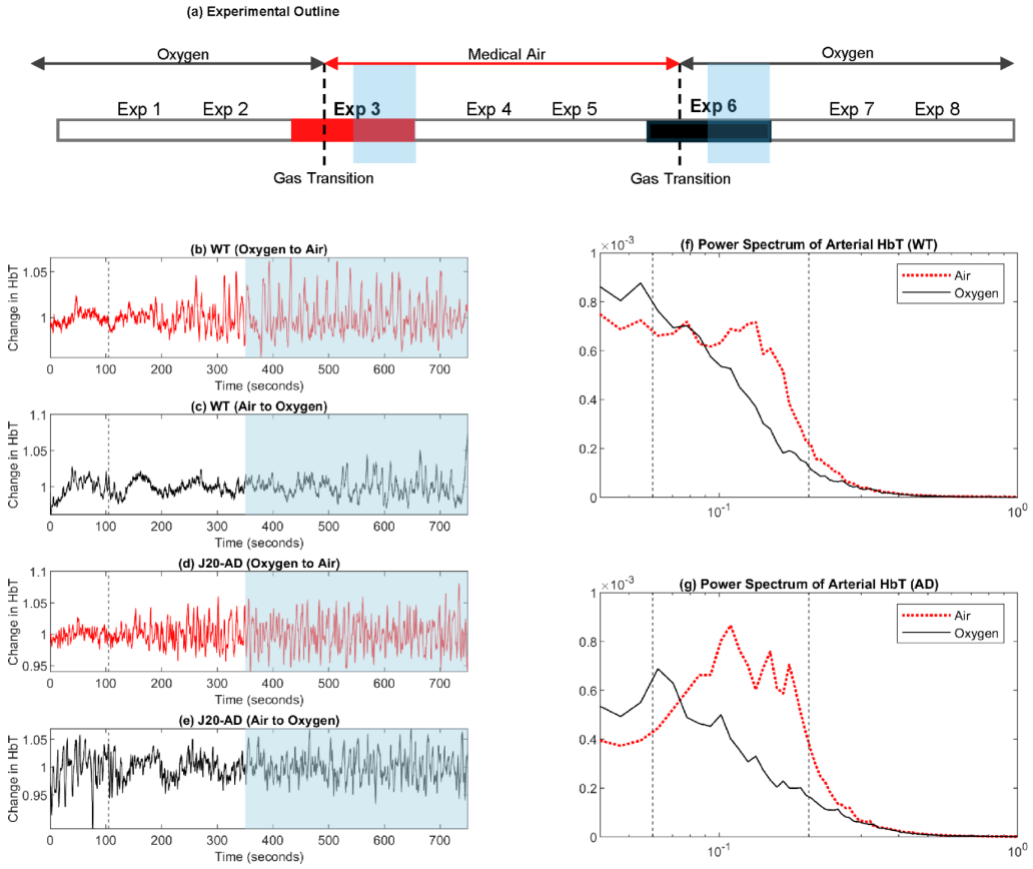

Fig 3. Time series and FFT of arterial HbT. (a) depiction of a single session, involving 8 experiments. The black dotted lines indicate where inspired gas had been changed. The current study used data from experiment 3 and experiment 6 (marked in bold). The blue highlighted area indicates the portion of the experiment used for the analysis of HbT in each inspired gas condition. Time series of arterial HbT occurring in a WT mouse in (b) an experiment in which the inspired gas was switched from 100% oxygen to medical air, and (c) an experiment in which the inspired gas was switched from medical air to 100% oxygen. Time series of arterial HbT occurring in a J20-AD mouse during (d) an experiment in which the inspired gas was switched from 100% oxygen to medical air, as well as (e) an experiment in which the inspired gas was switched from medical air to 100% oxygen. The grey dotted line indicates when the inspired gas was changed (105s), and blue highlighting indicates the portion of data used for the measurement of HbT for each inspired gas condition. Mean FFTs of HbT in the artery for both the oxygen (black) and air-breathing (red) conditions are shown for (f) WT and (g) J20-AD mice, the grey dotted lines indicate the 0.06 - 0.2 Hz range summed and used for analysis.

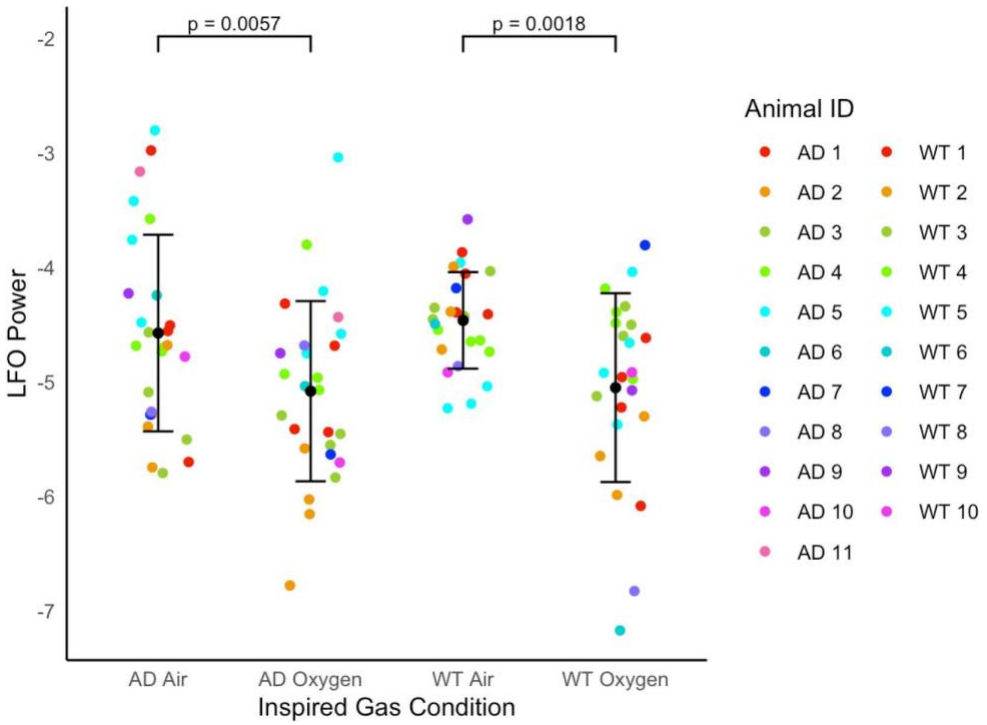

Fig 4. Power of LFOs in the artery of J20-AD and WT mice in oxygen and air-breathing conditions. Log-transformed powers of LFOs occurring in the 0.06-0.2 Hz range in the arterial region of J20-AD (n = 11) and WT (n = 10) mice in each inspired gas condition (oxygen and air). Each mouse contributed no more than 4 sessions. Each data point represents the summation of power occurring between 0.06-0.2 Hz in a session, with mean ± standard deviation (SD) for each group and inspired gas condition.

2.4.2 Arterial Low-Frequency Oscillations are Impaired in J20-AD Mice Compared to WT Controls in the Acute Imaging Session (with Electrode Implanted)

As we wanted to investigate whether HbT LFOs are driven by neural activity, data from mice during the acute session in which an electrode was in place were analysed. First, these data were analysed to determine the effect of group (J20-AD or WT C57Bl/6 control) and inspired gas

(oxygen or air) on the power of HbT LFOs in the artery ROI. A mixed ANOVA revealed that in the acute dataset, group differences were more pronounced. Specifically, we observed a significant main effect of group [$F(1,20) = 5.43$, $p = 0.030$)], such that J20-AD mice exhibited overall lower power of LFOs than WT controls (Fig. 5a). Similar to the chronic dataset, a significant effect of inspired gas was observed [$F(1,20) = 5.30$, $p = 0.0320$], in that LFOs were found to increase as inspired oxygen was reduced (Fig. 5b, Table S2).

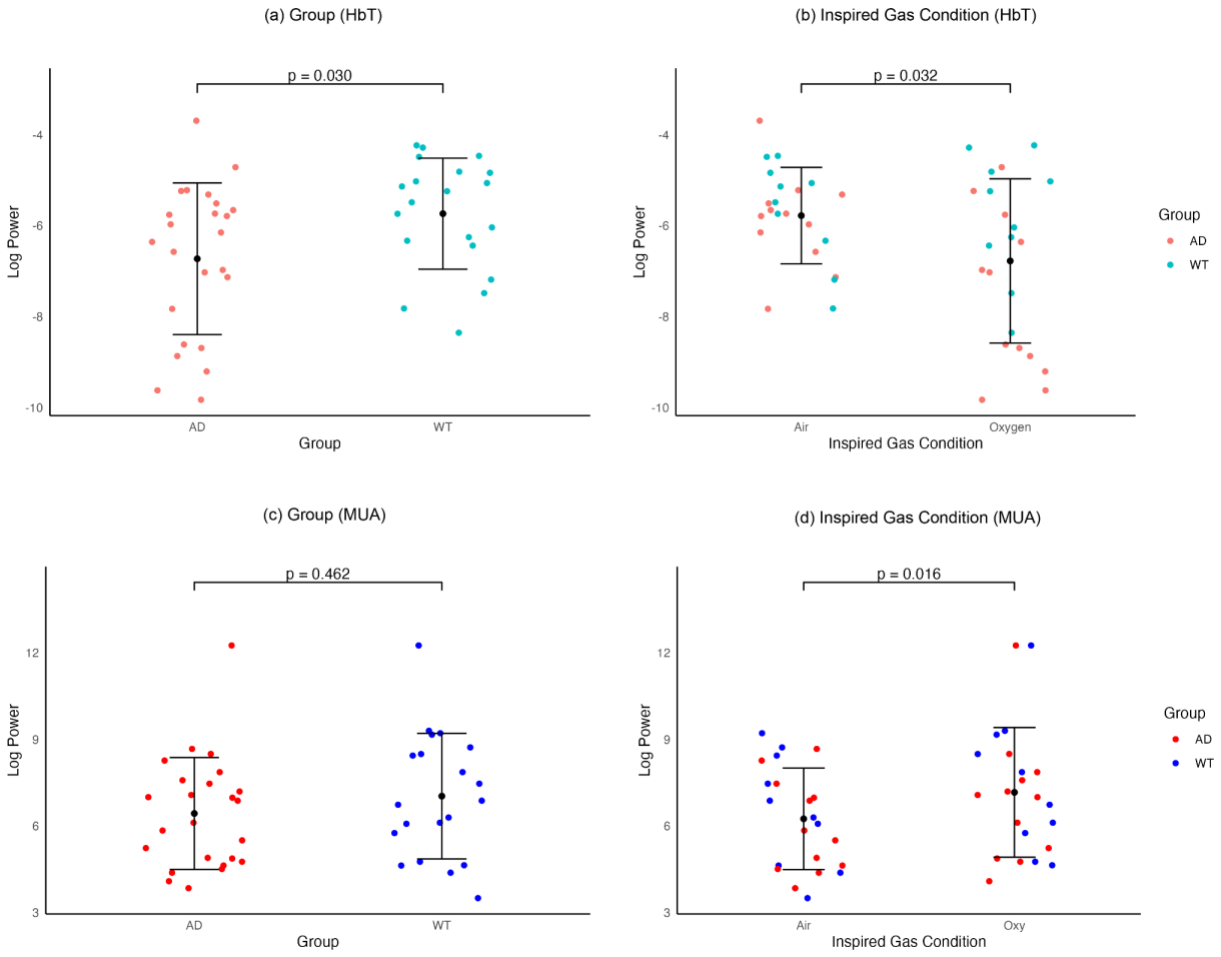

Fig 5. Power of LFOs in the artery of J20-AD and WT mice (with electrode implant) in oxygen and air-breathing conditions. Log-transformed powers of LFOs in HbT occurring in the 0.06-0.2 Hz range in the arterial region of (a) each group [J20-AD (n = 12) and WT (n = 10) mice], and (b) in each inspired gas condition (oxygen and air). Animals contributed one session to each of the inspired gas conditions. Each data point represents the summation of

power occurring between 0.06-0.2 Hz in a session, with mean ± standard deviation (SD) for each group and inspired gas condition. Log-transformed powers of low-frequency MUA oscillations occurring in the 0.06-0.2 Hz range in the somatosensory region of (a) J20-AD and WT mice (with electrode implant), and (b) power of MUA in the somatosensory region of J20-AD and WT mice (with electrode implant) in each inspired gas condition (oxygen and air). Data are plotted as individual values with mean ± standard deviation (SD).

2.4.3 MUA

In the ideal case, changes in inspired gas would affect only neural-independent vasomotion, without altering neural activity. Under such conditions, LFOs in MUA would be expected to remain consistent across breathing conditions. However, a mixed ANOVA on low-frequency MUA revealed significantly higher MUA power during the oxygen condition compared to the air condition ($F(1,20) = 6.864$, $p = 0.891$), with no significant differences observed across groups (Table S2, Fig. 5). These findings suggest that the LFOs observed in Fig. 5 may result from spontaneous neurovascular coupling (NVC), or from a combination of NVC and neural-independent vasomotion.

2.4.3.1 Neurovascular coupling

Variations in neural activity across different breathing conditions complicated the interpretation of LFOs in HbT. To address this, we investigated how inspired gas and group influence the relationship between neural activity and hemodynamic responses.

To quantify this relationship, we computed a kernel to model the linear relationship between the HbT signal and MUA (i.e., NVC; Fig. 6b). Predicted HbT was obtained by convolving the kernel with MUA data and then correlated with measured HbT (Fig. 6a). Five features of the kernel shape were defined (see Fig. 2), and a mixed ANOVA was applied to analyse these data. To correct for multiple comparisons, a Bonferroni-corrected α-level of 0.01 was applied.

The kernel shape represents the linear relationship between HbT and MUA, that is, the NVC. If the inspired gas or disease group alters NVC, significant differences in kernel shape parameters would be expected. The air breathing condition decrease slope to baseline ($F(1,20) = 9.279$, $p = 0.006$) and region before ($F(1,20) = 12.278$, $p = 0.002$), and increase region after ($F(1,20) = 9.428$, $p = 0.006$) were significantly different across breathing conditions. The kernel prediction reflects the extent to which changes in HbT can be explained by MUA. If the LFOs in HbT observed under air are primarily driven by neural-independent vasomotion—or a mixture of spontaneous NVC and vasomotion—then kernel prediction would be expected to be lower in the air group. Interestingly, a significant interaction was found in the correlation between predicted HbT and measured HbT ($F(1,20) = 6.643$, $p = 0.018$), although the main effects of group and inspired gas were not significant (Table S2). A follow-up simple effects test revealed that the group mean of kernel prediction for oxygen in the WT condition was significantly higher compared to the AD condition (Table S4; Oxy-WT, $M = .485$, $SD = .159$; Oxy-AD, $M = .304$, $SD = .231$). Importantly, no significant differences in kernel prediction were found across breathing conditions in either the WT or AD group, suggesting that LFO HbT changes across breathing conditions are likely neurally driven.

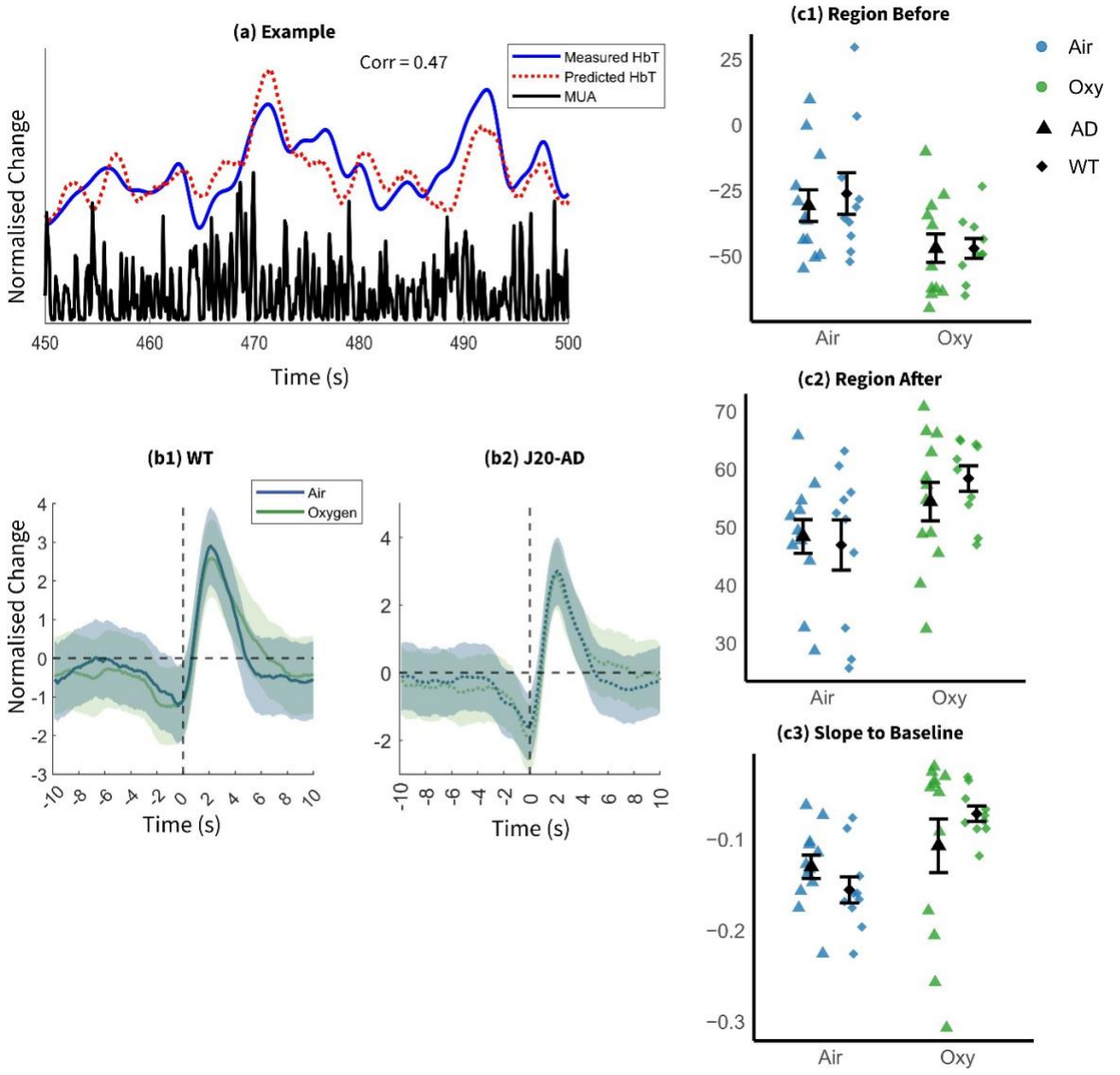

Fig 6. Kernel of MUA and HbT in the artery of J20-AD and WT mice (acute dataset) in oxygen and air-breathing conditions. **a**: The HbT and MUA data from a representative subject, over 50s. **b**: The average kernel for WT (b1) and J20-AD (b2) groups. The green line represents the oxygen-breathing condition, while the blue line represents the air-breathing condition. The shaded regions denote the standard deviation. **c**: The region before (c1), region after (c2), and slope to baseline of all subjects, plotted as individual values with mean ± standard deviation (SD). The green and blue represent air and oxygen-breathing condition, while square and diamond represent AD and WT mice group.

To further confirm that LFOs in HbT are driven by neural activity, we conducted an additional analysis. We manually identified HbT peaks in WT and AD animals under air and oxygen conditions, extracting corresponding hemodynamic time series for HbT, HbO, and HbR (averaged across animals; Fig. 7). MUA aligned to these hemodynamic peaks was subsequently extracted for neural correlational analysis. If vasomotion was independent of MUA the expectation would be that the MUA time series would be flat. As can be seen across all groups the MUA data peaks approximately 2s prior to the peak in HbT. Spatially the MUA data also arises from the middle cortical layers from around the depth of the whisker barrels in layer IV. This data supports the results from the kernel analysis suggesting in this study vascular oscillations were driven by coherent spontaneous neural responses and did not arise independently.

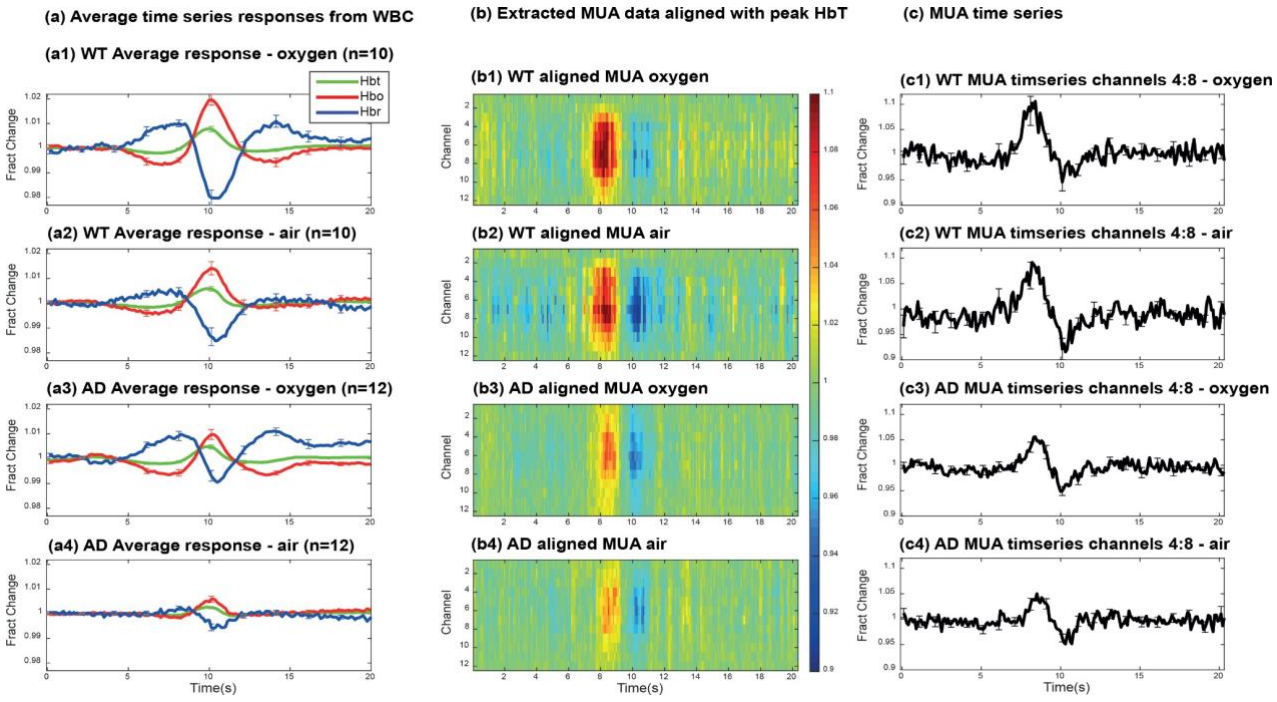

Fig 7. Alignment of spontaneous hemodynamic peak responses and MUA activity across all groups. Column (a) depicts average time series responses from the WBC in (a1) WT animals under oxygen (n = 10), (a2) WT animals under air (n = 10), (a3) AD animals under oxygen (n = 12), and (a4) AD animals under air (n = 12). Column (b) depicts extracted MUA data aligned from the peak Hbt response at 10s for (b1) WT animals under oxygen, (b2) WT

animals under air, (b3) AD animals under oxygen, and (b4) AD animals under air. The largest increase in MUA activity can be seen at 8s. Colour bar represents fractional change. Column (c) depicts MUA time series taken from channels 4 to 8 in (c1) WT animals under oxygen, (c2) WT animals under air, (c3) AD animals under oxygen, and (c4) AD animals under air. HbT = total haemoglobin, HbO = oxyhaemoglobin, HbR = deoxyhaemoglobin. Error bars=standard error of the mean.

2.4.3.2 Brain state

To examine whether brain states differ across groups and air-breathing conditions, we employed mixed ANOVA to assess the effects of breathing conditions and group differences on local field potential (LFP) band power across five frequency ranges: delta (0.5–4 Hz), theta (4–8 Hz), alpha (8–12 Hz), beta (12–30 Hz), and gamma (30–100 Hz). LFP band power was log-transformed to meet normality assumptions. The Bonferroni correction was applied and the significant level was reduced to 0.01 to account for multiple comparisons.

Significant differences were observed across breathing conditions in the delta, alpha, and gamma bands (Table S5). Delta and gamma band oscillations are associated with anaesthetic state and low-frequency hemodynamic fluctuations, respectively[50]. Additionally, alpha and beta band LFPs differed significantly between groups, consistent with previous findings[51].

All experiments were conducted in the same order (see Methods section and Fig. 3a). Therefore, it is crucial to determine whether changes in LFP band power reflect the effects of time or breathing condition. To further examine this, a follow-up ANOVA was performed on LFP power recorded at the beginning of Experiment 3 and the end of Experiment 6— the two experiments used for analysis in this study (Fig. 8). The results revealed no significant differences in delta-band power between the beginning of Exp. 3 and the end of Exp. 6 (Fig. 8a, grey and orange; Fig. 8b), indicating that anaesthetic depth remained stable throughout the recording sessions included in the current analysis. Similarly, delta power in the two air-breathing conditions (Fig. 8a, blue and yellow; Fig. 8b) remained unchanged. This suggests that although breathing condition may influence delta-band power and, by extension, anaesthetic depth, there was no time-dependent effect on anaesthetic depth. Furthermore, Fig. 8d shows that LFP power in the three

frequency bands significantly modulated by gas condition was not correlated with kernel prediction.

(a) Oxygen Level Change across Experiment

(b) LFP Power in Oxygen Breathing Condition

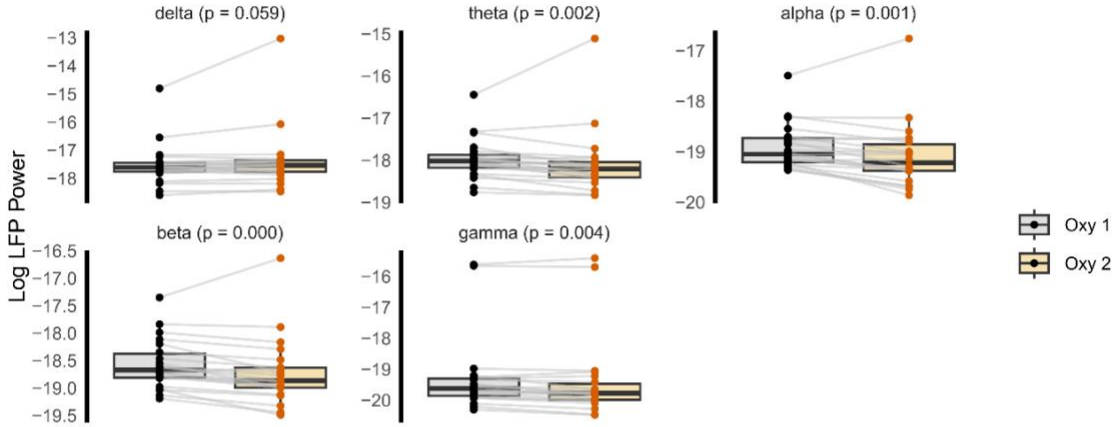

(c) LFP Power in Air Breathing Condition

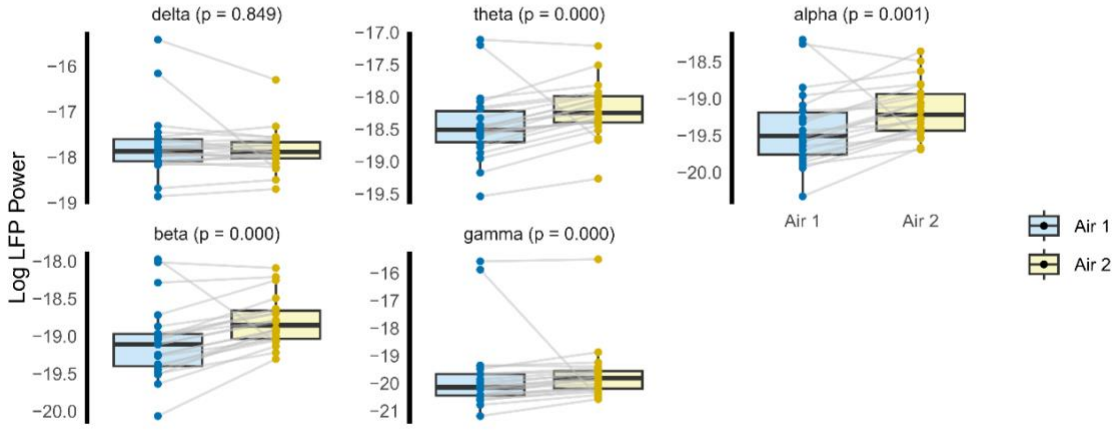

(d) LFP Power with Kernel Prediction

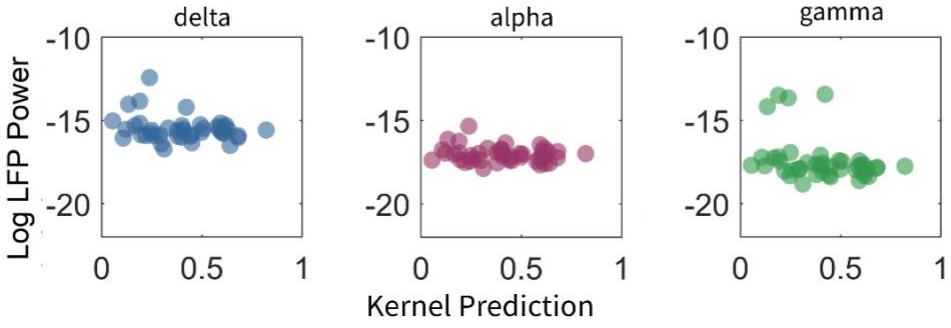

Fig 8. Anaesthesia depth remains constant throughout experiments and kernel prediction is independent of anaesthesia depth. **a:** Illustration of the experimental setup following electrode implantation. In Experiment 3, the breathing condition was switched from oxygen to medical air; in Experiment 6, it was switched from medical air to oxygen. The final 450 seconds of Experiments 3 and 6 were used, corresponding to the air and oxygen conditions, respectively. Two 100-second segments from each condition—oxygen (grey and orange) and air (blue and yellow)—were selected for further analysis. The black line represents the oxygen level. **b & c:** LFP power across frequency bands in the two oxygen and air conditions. **d:** Log-transformed delta, alpha, and gamma power plotted against kernel prediction.

2.5 Discussion

The current study found no differences in cortical arterial LFOs between J20-AD and WT mice. These results suggest that measurements of arterial LFOs may not be a suitable metric to distinguish J20-AD males from healthy male controls, as differences between diseased and healthy mice were not detected. Further, in line with our hypothesis that a mild respiratory challenge would drive vasomotion oscillations, we found a significant increase in arterial LFO power when inspired oxygen was reduced. It was determined that these LFOs were not entirely independent of neural activity, suggesting that our LFO measurement potentially reflects spontaneous low-frequency NVC rather than vascular-only derived activity.

There were no significant differences in arterial LFOs in HbT in the 0.06-0.2 Hz range observed between J20-AD and WT mice in the chronic condition. This aligns with previous findings from our laboratory and others which found no differences in the neurovascular function of AD mice[14,15,16]. However, when an electrode was inserted into the cortex, group differences were more pronounced. It was revealed that in acute sessions, J20-AD mice exhibited significantly lower powers of arterial LFOs than WT mice when an electrode implant was present in the brain. This aligns with previous literature reporting impaired neurovascular responses after electrode implantation[15,16]. This is a result of a cortical spreading depression (CSD) which is a wave of depolarization of neurons and thus silencing of synaptic activity which may result from electrical or mechanical perturbation of the brain[52] and is followed by a

spontaneous return to normal function after time. The effects of CSD have been reported to be more severe in J20-AD mice, resulting in a larger reduction in HbT and slower hemodynamic recovery than that seen in WT controls[15]. Thus, group differences in the acute experimental setting of the current study, in which mice underwent intracranial surgery (for electrode insertion) immediately prior to measurements taken of neurovascular function, may have become apparent due to differential effects of CSD on AD and WT mice, in that the J20-AD mice likely exhibited a reduction in HbT that was more prolonged and sustained than that of WT controls. For a more comprehensive report on the differential effects of CSD on J20-AD and WT mice, please see Shabir et al., 2022.

The electrode present for acute sessions allowed for the simultaneous measurement of neural activity alongside measurements of changes in cerebral haemodynamics, and this was investigated to see whether the LFOs were driven by neural activity. Significantly higher LFOs in HbT and lower LFOs in MUA were observed under air-breathing conditions. This finding suggested that the manipulation of oxygen concentration influenced neural activity in addition to LFOs in HbT. In the air-breathing experiment (Exp. 6), which always followed the oxygen-breathing experiment (Exp. 3), the observed increase in HbT LFOs may reflect mice recovering from CSD or the presence of neural-independent vasomotion. Furthermore, the MUA power differences suggest the LFOs in HbT across inspired gas conditions could be a result of spontaneous NVC and/or neural independent vascular movement, therefore, further analysis was undertaken to explore the relationship between HbT and neural activity to assess whether any of the hemodynamic LFO increase in air is due to neural-independent vasomotion. Analysis revealed that there were no differences in kernel shape between the groups, consistent with previous studies which reported that average HbT response to whisker stimulation (i.e., NVC) does not change significantly in J20-AD mice[15,16]. Since kernel shape reflects the linear relationship between neural activity and the subsequent hemodynamic response, manipulations which evoke changes solely in neural-independent vasomotion should not affect kernel shape. Additionally, neural-independent vasomotion is unpredictable based on neural activity, thus kernel prediction accuracy should decrease with increased neural-independent vasomotion. In the current study, significant differences in kernel shape were found across inspired gas conditions.

Analysis revealed a significant interaction between group and inspired gas on kernel prediction despite no significant main effect of group or inspired gas being found. If the breathing condition induces neural-independent vasomotion in both AD and WT mice, we should observe lower kernel prediction in the air compared with the oxygen condition. However, a simple effects test indicated that the mean predictive power in the oxygen-breathing condition is significantly higher in the WT group compared to the J20-AD group, and no significant differences in the kernel prediction across breathing condition were found. Our additional peak-triggered analysis demonstrated that hemodynamic LFOs consistently followed neural activity (i.e., NVC), as indicated by MUA peaks occurring approximately 2 seconds prior to HbT peaks across all groups and conditions. Collectively, these results suggest the LFO HbT change induced by oxygen level change is at least partially neurally induced. While our findings suggest a linear relationship between LFOs in HbT and MUA, we acknowledge that this approach provides only an indirect assessment of NVC. The NVC responses of the same animals to whisker stimulation have been reported in our previous work[15,16].

Interpretations of relationships between neural activity and hemodynamic response data between the WT and J20-AD groups must be approached with caution, as electrode implantation induces differential CSD effects in WT compared to J20-AD mice, in that the effects of the CSD appear to be more profound in the J20-AD model than WT mice[15]. Future research should prioritize less invasive techniques, such as the use of single-fluorophore genetically encoded calcium indicators (GECIs), such as GCaMP. This allows for in-vivo imaging of brain activity without the need for an electrode, thus, next steps may be to investigate LFOs in HbT using this technique. This would allow for a better assessment of differences in neural activity and kernel prediction between WT and J20-AD groups.

Classically, vasomotion has been defined as an ~0.1 Hz oscillation in vessel diameter that occurs independently of neuronal activity[18,33]. However, studies in mice have reported instances of entrainment or coupling between vasomotion and neuronal signals[35,50], suggesting a more intricate relationship. In the current study, changes in our LFO signal were seemingly induced by neural activity, contributing to the understanding of the connection between vasomotion and

neuronal activity in the mouse. The current study found no differences in LFO power between WT and J20-AD mice, results which contrast with studies reporting changes in vasomotion in several disease states, such as hypertension[22,23] and AD[29,30]. A better understanding of vasomotion in AD is of significant importance, as it has been postulated that this process may aid in the clearance of Aβ from the brain[31,32], and thus, could be a key therapeutic target for the prevention or treatment of AD. It has also been suggested that the oscillatory blood flow produced by vasomotion can help achieve better tissue oxygenation[25], which aligns with studies reporting higher amplitudes of vasomotion in conditions associated with hypoperfusion[20,21].

We had hypothesised that a mild respiratory challenge (inspired gas transition from 100% O_2 to 21% O_2) would drive vasomotion oscillations, however, this does not seem to be the case, as significant changes in low-frequency MUA and kernel shape were detected across the different inspired gas conditions. Vasomotion oscillations might have been more prominent using methods such as changing arterial pressure[33] or administering L-NAME[53], rather than changing inspired gases, although the aforementioned methods were implemented successfully in rat models, and thus it may be possible that cerebral vasomotion is more difficult to induce or measure successfully in the mouse. Further research is needed to characterize vasomotion both in the mouse and in the AD-state.

Methods such as blood-oxygen level dependent (BOLD) fMRI have been used to study brain activity in AD in both humans[54,55] and in animal models[56,57] of the disease. It is known that factors such as motion, respiratory and cardiac cycles, and vasomotion can confound BOLD signals[58], thus, highlighting the importance of investigating the role of non-neuronal factors such as vascular fluctuations, to better understand how these signals may impact the interpretation of resting-state fMRI data. Our study found that LFOs in arterial HbT were coupled to neuronal activity. This may contribute to the understanding of the resting-state BOLD signal as used in functional connectivity mapping, strengthening the interpretation of the relevant low-frequency vascular oscillations as reflective of underlying neuronal activity. It has been suggested that a dynamic relationship between vasomotion and neuronal activity may exist, in that vasomotion has been reported to be influenced by or tied to underlying neural activity in awake mice[35,59],

thus an avenue for future research may be to explore this relationship further. A study by Ma et al. (2016) investigating the relationship between resting-state haemodynamics and underlying neural activity using Thy1-GCaMP mice and wide-field optical mapping has found that Thy1-GCaMP signals were coupled to multiunit activity[50], providing further evidence that resting-state haemodynamics may reflect underlying patterns of neural activity.

There are some limitations of the current study to address, one being that the measurements of neurovascular function were taken in animals under anaesthesia. It is known that cerebral haemodynamics, neural activity, and NVC in anaesthetised animals is different from that of awake animals[60,61], and thus the state produced by anaesthetics does not reflect normal physiological conditions. However, previous research from our laboratory has indicated that the anaesthetic combination used in the current study results in a magnitude and speed of evoked hemodynamic responses to physiological whisker stimulation that resemble those found in the awake state[42]. Although, the impact that our anaesthetic regime may or may not have on LFOs specifically has not yet been determined. Further, the current experiments did not include the collection of additional physiological monitoring data (such as breathing rate, heart rate, and movement) during anaesthesia, making it challenging to accurately quantify the anaesthetic state. However, we have shown previously that baseline hemodynamic values remain stable throughout the duration of the experiments, apart from time points where an intervention took place to change the baseline state (i.e., gas challenges or hypercapnia), (see fig.5 in Sharp et al., 2020).

To further investigate the anaesthetic state of the animals in the present study, LFP power was analysed. Among the frequency bands, delta-band activity (0.5–4 Hz) has emerged as the most reliable indicator of anaesthetic depth in the experimental setting[62]. There was significant difference in delta-band LFP in air compared to oxygen breathing condition, but no significant differences were observed in the delta band LFP power in the beginning and end of the experimental data that were used in the current study (i.e., the beginning of Exp. 3 and end of Exp. 6). Thus, while breathing condition may influence brain state, no evidence of a time-dependent change in brain state was observed. Furthermore, no significant correlation was found

between the fraction of LFO HbT explained by neural activity (as assessed by kernel prediction) and changes in LFP bands across different breathing conditions. Therefore, we suggest that the observed LFP variations across breathing conditions do not undermine the conclusions drawn. Nevertheless, future studies employing anaesthetised models should incorporate anaesthetic state monitoring and adopt a counterbalanced experimental design.

The current study also cannot quantify whether mice experienced different sleep states while under anaesthesia. This may be an interesting avenue for future research as Hauglund et al., 2025 has demonstrated that norepinephrine-mediated vasomotion occurs during NREM sleep and may also aid in driving glymphatic clearance[63]. Another limitation of the current study is that the measurements taken for neurovascular function in the oxygen and air-breathing conditions were taken at different points of time following electrode insertion (i.e., experiment 3 and experiment 6 of 8 total experiments). This means that recovery after electrode insertion will vary slightly, in that measurements taken in the later session would have been after the animals had more time to recover following the CSD, and thus NVC responses may not be as diminished as those observed in the earlier experiment (i.e., in experiment 3). All animals experienced one CSD event immediately following electrode insertion, the hemodynamic effects of which persisted for some time before recovery[15] (see Shabir et al., 2022). However, electrode insertion occurred 30 minutes prior to experiment 1, meaning that experiment 3 took place ~1 hour after insertion, which should be sufficient time to allow for hemodynamic recovery, at least in healthy mice[15]. In addition, it should be noted that all mice included in the current study were male, thus our findings do not account for any potential sex differences. As female mice often exhibit a more severe AD phenotype[64,65], an investigation into arterial LFOs in female mice would be an important avenue for future research. Future work may also benefit from use of an imaging apparatus with greater spatial resolution and depth specificity than that which can be achieved by OIS imaging, such as two-photon microscopy, to potentially provide more precise insights into the relationship between cerebral haemodynamics and neural activity. This could also allow for the quantification of diameter fluctuations in cerebral arterial vessels, which would be valuable in the investigation of cerebral vasomotion in vivo.

2.5.1 Conclusion

The current study found no differences in arterial LFOs of J20-AD and healthy WT mice, except for in our acute preparation in which an electrode implant was present, likely due to the effects of a CSD from electrode insertion. Thus, measurements of LFOs in the artery may not be a feasible biomarker to distinguish between diseased and healthy states in male J20-AD mice. We had hypothesised that a mild respiratory challenge would drive vasomotion oscillations, and we observed an increase in LFO power as inspired oxygen was reduced. Upon further analysis, it was revealed that these LFOs were not independent of neuronal activity. Our results suggest that low-frequency vascular oscillations may be driven by spontaneous neural activity, thus adding to the understanding of how vascular fluctuations may contribute to the resting-state BOLD response. The current study also revealed that hemodynamic oscillations occurring within the same frequency range as vasomotion were coupled to neuronal activity, providing evidence that a dynamic relationship might exist between vasomotion and neuronal activity in the mouse. Further work in this area is needed, both to obtain a better understanding and characterization of vasomotion in AD and to find potential vascular biomarkers for the early detection of the disease.

Disclosures

The authors declare that there are no potential conflicts of interest that could have influenced the objectivity of this research or the writing of this paper.

Code, Data, and Materials Availability

Data presented in this paper are available on the Dryad Digital Repository: https://doi.org/10.5061/dryad.q83bk3jt4

Acknowledgements

This work was funded by a Medical Research Council UK grant [Grant number MR/M013553/1] and an ARUK grant [Grant number ARUK-IRG2014-10].

We thank Dr. Lennart Mucke (Gladstone Institute of Neurological Disease and Department of Neurology, UCSF, CA) and the J. David Gladstone Institutes for the hAPPSwe, Ind mice.

2.6 Supplementary Material

Table S1. Linear Mixed Model - Pairwise Comparisons

	b	SE	t	p
AD Air vs. AD O2	0.5076	0.146	3.485	0.0057*
AD Air vs. WT Air	-0.0367	0.279	-0.131	0.9992
AD Air vs. WT O2	0.5506	0.279	1.974	0.2255
AD O2 vs. WT Air	-0.5442	0.279	-1.951	0.2342
AD O2 vs. WT O2	0.0431	0.279	0.154	0.9986
WT Air vs. WT O2	0.5873	0.152	3.874	0.0018*

Note. significant terms are denoted with an asterisk. P-values are Tukey-adjusted for multiple comparisons.

Table S2 ANOVA

	Inspired Gas (Oxygen vs Air)			**Group (J20-AD vs WT)**			**Inspired Gas*Group**		
	F(1,20)	p	η^2	F(1,20)	p	η^2	F(1,20)	p	η^2
HbT (Acute)	5.30	.032*	.209	5.43	.030*	.213	3.62	.072	.153
MUA	6.864	.016*	.052	.562	.462	.023	.007	.934	.056
Kernel Prediction	.019	.891	.000	.775	.389	.026	6.643	.018*	.091

Note. 'HbT' in the table refers to power of LFOs in HbT within the 0.06-0.2 Hz range. Significant terms are denoted with an asterisk.

Table S3 ANOVA with Multiple Comparison on Kernel Shape Parameters

	Inspired Gas (Oxygen vs Air)			**Group (J20-AD vs WT)**			**Inspired Gas*Group**		
	F(1,20)	p	η^2	F(1,20)	p	η^2	F(1,20)	p	η^2
Slope to Baseline	9.279	.006*	.162	.056	.815	.002	2.969	.100	.058
Region Before	12.278	.002*	.194	.119	.733	.004	0.189	.668	.004
Region After	9.428	.006*	.150	.117	.736	.004	.931	.346	.017
Peak	1.437	.245	.025	0.145	.707	.005	0.219	.645	.004
	Q(1,20)	p	η^2	Q(1,20)	p	η^2	Q(1,20)	p	η^2
Slope to Peak	.029	.869	.003	2.101	.173	.151	.051	.825	.005

Note. significant terms are denoted with an asterisk.

Table S4 Simple Effects Test on Kernel Prediction

	Contrast	estimate	p	t- ratio
J20-AD	Inspired Gas	.126	.125	1.566
WT	Inspired Gas	-.113	.207	-1.284
Air	Group	.058	.499	.682

Oxygen	Group	-.182	.037*	-2.152

Note. significant terms are denoted with an asterisk.

Table S5 ANOVA with Multiple Comparison on LFP Band Powers

	Inspired Gas (Oxygen vs Air)			**Group (J20-AD vs WT)**			**Inspired Gas*Group**		
	F(1,20)	p	η^2	F(1,20)	p	η^2	F(1,20)	p	η^2
Log-delta	9.851	.005*	.033	2.950	.101	.121	<.001	.994	<.001
Log-theta	6.818	.021	.026	6.283	.017	.225	.092	.764	<.001
Log-alpha	14.188	.001*	.047	8.139	.010*	.275	.161	.692	<.001
log-beta	21.135	<.001*	.075	11.771	.003*	.352	.029	.867	<.001
log-gamma	35.697	<.001*	.010	3.548	.074	.150	.609	.444	<.001

Note. significant terms are denoted with an asterisk.

2.7 References

1. Klohs, J. (2019). An integrated view on vascular dysfunction in Alzheimer's disease. *Neurodegenerative Diseases*, 19 (3-4), 109–127. http://doi.org/10.1159/000505625

2. Donato, A. J., Machin, D. R., & Lesniewski, L. A. (2018). Mechanisms of dysfunction in the aging vasculature and role in age-related disease. *Circulation Research*, 123(7), 825-848. http://doi.org/10.1161/CIRCRESAHA.118.312563

3. Iturria-Medina, Y., Sotero, R. C., Toussaint, P. J., Mateos-Pérez, J. M., Evans, A. C., & The Alzheimer's Disease Neuroimaging Initiative (2016). Early role of vascular dysregulation on late-onset Alzheimer's disease based on multifactorial data-driven analysis. *Nature Communications*, 7, 11934. https://doi.org/10.1038/ncomms11934

4. Iadecola, C. (2010). The overlap between neurodegenerative and vascular factors in the pathogenesis of dementia. *Acta Neuropathologica*, 120, 287–296. https://doi.org/10.1007/s00401-010-0718-6

5. Zlokovic, B. V. (2011). Neurovascular pathways to neurodegeneration in Alzheimer's disease and other disorders. *Nature Reviews Neuroscience*, 12(12), 723-738. https://doi.org/10.1038/nrn3114

6. Hardy, J., & Selkoe. D.J. (2002). The amyloid hypothesis of Alzheimer's disease: progress and problems on the road to therapeutics. *Science*, 297(5580), 353-356. https://doi.org/10.1126/science.1072994

7. Presa, J. L., Saravia, F., Bagi, Z., & Filosa, J. A. (2020). Vasculo-Neuronal Coupling and Neurovascular Coupling at the Neurovascular Unit: Impact of Hypertension. *Front Physiol*, 11, 584135. https://doi.org/10.3389/fphys.2020.584135

8. Verweij, B.H., Amelink, G.J., & Muizelaar, J.P. (2007). Current concepts of cerebral oxygen transport and energy metabolism after severe traumatic brain injury. *Progress in Brain Research*, 161, 111-24. https://doi.org/10.1016/S0079-6123(06)61008-X

9. Hock, C., Villringer, K., Müller-Spahn, F., Wenzel, R., Heekeren, H., Schuh-Hofer, S., Hofmann, M., Minoshima, S., Schwaiger, M., Dirnagl, U., & Villringer, A. (1997). Decrease in parietal cerebral hemoglobin oxygenation during performance of a verbal fluency task in patients with Alzheimer's disease monitored by means of near-infrared spectroscopy (NIRS) — correlation with simultaneous rCBF-PET measurements. *Brain Research*, 755(2), 293-303. https://doi.org/https://doi.org/10.1016/S0006-8993(97)00122-4

10. Lacoste, B., Tong, X. K., Lahjouji, K., Couture, R., & Hamel, E. (2013). Cognitive and cerebrovascular improvements following kinin B1 receptor blockade in Alzheimer's disease mice. *J Neuroinflammation*, 10, 57. https://doi.org/10.1186/1742-2094-10-57

11. Li, L., Tong, X. K., Hosseini Kahnouei, M., Vallerand, D., Hamel, E., & Girouard, H. (2021). Impaired Hippocampal Neurovascular Coupling in a Mouse Model of Alzheimer's Disease. *Front Physiol*, 12, 715446. https://doi.org/10.3389/fphys.2021.715446

12. van Dijk, S.E., Drenth, N., Hafkemeijer, A., Labadie, G., Witjes-Ané, M.W., Blauw, G.J., Rombouts, S.A., van der Grond, J., van Rooden, S. (2024). Neurovascular coupling in early stage dementia - A case-control study. *Journal of Cerebral Blood Flow & Metabolism*, 44(6):1013-1023. https://doi.org/10.1177/0271678X231214102

13. Royea, J., Zhang, L., Tong, X. K., & Hamel, E. (2017). Angiotensin IV Receptors Mediate the Cognitive and Cerebrovascular Benefits of Losartan in a Mouse Model of Alzheimer's Disease. *J Neurosci*, 37(22), 5562-5573. https://doi.org/10.1523/jneurosci.0329-17.2017

14. Munting, L.P., Derieppe, M., Suidgeest, E., Hirschler, L., van Osch, M.J., Denis de Senneville, B., van der Weerd, L. (2021). Cerebral blood flow and cerebrovascular reactivity are preserved in a mouse model of cerebral microvascular amyloidosis. *eLife*, 10, e61279. https://doi.org/10.7554/eLife.61279

15. Shabir, O., Pendry, B., Lee, L., Eyre, B., Sharp, P. S., Rebollar, M. A., Drew, D., Howarth, C., Heath, P. R., Wharton, S. B., Francis, S. E., & Berwick, J. (2022). Assessment of neurovascular coupling and cortical spreading depression in mixed mouse models of atherosclerosis and Alzheimer's disease. *eLife*, 11, e68242. https://doi.org/10.7554/eLife.68242

16. Sharp, P. S., Ameen-Ali, K. E., Boorman, L., Harris, S., Wharton, S., Howarth, C., Shabir, O., Redgrave, P., & Berwick, J. (2020). Neurovascular coupling preserved in a chronic mouse model of Alzheimer's disease: Methodology is critical. *Journal of Cerebral Blood Flow and Metabolism*, 40(11), 2289–2303. https://doi.org/10.1177/0271678X19890830

17. Drew, P.J., Shih, A.Y., and Kleinfeld, D. (2011). Fluctuating and sensory-induced vasodynamics in rodent cortex extends arteriole capacity. *Proceedings of the National Academy of Sciences*, 108, 8473–8478. https://doi.org/10.1073/pnas.1100428108

18. Mayhew, J. E., Askew, S., Zheng, Y., Porrill, J., Westby, G. W., Redgrave, P., Rector, D. M., & Harper, R. M. (1996). Cerebral vasomotion: a 0.1-Hz oscillation in reflected light imaging of neural activity. *Neuroimage*, 4(3.1), 183-193. https://doi.org/10.1006/nimg.1996.0069

19. Noordmans, H. J., van Blooijs, D., Siero, J. C. W., Zwanenburg, J. J. M., Klaessens, J. H. G. M., & Ramsey, N. F. (2018). Detailed view on slow sinusoidal, hemodynamic oscillations on the human brain cortex by Fourier transforming oxy/deoxy hyperspectral images. *Human brain mapping*, 39(9), 3558–3573. https://doi.org/10.1002/hbm.24194

20. Hollenberg, N. K., & Sandor, T. (1984). Vasomotion of renal blood flow in essential hypertension. Oscillations in xenon transit. *Hypertension*, 6(4), 579-585. https://doi.org/10.1161/01.hyp.6.4.579

21. Intaglietta, M. (1991). Arteriolar vasomotion: implications for tissue ischemia. *Blood Vessels*, 28(Suppl. 1): 1-7. https://doi.org/10.1159/000158912

22. Lefer, D.J., Lynch, C.D., Lapinski, K.C., Hutchins, P.M. (1990). Enhanced vasomotion of cerebral arterioles in spontaneously hypertensive rats. *Microvascular Research*, 39(2), 129-139. https://doi.org/10.1016/0026-2862(90)90065-Y

23. Pascoal, I. F., Lindheimer, M. D., Nalbantian-Brandt, C., & Umans, J. G. (1998). Preeclampsia selectively impairs endothelium-dependent relaxation and leads to oscillatory activity in small omental arteries. *Journal of Clinical Investigation*, 101(2), https://doi.org/464-470. 10.1172/JCI557

24. Di Marco, L. Y., Farkas, E., Martin, C., Venneri, A., & Frangi, A. F. (2015). Is Vasomotion in Cerebral Arteries Impaired in Alzheimer's Disease? *Journal of Alzheimer's Disease*, 46(1), 35-53. https://doi.org/10.3233/JAD-142976

25. Nilsson, H., & Aalkjaer, C. (2003). Vasomotion: mechanisms and physiological importance. *Molecular Interventions*, 3(2), 79-89, 51. https://doi.org/10.1124/mi.3.2.79

26. Bertuglia, S., Colantuoni, A., Coppini, G., & Intaglietta, M. (1991). Hypoxia- or hyperoxia-induced changes in arteriolar vasomotion in skeletal muscle microcirculation. *American Journal of Physiology*, 260(2.2), H362-372. https://doi.org/10.1152/ajpheart.1991.260.2.H362

27. Kotliar, K., Ortner, M., Conradi, A., Hacker, P., Hauser, C., Günthner, R., Moser, M., Muggenthaler, C., Diehl-Schmid, J., Priller, J., Schmaderer, C., Grimmer, T. (2022). Altered retinal cerebral vessel oscillation frequencies in Alzheimer's disease compatible with impaired amyloid clearance. *Neurobiology of Aging*, 120, 117-127. https://doi.org/10.1016/j.neurobiolaging.2022.08.012

28. van Beek, A.H.E.A, Lagro, J., Olde-Rikkert, M. G. M., Zhang, R., & Claassen, J.A.H.R. (2012). Oscillations in cerebral blood flow and cortical oxygenation in Alzheimer's disease. *Neurobiology of Aging*, 33(2), 428.e21-428.e31. https://doi.org/10.1016/j.neurobiolaging.2010.11.016

29. Rivera-Rivera, L. A., Cody, K. A., Rutkowski, D., Cary, P., Eisenmenger, L., Rowley, H. A., Carlsson, C. M., Johnson, S. C., & Johnson, K. M. (2020). Intracranial vascular flow oscillations in Alzheimer's disease from 4D flow MRI. *NeuroImage: Clinical*, 28, 102379. https://doi.org/10.1016/j.nicl.2020.102379

30. Bonnar, O., Shaw, K., Grijseels, D. M., Clarke, D., Bell, L., Anderle, S., King, S. L., & Hall, C. N. (2022). APOE4 expression confers a mild, persistent reduction in neurovascular function in the visual cortex and hippocampus of awake mice. *Journal of Cerebral Blood Flow & Metabolism,* 43(11), 1826-1841. https://doi.org/10.1177/0271678X231172842

31. Aldea, R., Weller, R. O., Wilcock, D. M., Carare, R. O., & Richardson, G. (2019). Cerebrovascular smooth muscle cells as the drivers of intramural periarterial drainage of the brain. *Frontiers in Aging Neuroscience*, 11, 1. https://doi.org/10.3389/fnagi.2019.00001

32. van Veluw, S. J., Hou, S. S., Calvo-Rodriguez, M., Arbel-Ornath, M., Snyder, A. C., Frosch, M. P., Greenberg, S. M., & Bacskai, B. J. (2020). Vasomotion as a Driving Force for Paravascular Clearance in the Awake Mouse Brain. *Neuron*, 105(3), 549-561 e545. https://doi.org/10.1016/j.neuron.2019.10.033

33. Hudetz, A.G., Roman, R.J., Harder, D.R. (1992). Spontaneous flow oscillations in the cerebral cortex during acute changes in mean arterial pressure. *Journal of Cerebral Blood Flow and Metabolism*, 12(3), 491-499. https://doi.org/10.1038/jcbfm.1992.67

34. Das, A., Murphy, K., Drew, P.J. (2021). Rude mechanicals in brain haemodynamics: non-neural actors that influence blood flow. *Phil. Trans. R. Soc. B,* 376(1815), 20190635. http://doi.org/10.1098/rstb.2019.0635

35. Mateo, C., Knutsen, P. M., Tsai, P. S., Shih, A. Y., & Kleinfeld, D. (2017). Entrainment of arteriole vasomotor fluctuations by neural activity is a basis of blood-oxygenation-level-dependent "resting-state" connectivity. *Neuron*, 96(4), 936–948.e3. https://doi.org/10.1016/j.neuron.2017.10.012.

36. Winder, A.T., Echagarruga, C., Zhang, Q., Drew, P.J. (2017). Weak correlations between hemodynamic signals and ongoing neural activity during the resting state. *Nature Neuroscience*, 20, 1761–1769. https://doi.org/10.1038/s41593-017-0007-y.

37. Mucke, L., Masliah, E., Yu, G.Q., Mallory, M., Rockenstein, E.M., Tatsuno, G., Hu, K., Kholodenko, D., Johnson-Wood, K., McConlogue, L.. (2000). High-level neuronal expression of abeta 1-42 in wild-type human amyloid protein precursor transgenic mice: synaptotoxicity without plaque formation. *Journal of Neuroscience*, 20(11), 4050-4058. https://doi.org/10.1523/JNEUROSCI.20-11-04050.2000.

38. Hong, S., Beja-Glasser, V.F., Nfonoym, B.M., Frouin, A., Li, S., Ramakrishnan, S., Merry, K.M., Shi, Q., Rosenthal, A., Barres, B.A., Lemere, C.A., Selkoe, D.J., Stevens, B. (2016). Complement and microglia mediate early synapse loss in Alzheimer mouse models. *Science*, 352(6286), 712-716. https://doi.org/10.1126/science.aad8373

39. Karl, T., Bhatia, S., Cheng, D., Kim, W.S., Garner, B. (2012). Cognitive phenotyping of amyloid precursor protein transgenic J20 mice. *Behavioural Brain Research*, 228(2), 392-397. https://doi.org/10.1016/j.bbr.2011.12.021

40. Ameen-Ali, K.E., Simpson, J.E., Wharton, S.B., Heath, P.R., Sharp, P.S., Brezzo, G., Berwick, J. (2019). The time course of recognition memory impairment and glial pathology in the hAPP-J20 mouse model of Alzheimer's disease. *Journal of Alzheimer's Disease*, 68(2), 609-624. https://doi.org/10.3233/JAD-181238

41. Kennerley, A. J., Harris, S., Bruyns-Haylett, M., Boorman, L., Zheng, Y., Jones, M., & Berwick, J. (2012). Early and late stimulus-evoked cortical hemodynamic responses provide insight into the neurogenic nature of neurovascular coupling. *Journal of Cerebral Blood Flow and Metabolism*, 32(3), 468-480. https://doi.org/10.1038/jcbfm.2011.163

42. Sharp, P., Shaw, K., Boorman, L., Harris, S., Kennerley, A., Azzouz, M., & Berwick, J. (2015). Comparison of stimulus-evoked cerebral hemodynamics in the awake mouse and under a novel anesthetic regime. *Scientific Reports*, 5, 12621. https://doi.org/10.1038/srep12621

43. The MathWorks Inc. (2022). MATLAB version: 9.12 (R2022a), Natick, Massachusetts: The MathWorks Inc. https://www.mathworks.com

44. Aalkjaer, C., & Nilsson, H. (2005). Vasomotion: cellular background for the oscillator and for the synchronization of smooth muscle cells. Br J Pharmacol, 144(5), 605-616. https://doi.org/10.1038/sj.bjp.0706084

45. Stefanovska, A. (2007). Coupled oscillators: complex but not complicated cardiovascular and brain interactions. *IEEE Engineering in Medicine and Biology Magazine*, 26(6), 25-29. https://doi.org/10.1109/EMB.2007.907088

46. Aster, R. C., Borchers, B., & Thurber, C. H. (2019). Chapter Eight—Fourier Techniques. In R.C. Aster, B. Borchers, & C. H. Thurber (Eds.), *Parameter Estimation and Inverse Problems (Third Edition)* (pp. 211–233). Elsevier. https://doi.org/10.1016/B978-0-12-804651-7.00013-4.

47. Bates, D., Mächler, M., Bolker, B., Walker, S. (2015). “Fitting Linear Mixed-Effects Models Using lme4.” *Journal of Statistical Software*, 67(1), 1–48. doi:10.18637/jss.v067.i01

48. Kassambara, A. (2021). *rstatix: Pipe-friendly framework for basic statistical tests* (Version 0.7.0) [R package]. Comprehensive R Archive Network (CRAN). https://CRAN.R-project.org/package=rstatix

49. Mair, P., & Wilcox, R. (2020). *WRS2: A collection of robust statistical methods* (Version 1.1-3) [R package]. Comprehensive R Archive Network (CRAN). https://CRAN.R-project.org/package=WRS2

50. Ma, Y., Shaik, M.A., Kozberg, M.G., Kim, S.H., Portes, J.P., Timerman, D., Hillman, E.M. (2016). Resting-state hemodynamics are spatiotemporally coupled to synchronized and symmetric neural activity in excitatory neurons. *Proceedings of the National Academy of Sciences of the United States of America*, 113(52), E8463-E8471. https://10.1073/pnas.1525369113

51. van Heusden, F.C., van Nifterick, A.M., Souza, B.C., França, A.S.C., Nauta, I.M., Stam, C.J., Scheltens, P., Smit, A.B., Gouw, A.A., van Kesteren, R.E. (2023). Neurophysiological alterations in mice and humans carrying mutations in APP and PSEN1 genes. *Alzheimer’s Research & Therapy*, 15, 142. https://doi.org/10.1186/s13195-023-01287-6

52. Lauritzen, M., Dreier, J. P., Fabricius, M., Hartings, J. A., Graf, R., & Strong, A. J. (2011). Clinical relevance of cortical spreading depression in neurological disorders: migraine, malignant stroke, subarachnoid and intracranial hemorrhage, and traumatic brain injury. *Journal of Cerebral Blood Flow and Metabolism*, 31(1), 17–35. https://doi.org/10.1038/jcbfm.2010.191

53. Lindauer, U., Megow, D., Matsuda, H., Dirnagl, U. (1999). Nitric oxide: a modulator, but not a mediator, of neurovascular coupling in rat somatosensory cortex. *American Journal of Physiology*, 277(2), H799-H811. https://doi.org/10.1152/ajpheart.1999.277.2.H799

54. Sperling, R. A., Bates, J. F., Chua, E. F., Cocchiarella, A. J., Rentz, D. M., Rosen, B. R., Schacter, D. L., & Albert, M. S. (2003). fMRI studies of associative encoding in young and elderly controls and mild Alzheimer’s disease. *Journal of Neurology, Neurosurgery & Psychiatry*, 74(1), 44. https://doi.org/10.1136/jnnp.74.1.44

55. Zheng, W., Liu, X., Song, H., Li, K., & Wang, Z. (2017). Altered Functional Connectivity of Cognitive-Related Cerebellar Subregions in Alzheimer's Disease. *Frontiers in Aging Neuroscience*, 9. https://doi.org/10.3389/fnagi.2017.00143

56. Liu, X., Hike, D., Choi, S., Man, W., Ran, C., Zhou, X.A., Jiang, Y., Yu, X. (2024). Identifying the bioimaging features of Alzheimer's disease based on pupillary light response-driven brain-wide fMRI in awake mice. *Nature Communications*, 15, 9657. https://doi.org/10.1038/s41467-024-53878-y

57. Sanganahalli, B.G., Herman, P., Behar, K.L., Blumenfeld, H., Rothman, D.L., Hyder, F. (2013). Functional MRI and neural responses in a rat model of Alzheimer's disease. *NeuroImage*, 79, 404-411. https://doi.org/10.1016/j.neuroimage.2013.04.099

58. Murphy, K., Birn, R.M., Bandettini, P.A. (2013). Resting-state fMRI confounds and cleanup. *Neuroimage*, 80, 349-59. https://doi.org/10.1016/j.neuroimage.2013.04.001.

59. Broggini, T., Duckworth, J., Ji, X., Liu, R., Xia, X., Mächler, P., Shaked, I., Munting, L.P., Iyengar, S., Kotlikoff, M., van Veluw, S.J., Vergassola, M., Mishne, G., Kleinfeld, D. (2024). Long-wavelength traveling waves of vasomotion modulate the perfusion of cortex. *Neuron*, 112(14), 2349-2367.e8. https://doi.org/10.1016/j.neuron.2024.04.034

60. Gao, Y-R., Ma, Y., Zhang, Q., Winder, A.T., Liang, Z., Antinori, L., Drew, P.J., Zhang, N. (2017). Time to wake up: Studying neurovascular coupling and brain-wide circuit function in the un-anesthetized animal. *NeuroImage*, 153, 382-398. https://doi.org/10.1016/j.neuroimage.2016.11.069

61. Martin, C., Martindale, J., Berwick, J., Mayhew, J. (2006). Investigating neural-hemodynamic coupling and the hemodynamic response function in the awake rat. *Neuroimage*, 32(1), 33-48. https://doi.org/10.1016/j.neuroimage.2006.02.021

62. Sorrenti, V., Cecchetto, C., Maschietto, M., Fortinguerra, S., Buriani, A., Vassanelli, S. (2021). Understanding the Effects of Anesthesia on Cortical Electrophysiological Recordings: A Scoping Review. *International Journal of Molecular Sciences*, 22(3), 1286. https://10.3390/ijms22031286

63. Hauglund, N.L., Andersen, M., Tokarska, K., Radovanovic, T., Kjaerby, C., Sørensen, F.L., Bojarowska, Z., Untiet, V., Ballestero, S.B., Kolmos, M.G., Weikop, P., Hirase, H., Nedergaard, M. (2025). Norepinephrine-mediated slow vasomotion drives glymphatic clearance during sleep. *Cell*, 188(3), 606-622.e17. https://doi.org/10.1016/j.cell.2024.11.027

64. Sil, A., Erfani, A., Lamb, N., Copland, R., Riedel, G., Platt, B. (2022). Sex Differences in Behavior and Molecular Pathology in the 5XFAD Model. *Journal of Alzheimer's Disease*, 85(2), 755-778. https://10.3233/JAD-210523. PMID: 34864660

65. Wang, J., Tanila, H., Puoliväli, J., Kadish, I., van Groen, T. (2003). Gender differences in the amount and deposition of amyloidβ in APPswe and PS1 double transgenic mice. Neurobiology of Disease, 14(3), 318-327. https://doi.org/10.1016/j.nbd.2003.08.009

Chapter 3 - Effects of angiotensin-II on cerebral haemodynamics and low-frequency vascular oscillations in awake mice

This chapter is a research paper in preparation for publication.

Chapter Summary

This chapter explores the impact of angiotensin II–induced hypertension on brain vascular function. As discussed in Chapter 1, hypertension has emerged as a leading risk factor for Alzheimer's disease, yet the mechanisms linking the two conditions remain incompletely understood. Given the growing recognition of vascular dysregulation as a contributing factor in Alzheimer's disease, this study aimed to investigate how hypertension may alter vascular function, with a particular focus on neurovascular coupling and vasomotion.

3.1 - Paper Title and Authors

Effects of angiotensin-II on cerebral haemodynamics and low-frequency vascular oscillations in awake mice

Shannon M O'Connor[a], Kira Shaw[a], Jessica D Westbourne[c], Osman Shabir[c,d], Clare Howarth[a,d,f], Jason Berwick[a,d,f] , Chris Martin[a,d]

[a]University of Sheffield, Faculty of Science, School of Psychology, Sheffield, UK

[b]Medicines Discovery Catapult, Macclesfield, UK

[c]University of Sheffield, Division of Clinical Medicine, School of Medicine and Population Health, Sheffield, UK

[d]University of Sheffield, Neuroscience Institute, Sheffield, UK

[e]University of Nottingham, School of Life Sciences, Nottingham, UK

[f]University of Sheffield, Healthy Lifespan Institute, Sheffield, UK

I, Shannon O'Connor, perfomed all in-vivo experiments, IHC staining, data analyses, and wrote the manuscript. Kira Shaw helped with data processing and statistical analyses. Jessica Westbourne and Osman Shabir performed IHC slide imaging and analysis. Jason Berwick helped with MATLAB data analysis. Chris Martin helped with analysis, and conception and design of the study. Clare Howarth, Jason Berwick. and Chris Martin supervised the research, proofread and helped edit the manuscript.

3.2 Introduction

Vascular risk factors, particularly hypertension (HTN), have emerged as key contributors to the development of Alzheimer's disease (AD) (O'Brien & Markus, 2014), the most common form of dementia. Despite decades of research, AD remains without a cure or effective treatment. Increasing evidence supports the vascular hypothesis of AD, which proposes that cerebrovascular dysfunction may lead to the development or progression of AD via factors such as blood-brain barrier (BBB) dysfunction and impairments in cerebral blood flow (CBF), promoting the accumulation of amyloid-beta peptide (Aβ) and development of tau-related pathology (Iadecola, 2010; Zlokovic, 2011), further exacerbating vascular impairment in a detrimental feedback loop.

HTN is linked to deleterious changes to the structure and function of the cerebral vasculature, as chronically elevated blood pressure is associated with vascular stiffening (Laurent & Boutouyrie, 2020), remodeling (Intengan & Schiffrin, 2001), and rarefaction (Antonios et al., 1999), all of which affect resistance to flow. Functionally, HTN is associated with endothelial dysfunction and reduced nitric oxide availability (Bruno et al., 2018), impairing vasodilation and increasing vascular resistance, ultimately reducing CBF. Additionally, HTN contributes to blood-brain barrier (BBB) disruption through factors such as inflammation and oxidative stress (Zhang et al., 2010), and is also associated with impairments in neurovascular coupling (NVC) (Girouard & Iadecola, 2006). NVC is the process by which neural activity induces localised increases in cerebral blood flow, allowing for the delivery of nutrients such as oxygen and glucose, which are essential for optimal brain function. Impaired NVC is observed in various pathological states, including HTN (Jennings et al., 2005; Kazama et al., 2003; Youwakim et al., 2023) and AD (Girouard & Iadecola, 2006; Hock et al., 1997; Park et al., 2020; Tarantini et al., 2017), and has been linked to cognitive decline (Tarantini et al., 2017).

Another vascular process affected by HTN is vasomotion (Hollenberg & Sandor, 1984; Liu et al., 2017; Pascoal et al., 1998), a low-frequency oscillation in vessel diameter typically centered around 0.1 Hz (Mayhew et al., 1996). Although its physiological role remains incompletely understood, it has been postulated that the oscillatory blood flow produced by vasomotion may achieve better tissue perfusion compared to that which can be achieved with

steady blood flow (Nilsson & Aalkjaer, 2003). This theory is supported by findings of increases in vasomotion in hypoxic conditions (Bertuglia et al., 1991; Colantuoni et al., 2001; Salvi et al., 2018). In both animal models and human studies of HTN, alterations in vasomotion have been reported, including changes in amplitude and frequency (Hollenberg & Sandor, 1984; Liu et al., 2017; Pascoal et al., 1998). Interestingly, these changes may depend on the severity of HTN, as a study by Fujii et al., 1990, reported an increase in the frequency of vasomotion in moderate HTN, while marked HTN was found to abolish vasomotion (Fujii et al., 1990). As vasomotion may contribute to solute clearance from the brain (Aldea et al., 2019; van Veluw et al., 2020), a better understanding and characterisation of this process could reveal novel therapeutic targets for the prevention or treatment of AD in terms of aiding in the clearance of Aβ from the brain.

Given the strong association between HTN and AD, the current study aimed to investigate how chronic HTN affects brain vascular function. The current study used the angiotensin-II (Ang-II) model of experimental HTN, a well-established approach that mimics the gradual onset of HTN observed in humans. Wild-type (WT) C57Bl/6 mice were treated with 600 ng/kg/min of Ang-II via subcutaneously implanted osmotic minipump. This model enabled the assessment of neurovascular function using in vivo neuroimaging and electrophysiological techniques, as well as the assessment of cognition and cellular changes through behavioural paradigms and immunohistochemistry, respectively.

3.3 Materials and Method

3.3.1 Animals

The current study used 6-8 month old C57Bl6/J mice, both sexes, N = 14 (n = 8 males, n = 6 females) obtained from *Charles River UK*. Of the 14 mice in the study, 8 were randomly assigned to the experimental group and treated with ang-II (n = 4 males, n = 4 females), whilst 6 were assigned to the control group (n = 4 males, n = 2 females). Mice were housed in a temperature-controlled room with *ab libitum* access to food and water. All animal procedures were performed with approval from the UK Home Office in accordance with the guidelines and

regulations of the Animal (Scientific Procedures) Act 1986 and were approved by the University of Sheffield ethical review and licensing committee.

3.3.2 Thinned cranial window

To allow for in-vivo imaging of cortical haemodynamics, a thinned cranial window implant was installed on all mice (Eyre et al., 2022; Shabir et al., 2020; Sharp et al., 2020). Surgery was performed on the animals under sterile conditions. Mice were anaesthetised with isoflurane (5% induction, 2-3% maintenance) and the depth of the surgical plane was repeatedly checked via the pedal reflex. To control pain, mice were administered ~0.01ml Carprofen (s/c), in addition to local anaesthetic (bupivacaine) applied to the scalp. Temperature was monitored using a rectal probe and homeothermic blanket, and eye gel was administered. A thinned cranial window (measuring ~3mm^2) was installed over the somatosensory cortex using a dental drill and a thin layer of cyanoacrylate glue was applied to reinforce the window and reduce specularities. Dental cement (Super Bond C&B, Sun Medical, Shiga, Japan) was applied around the perimeter of the window to attach a titanium head-plate to the skull, allowing for chronic imaging to take place. Following surgery, mice were continuously monitored for signs of pain and abnormal behaviour using MGS scoring (Langford et al., 2010). Mice were given analgesia (10mg/kg carprofen in jelly) for several days following the procedure.

3.3.3 Induction of HTN

To induce experimental hypertension, osmotic minipumps (*Alzet*, model 2004) containing ang-II (or saline for controls) were implanted into the mice subcutaneously, a method that has been widely used in hypertension studies (Cifuentes et al., 2015; Csiszar et al., 2013; Gonzalez-Villalobos et al., 2008; Kawada et al., 2002; Meissner et al., 2017; Toth et al., 2013). Osmotic pump surgery was performed on the animals under sterile conditions. To control pain, a subcutaneous injection of buprenorphine (0.05mg/kg s/c) was given before surgery in addition to local anaesthesia (bupivacaine (50-100mcL) at the incision site. Animals were anaesthetised with isoflurane (5% induction, 2-3% maintenance), and the flank of the animal was shaved and sterilised with iodine. A sterile blade was then used to make a small incision on the flank of the

mouse and a subcutaneous pocket was formed longitudinally across the side of the mouse. The prefilled sterile minipump was then inserted into the mouse and the wound secured with vicryl sutures (6-0). Mice were given analgesia (10mg/kg carprofen in jelly) for several days following the procedure. The osmotic minipumps administered ang-II (600 ng/kg/min) (Cao et al., 2012; Capone et al., 2011; Marques-Lopes et al., 2014; Youwakim et al., 2023; Zimmerman et al., 2004) or saline for a total of 28 days.

3.3.4 Imaging

Chronic imaging was conducted using 2-dimensional optical imaging spectroscopy (2D-OIS). 2D-OIS offers a measurement of changes in total haemoglobin (HbT), oxyhaemoglobin (HbO), and deoxyhaemoglobin (HbR) that are reflective of changes in cerebral blood volume and oxygenation. The right somatosensory cortex was illuminated with 4 wavelengths of light according to the absorption profiles of each haemoglobin state (495 nm ± 31, 559 nm ± 16, 575 nm ± 14 & 587 nm ± 9) using a Lambda DG-4 high-speed galvanometer (*Sutter Instrument Company*, US). A CCD camera (Dalsa 1M60) was used to capture remitted light from the cortical surface. During 2D-OIS imaging sessions, awake mice were placed on a spherical polystyrene foam treadmill with head-fixation. An optical motion sensor was attached to the spherical treadmill, allowing for the collection and quantification of locomotion. Whisker stimulation was used in somatosensory stimulation trials to evoke a neurovascular response, in which a plastic T-shaped stimulator would mechanically deflect the whiskers of the mouse when activated (Figure 9). Mice underwent two timepoints of awake imaging using 2D-OIS, one approximately 5 days after osmotic pump implantation, and one in the final week of ang-II infusion. The experimental paradigm used for awake imaging is outlined below:

Day 0 (Habituation) - Mice are given time to become acclimated to the awake imaging room and to the spherical treadmill. Mice were placed on the treadmill, and allowed to explore/walk un-headfixed for approximately 10 minutes each.

Day 1 - Experiment 1: Mice were headfixed and imaged using 2D-OIS. Experiment consisted of 30 trials, with a 2s mechanical whisker stimulation.

Day 2 - Repeat of experiment 1, followed by experiment 2. Experiment 2 is a spontaneous

activity trial which consisted of 30 trials with no stimulation.

Day 3 - Repeat of experiments 1 and 2, followed by experiment 3. Experiment 3 consisted of 15 trials, with a 16s mechanical whisker stimulation.

Day 4 - Repeat of experiments 1, 2, and 3.

Day 5 - Second timepoint of awake imaging, which took place in the final week of ang-II infusion (or saline). Consisted of a repeat of experiments 1, 2, and 3.

Day 6 - Second timepoint of awake imaging, which took place in the final week of angiotensin-II infusion. Consisted of a repeat of experiments 1, 2, and 3.

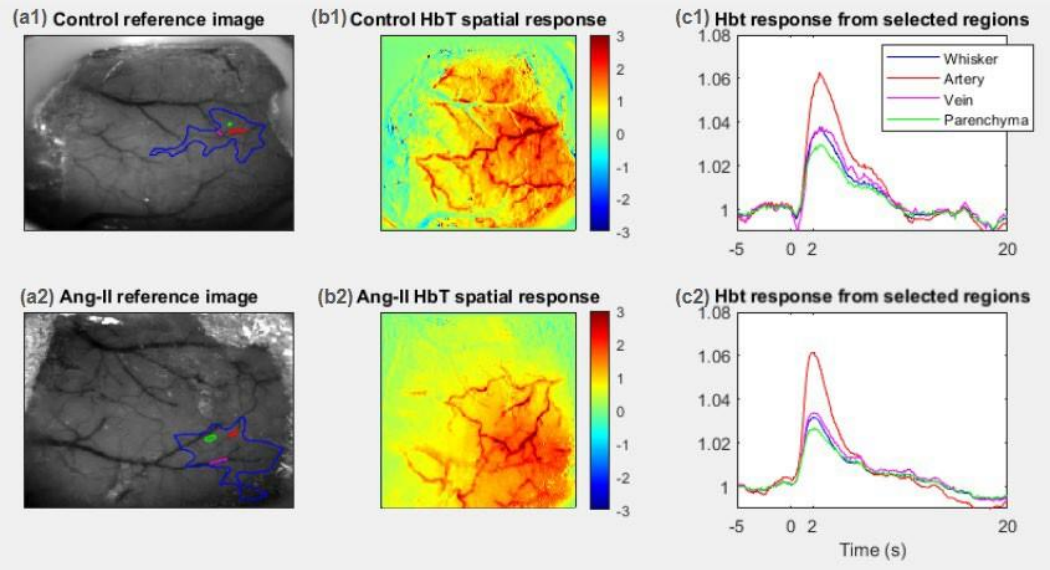

Fig 9. Regions of Interest and HbT Response to Whisker Stimulation. A reference image of the thinned cranial window over the somatosensory cortex with four regions of interest (ROIs) selected: whisker region (blue), artery (red), vein (pink), and parenchyma (green) for (a1) saline-treated control, and (a2) ang-II-treated mice. The corresponding HbT spatial response to a 2-second mechanical whisker stimulation of (b1) saline-treated control, and (b2) ang-II-treated mice. HbT time series for (c1) saline-treated control, and (c2) ang-II-treated mice. Whisker stimulation occurred at 0 seconds (after a 5-second baseline) for a 2-second duration. Colour bar represents fractional change.

3.3.5 Novel Object Recognition Test

Behavioural testing took place after approximately 2 weeks of ang-II infusion. The novel object recognition (NOR) test was used to assess short and long-term memory of the mice. The test was conducted in an open-field, square arena over the span of 4 days. On day one, mice were habituated to the experimenter and the arena by being handled and allowed to explore the arena freely for 10 minutes before being placed back into their home cage. On day 2, short-term memory was assessed. Each mouse was placed into the arena with two identical objects and allowed to explore freely for 10 minutes before being removed from the arena and placed back into the home cage. The arena and objects were cleaned with ethanol (70%), and one of the same objects was placed back into the arena along with one novel object. After 3 minutes, the mouse was placed back into the arena with the familiar object and novel object, and allowed to explore freely for 10 minutes before being placed back into the home cage. On day 3-4, long-term memory was assessed. Each mouse was placed into the arena with two familiar objects and allowed to explore for 10 minutes before being returned to the home cage as described above, however, rather than a 3-minute interval, mice were placed back into the arena with one familiar object and one novel object 24 hours later. During each trial, the arena was filmed by an overhead camera to record the time spent exploring each object. Objects were counterbalanced during the course of the behavioural experiments. Video tracking and analysis were done using EthoVision XT, *Noldus*.

3.3.6 Anaesthetised imaging and electrophysiology

An acute imaging session took place at the end of the study period, in which mice were anaesthetised [fentanyl-fluanisone, midazolam, and sterile water (ratio of 1:1:2 by volume; 7 mL/kg, i.p.) for induction, and 0.1-1% isoflurane for maintenance] and a 16-channel electrode (100 µm spacing, site area 177 µm2, 1.5–2.7 MΩ impedance; Neuronexus Technologies, Ann Arbor, MI, USA) was inserted into the right whisker barrel cortex (WBC), allowing for the simultaneous measurement of neural activity and haemodynamic function using 2D-OIS. Each 2D-OIS session consisted of 9 experiments performed in the same order as outlined below. Electrode insertion took place during experiment 2.

Exp1: Baseline measure. Sensory stimulation while breathing 100% oxygen. Experiment consisted of 20 trials of 25s each, with whisker stimulation administered 5s after the start of each trial. Whiskers were mechanically deflected using a plastic T-shaped stimulator for a 2s duration to evoke a haemodynamic response in the somatosensory cortex of the mouse. 2D-OIS lasted 500s.

Exp2: Long-duration sensory stimulation while breathing oxygen. Experiment consisted of 15 trials of 70s each, with 16s whisker stimulation administered 10s after the start of each trial. Electrode insertion occurred during trial 2 of 15. 2D-OIS lasted 1050s.

Exp3: Short-duration sensory stimulation while breathing 100% oxygen. Experimental paradigm is the same as experiment 1.

Exp4: Long-duration sensory stimulation while breathing 100% oxygen. Paradigm is the same as experiment 2 but included 10 trials instead of 15. 2D-OIS lasted 700s.

Exp5: Mild gas challenge: transition of anaesthetic carrier gas from 100% oxygen to medical air (21% oxygen). 2D-OIS lasted 500 seconds with the transition to air occurring after 125 seconds.

Exp6: Short-duration sensory stimulation while breathing air. Paradigm is the same as experiment 3, except the animal was breathing air rather than oxygen.

Exp7: Long-duration sensory stimulation while breathing air. Paradigm is the same as experiment 4, except the animal was breathing air rather than oxygen.

Exp8: Mild gas challenge: transition of anaesthetic carrier gas from air back to 100% oxygen. 2D-OIS lasted 500 seconds with the transition to air occurring after 125 seconds.

Exp9: Major gas challenge in the form of hypercapnia. Animal was switched from breathing 100% oxygen to 90% oxygen and 10% carbon dioxide. Duration of challenge was 250s.

3.3.7 Immunohistochemistry

Following terminal experiments, mice were euthanised with an i.p. injection of sodium pentobarbital (100 mg/kg) and transcardially perfused with saline, after which brains were

dissected. Coronal slices were obtained (5 μm) and immunohistochemistry was performed using an avidin-biotin complex (ABC) method, as described previously in Ameen-Ali et al., 2019. Sections were deparaffinised, rehydrated, and endogenous peroxidase activity was blocked through placing the sections in 3% methanol/12ml H_2O_2 for 20 minutes. Immunolabelling for GFAP, Iba1, and α-SMA underwent microwave antigen retrieval for 10 minutes (pH6 trisodium citrate buffer). Following antigen retrieval, sections were incubated in blocking solution for 30 minutes, after which they were incubated in the primary antibody (GFAP – 1:200, ab68428; Iba1 – 1:2000, ab178846; SMA 1:1000, ab5694; Abcam, UK) for 24 hours at 4°C. The horseradish peroxidase avidin-biotin complex method (Vectastain Elite kit, Vector Laboratories, UK) was used to visualise antibody binding, with 3,3-diaminobenzidinetetrahydrochloride (DAB) as the chromogen (Vector Laboratories, UK; brown). Sections were then counterstained with haematoxylin, dehydrated, and mounted in DPX. Negative controls (omission of primary antibody) were included with every run. For each animal, all brain sections were inspected manually, and slices with tissue damage or artefacts were excluded to ensure high-quality staining and reliable quantification. Three coronal sections per animal were then selected, evenly spaced along the rostro-caudal axis, and drawn from comparable anatomical levels. Slides were imaged using a Nikon Eclipse E800M microscope at x20 magnification of the section and x40 magnification of two (non-overlapping) regions in the hippocampus and cortex.

For each image, the area coverage of the stain was calculated as the percentage of the total tissue area that showed positive immunoreactivity, representing the spatial extent of marker expression. Resting percentage was also calculated to estimate the relative abundance of resting versus activated cells, i.e., the proportion of cells exhibiting a morphologically resting phenotype as opposed to activated or reactive forms. Images were imported into *Fiji ImageJ* and calibrated using the scale bar. All images were converted to 8-bit greyscale, and a uniform, pre-determined threshold was applied for each stain to ensure consistency across slices. Analysis settings were configured to *Area, Area Function* and *Limit to threshold* to obtain results. For cell-based stains, area coverage of the stain was assessed by calculating the percentage area above threshold. For blood vessel markers, vessel density was quantified as the percentage of area positive for staining. In all cases, analysis was restricted to consistently sized, anatomically matched regions of interest. Images in which the threshold did not reliably detect the relevant structures were

excluded to avoid skewing of the results. Astrocytes and microglia were assessed for reactive versus resting phenotypes based on cellular morphology. Images of slices stained with GFAP and IBA1 were acquired at 40x magnification to resolve cell bodies and processes. Reactive astrocytes were identified by enlarged soma and thickened processes with altered branching patterns. For microglia, reactive cells were characterised by enlarged, more amoeboid somata and retracted or thickened processes. Resting phenotypes exhibited smaller somata with fine, highly ramified processes.

3.3.8 Procedure

Mice were first fitted with a thinned cranial window implant as described above, after which they were given ~1 week recovery time before the implantation of a subcutaneous osmotic minipump containing either angiotensin-II or saline. The experimenter was blinded to the contents of each minipump during surgery. Approximately 5 days after osmotic pump implantation, habituation to the awake imaging apparatus occurred and the first sessions (timepoint 1; T1) of awake imaging took place. Following this, mice underwent the NOR test. In the final week of angiotensin-II infusion, mice underwent the second timepoint of awake imaging (timepoint 2; T2), before undergoing a single terminal session in which mice were anaesthetised and 2D-OIS and electrophysiology were performed simultaneously. At the end of this experiment, mice were killed via cardiac perfusion, and brains were extracted for histology. See Figure 10 below for experimental outline.

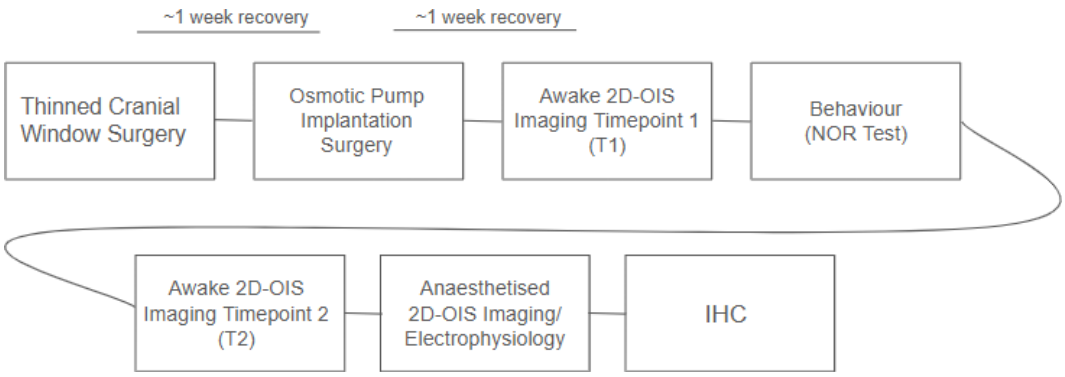

Fig 10. Experimental outline. Diagram shows order in which experiments took place in the current study.

3.3.9 Statistical Analysis

3.3.9.1 HbT responses to sensory stimulation in awake mice

Analysis was conducted on 111 sessions from N = 14 awake mice [n = 8 ang-II treated (4 females, 4 males), n = 6 saline-treated control (2 females, 4 males)]. Linear mixed modelling (LMM) (R version 2024.04.2+764, lme4 package, Bates et al. 2015) was performed to examine the effects of group [ang-II-treated vs control (saline)], sex, and timepoint (T1 vs T2) on haemodynamic responses to sensory stimulation (2s and 16s whisker stimulation) while accounting for animal ID, as each animal contributed multiple sessions to the analysis. The LMM was used to explore 4 metrics of interest: maximum peak of HbT (in response to the stimulation), HbT area under the curve, HbT time to peak, and HbT time to onset. This analysis was conducted on 4 regions of interest (ROIs): artery, whisker barrel cortex (WBC), vein, and parenchyma. Where post-hoc tests were performed, Tukey's method for multiple comparisons was applied. An α-level of 0.05 was considered to be statistically significant.

3.3.9.2 Locomotion

Locomotion was assessed in the animals using walking data from experiment one (30 trials, 2s stim) of each day of awake imaging. An LMM was used to assess the effects of group (ang-II-treated vs control) and sex on cumulative walking distance while accounting for inter-animal variability by including animal ID as a random effect.

3.3.9.3 Low-frequency oscillations in HbT

To assess whether LFOs in cerebral blood volume differ between ang-II-treated mice and saline-treated controls, data from experiments in which the cerebral haemodynamics of ang-II-treated mice and healthy controls recorded with 2D-OIS were analysed. Analysis was conducted on spontaneous sessions to assess low-frequency oscillations (LFOs) in HbT. HbT data from experiment 2 of awake imaging sessions (30 trials, no stimulation) were used to assess LFOs at two time points (T1 vs T2). 56 sessions were included in the analysis from N = 14 mice [n = 8 ang-II treated (4 females, 4 males), n = 6 saline-treated controls (2 females, 4 males)]. Data were imported to MATLAB (R2022a; MathWorks) for analysis. Data were high-pass filtered (0.01 Hz cutoff frequency) to remove low-frequency noise, and a fast Fourier transform (FFT) was performed to obtain the data in the frequency range for analysis (Figure 11). Oscillations within the 0.06 - 0.2 Hz range were summed for each animal, as this is a range typically associated with vasomotion (Aalkjaer & Nilsson, 2005; Stefanovska, 2007). As the strongest response was expected to occur in the arterial region, data analysis was focused on this ROI. An LMM was performed to examine the effects of group (ang-II-treated or saline-treated control), sex, and timepoint (T1 vs T2) on arterial LFO power while accounting for animal ID as a random effect, as each mouse contributed more than one session to the analysis.

a.

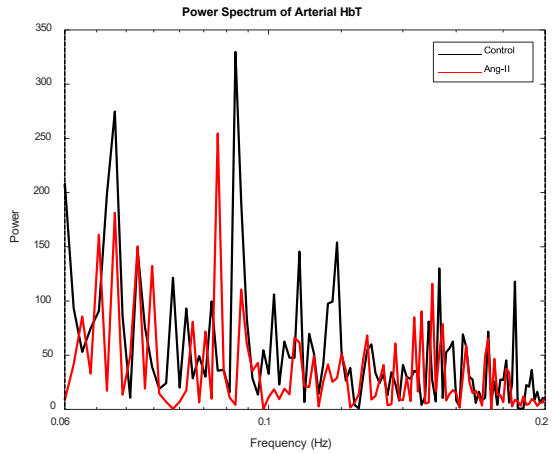

b.

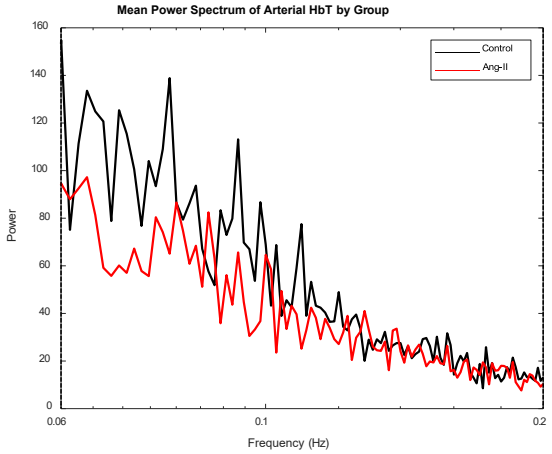

Fig 11. FFT of Arterial HbT. (a) Example FFT from a saline-treated control (indicated in black) and ang-II-treated mouse (indicated in red) in the 0.06 - 0.2 Hz range used for analysis, and (b) mean FFT for each group in the same frequency range.

3.3.9.4 Cognition

The preference index of the mice to the novel object compared to the familiar object was calculated as follows:

$$\text{Preference index (\%)} = (\text{time exploring novel object} / \text{total exploration time}) * 100$$

where the cumulative duration (seconds) spent exploring the novel object is divided by the total exploration time (i.e., the cumulative time spent exploring both the familiar and novel object). A t-test was conducted to assess whether the mean preference index (%) differed between ang-II-treated and saline-treated control mice. All required assumptions for the statistical test were met and an α-level of 0.05 was considered to be statistically significant.

3.3.9.5 MUA

A repeated measures analysis of variance (ANOVA) (R 2024.04.2+764, rstatix package; Kassambara, 2021) was conducted to assess whether group (ang-II-treated vs saline-treated control) or sex had an effect on peak and sum (AUC) of MUA in two inspired gas-breathing conditions [100% oxygen and medical air (21% oxygen)]. The assumptions of normality and homogeneity of variance were assessed using Q–Q plots, and Levene's test, as implemented in the rstatix package (Kassambara, 2021). All required assumptions of the statistical test were met, and an α-level of 0.05 was considered to be statistically significant.

3.3.9.6 IHC

An ANOVA (R 2024.04.2+764, rstatix package; Kassambara, 2021) was performed to assess the effects of group (ang-II-treated vs. saline-treated control) and sex on area coverage of each stain (GFAP, Iba1, and α-SMA). An ANOVA was also performed to assess the effects of group and sex on resting percentage of GFAP and Iba1.

3.4 Results

3.4.1 HbT (Awake Mice)

Analysis was conducted on haemodynamic responses of awake mice to sensory stimulation [2s whisker stimulation (Fig 12a) and 16s whisker stimulation (Fig 12b)] recorded by 2D-OIS. Several metrics of the evoked response were examined: peak HbT in response to stimulation, the area under the curve (AUC) of the HbT response, as well as the time to peak and time to onset of the HbT response.

3.4.1.1 Peak HbT

An LMM revealed a significant main effect of sex on the peak of HbT (b = 0.00201, SE = 0.00294, p = 0.0216) in the artery ROI in response to a 2s whisker stimulation (Figure 13; Table 1). Specifically, male mice exhibited a greater peak of HbT than that observed in female mice. There were no significant effects of treatment group (i.e., ang-II or vehicle), or timepoint (T1 vs T2) observed in response to a 2s whisker stimulation. There were also no significant effects of sex, treatment group, or timepoint on peak arterial HbT in response to a 16s whisker stimulation (Table 2).

In the other ROIs, a significant main effect of sex was also observed on the peak of HbT in response to a 2s whisker stimulation [vein (b = 0.000957, SE = 0.00174, p = 0.0445); WBC (b = 0.00195, SE = 0.00170, p = 0.0166); parenchyma (b = 0.00165, SE = 0.00142, p = 0.00436)], with male mice exhibiting a greater peak of HbT. No other significant effects of group or timepoint were observed on peak HbT in any of the ROIs.

a.

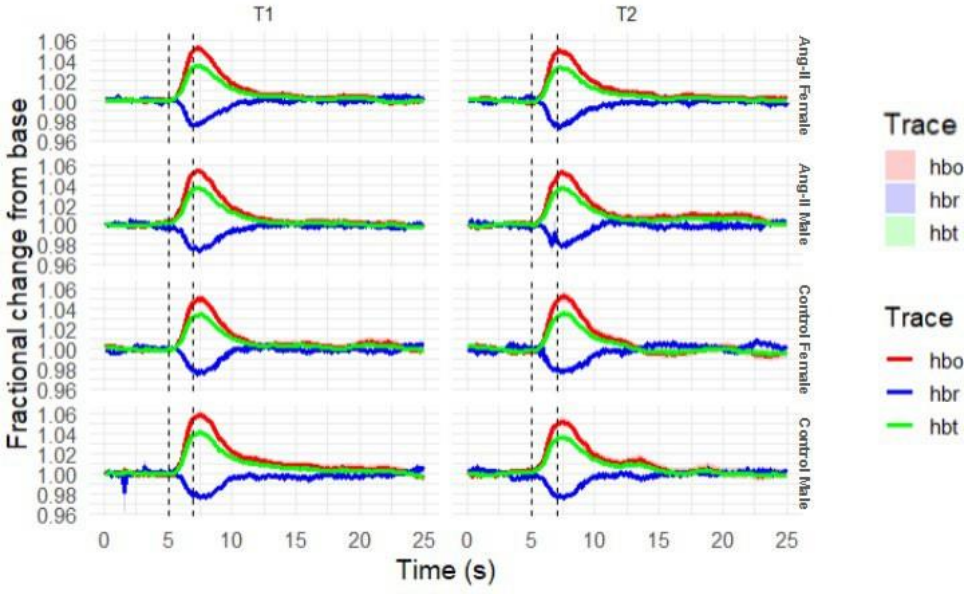

b.

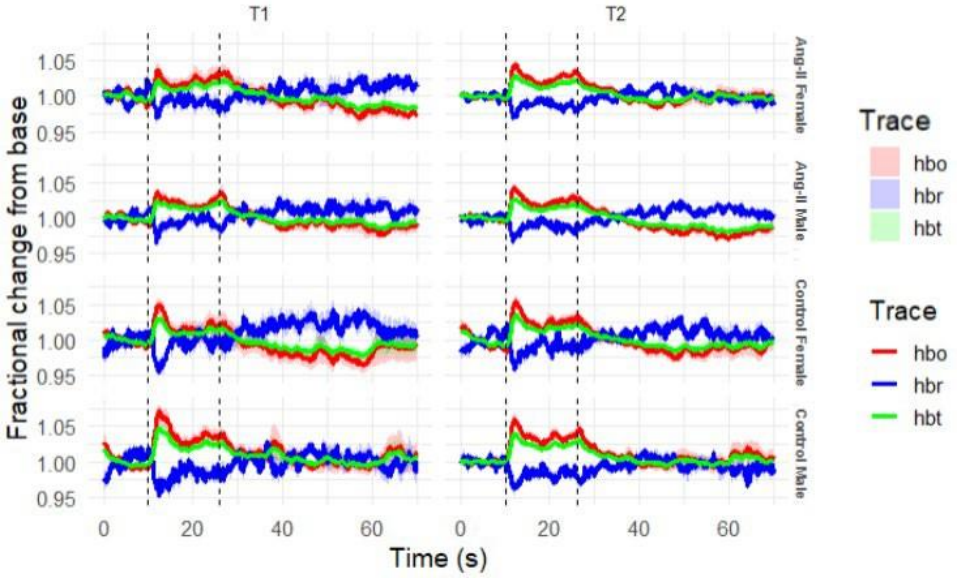

Fig 12. Time series of haemodynamic responses to whisker stimulation. HbT (green), HbO (red), and HbR (blue) responses of ang-II-treated and saline-treated mice are shown in response to (a) a 2s whisker stimulation, and (b) a 16s whisker stimulation in T1 and T2. Dotted lines indicate start and end of stimulation period.

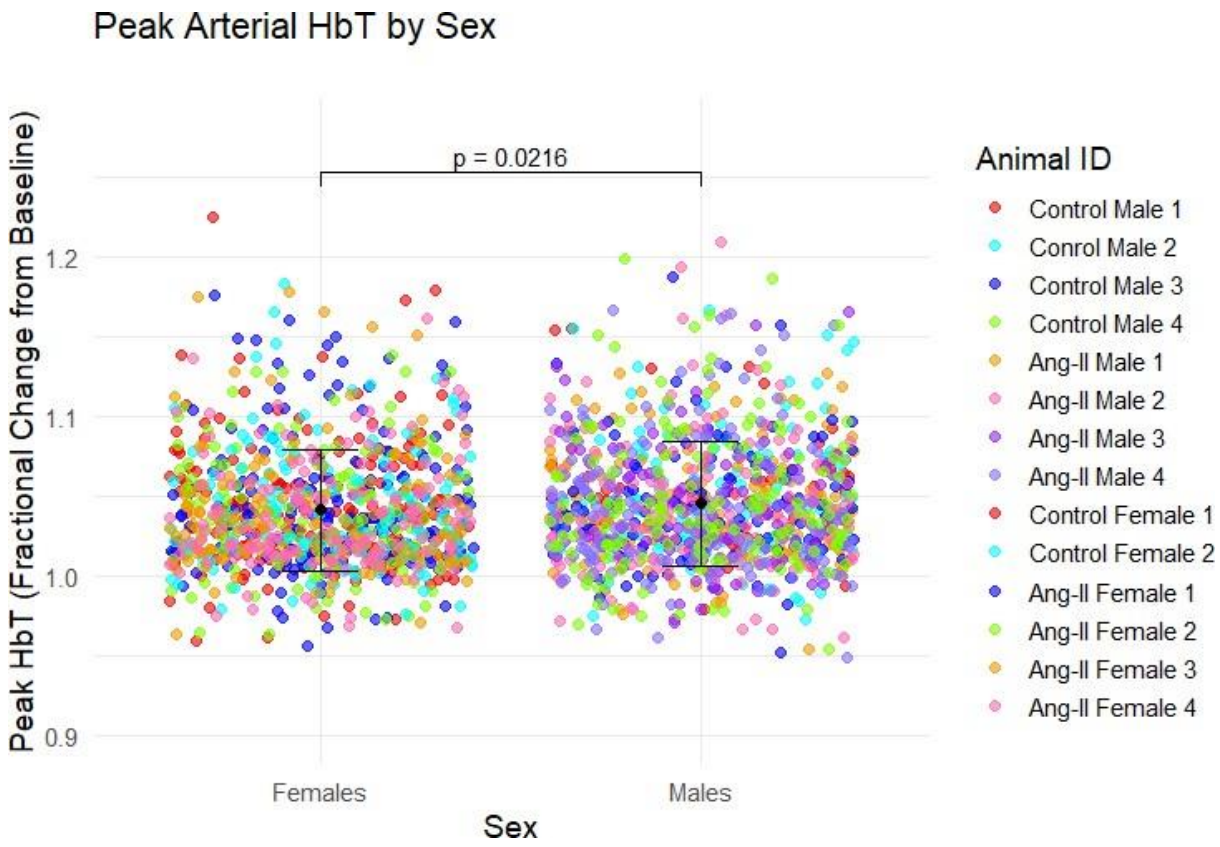

Fig 13. Mean peak of arterial HbT response evoked by 2s whisker stimulation in female and male mice. Data points represent peak HbT in a single session and are labelled by animal ID, with mean ± standard deviation (SD) of each sex displayed.

Table 1 HbT by Region (2s Stim)

	Artery	WBC	Vein	Parenchyma
HbT Peak (Males)	1.05(0.04)	1.03(0.02)	1.03(0.02)	1.02(0.02)
HbT Peak (Females)	1.04(0.04)	1.02(0.02)	1.02(0.02)	1.02(0.02)
HbT AUC (Males)	4.10(0.12)	4.06(0.07)	4.06(0.07)	4.05(0.06)
HbT AUC (Females)	4.09(0.11)	4.05(0.06)	4.05(0.06)	4.04(0.05)

HbT Time to Peak (Males)	2.37(0.97)	2.36(0.96)	2.40(0.99)	2.37(0.98)
HbT Time to Peak (Females)	2.36(0.93)	2.36(0.94)	2.35(0.96)	2.36(0.96)
HbT Time to Onset(Males)	0.76(0.59)	0.72(0.57)	0.70(0.59)	0.67(0.55)
HbT Time to Onset (Females)	0.77(0.60)	0.74(0.57)	0.70(0.56)	0.69(0.56)

Note. Values are mean and SD

Table 2 HbT by Region (16s Stim)

	Artery	WBC	Vein	Parenchyma
HbT Peak (Males)	1.06(0.05)	1.04(0.03)	1.04(0.03)	1.03(0.02)
HbT Peak (Females)	1.06(0.04)	1.04(0.03)	1.04(0.03)	1.03(0.02)
HbT AUC (Males)	20.52(0.58)	20.36(0.40)	20.37(0.40)	20.32(0.34)
HbT AUC (Females)	20.50(0.54)	20.35(0.35)	20.37(0.42)	20.31(0.35)
HbT Time to Peak (Males)	9.87(6.29)	10.66(6.21)	10.86(6.16)	11.12(6.12)
HbT Time to Peak (Females)	10.02(6.28)	10.96(6.14)	11.37(6.18)	11.59(6.16)
HbT Time to Onset (Males)	1.65(2.44)	1.48(2.34)	1.50(2.37)	1.43(2.28)
HbT Time to Onset (Females)	1.85(2.99)	1.94(3.07)	1.62(2.63)	1.64(2.66)

Note. Values are mean and SD

3.4.1.2 Area under the curve of HbT

Analysis revealed a significant main effect of sex on the area under the curve (AUC) of the HbT response in the artery ($b = 0.00793$, $SE = 0.00888$, $p = 0.0427$, Figure 14), WBC ($b = 0.00621$, $SE = 0.00514$, $p = 0.0322$), and parenchyma ($b = 0.00535$, $SE = 0.00431$, $p = 0.0163$) in response to a 2s whisker stimulation. It was revealed that female mice exhibited a smaller AUC response of HbT to sensory stimulation than that of male mice. There were no significant effects of

treatment group (i.e., ang-II vs control), or timepoint (T1 vs T2) observed in response to a 2s whisker stimulation. There were also no significant effects of sex, treatment group, or timepoint on AUC of the arterial HbT response to a 16s whisker stimulation.

Fig 14. Mean AUC of arterial HbT response evoked by 2s whisker stimulation in each session in female and male mice. Data points represent AUC of HbT in a single session and are labelled by animal ID, with mean ± standard deviation (SD) of each sex displayed.

3.4.1.3 Time to peak of HbT

There was a significant main effect of timepoint (T1 vs T2) observed on time to peak of the HbT response in the artery ($b = 0.574$, $SE = 0.948$, $p = 0.00108$) and WBC ($b = 0.400$, $SE = 0.939$, $p = 0.0185$) to a 16s whisker stimulation (Figure 15). Specifically, time to peak was lower at T1 compared to the time to peak in T2 in response to sensory stimulation. There were no significant

effects of sex, treatment group, or timepoint on time to peak of the HbT response to a 2s whisker stimulation in any of the ROIs.

In the parenchyma, there was a significant interaction between sex and timepoint ($b = 0.230$, $SE = 0.112$, $p = 0.0482$), such that there was a significant difference in the time to peak of HbT in female mice between T1 and T2 (Table 3; Figure 16).

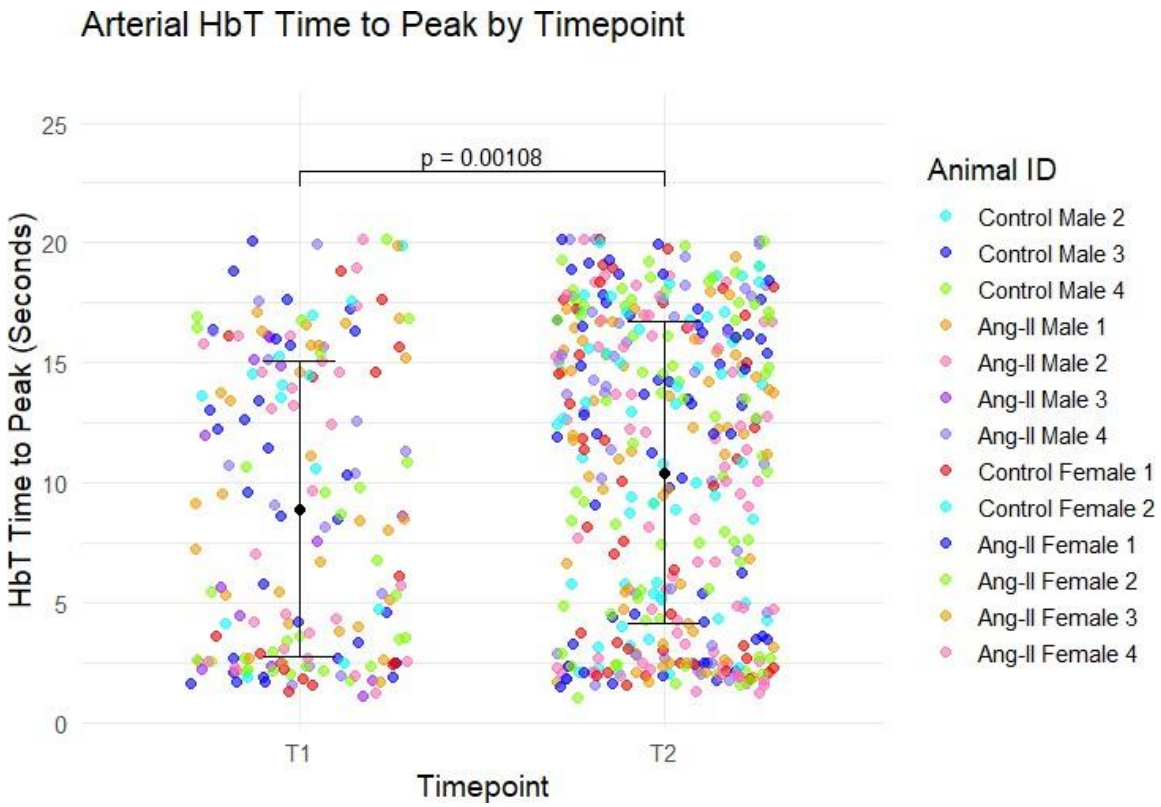

Fig 15. Depicted above is the mean time to peak of HbT response evoked by a 16s whisker stimulation in each session in timepoint 1(T1) and timepoint 2 (T2). Data points are labelled by animal ID, with mean ± standard deviation (SD) of each timepoint provided.

Table 3 Simple Effects Time to Peak of HbT Evoked by 16s Whisker Stimulation (Parenchyma)

	Contrast	estimate	p	t- ratio
T1	Female - Male	0.0745	0.2266	1.234
T2	Female - Male	-0.1106	0.1150	-1.609
Female	T1 - T2	0.126	0.0451*	2.005
Male	T1 - T2	-0.059	0.3390	-0.957

Note. significant terms are denoted with an asterisk.

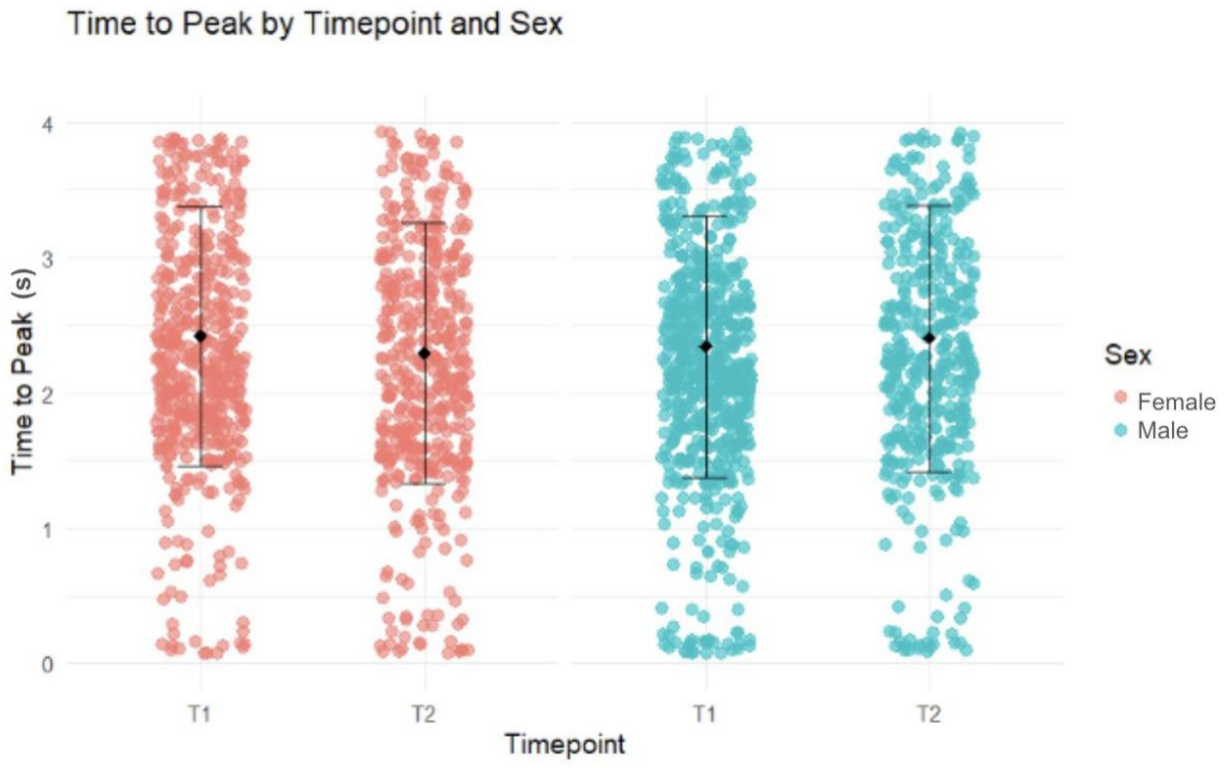

Fig 16. Shown above is the time to peak of HbT in time point 1 (T1) and time point 2 (T2) of female and male mice in the parenchyma ROI. Data points represent the time to peak of HbT in a single session. Data points are labelled by sex, with mean ± standard deviation (SD) of each sex in T1 and T2 provided.

3.4.1.4 Time to onset of HbT

In the WBC, a main effect of sex was observed on the time to onset of the HbT response evoked by a 16s whisker stimulation (b = -0.340, SE = 0.495, p = 0.0279), in that male mice exhibited a lower time to onset of HbT than female mice. In the parenchyma, there was a significant interaction between group and timepoint (b = -0.0788, SE = 0.0755, p = 0.0452), such that the time to onset differed significantly between ang-II treated and control mice at T1 (Table 4), with ang-II-treated mice exhibiting a lower time to onset of HbT in the parenchyma in response to a 2s whisker stimulation (Figure 17). No other significant effects were observed on the time to onset of HbT in any of the other ROIs.

Table 4 Simple Effects Time to Onset of HbT Evoked by a 2s Whisker Stimulation (Parenchyma)

	Contrast	estimate	p	t- ratio
T1	Ang-II - Control	-0.0743	0.0337*	-2.208
T2	Ang-II - Control	0.0337	0.3913	0.864
Ang-II	T1 - T2	-0.0586	0.0674	-1.831
Control	T1 - T2	0.0494	0.2203	1.226

Note. significant terms are denoted with an asterisk.

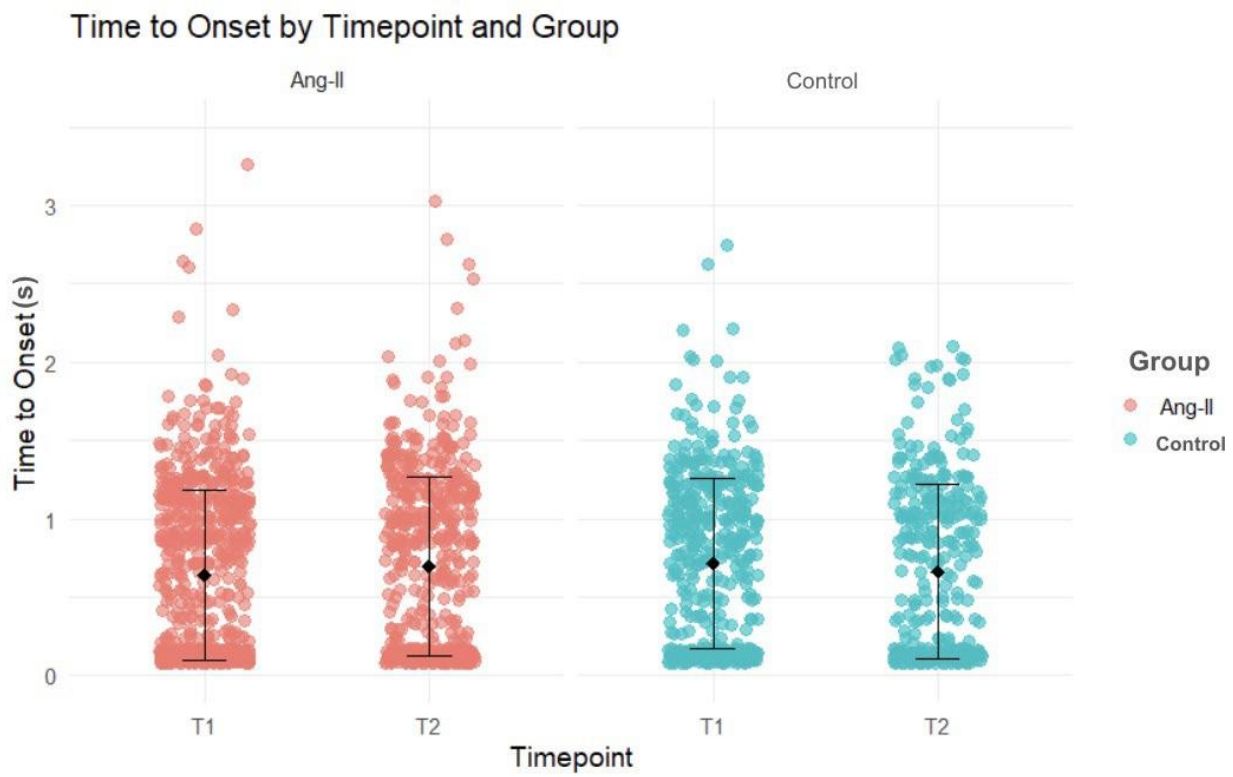

Fig 17. Depicted above is the time to onset of HbT in time point 1(T1) and time point 2 (T2) of ang-II-treated and saline-treated control mice in the parenchyma ROI. Data points represent the time to onset of HbT in a single session. Data points are labelled by treatment group (ang-II vs control), with mean ± standard deviation (SD) of each group in T1 and T2 provided.

3.4.2 Locomotion

As locomotion is known to affect haemodynamic responses (Eyre et al., 2022), potential differences in locomotion between male and female ang-II-treated and control mice were investigated. An LMM assessing the effects of group (ang-II-treated vs control) and sex on cumulative walking distance revealed a significant main effect of sex (b = 3158.26, SE = 1350.69, p = 0.04426). Specifically, it was found that males exhibited higher levels of locomotion than female mice (Figure 18).

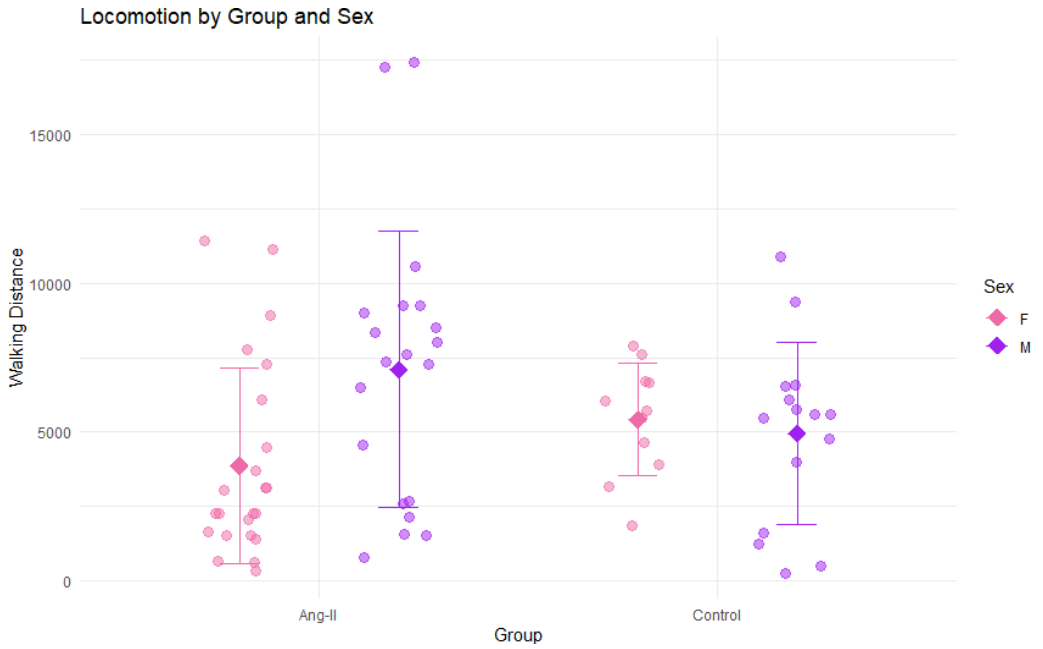

Fig 18. Plot depicts cumulative walking distance of ang-II-treated and control mice from experiment one of each awake imaging day. Data are plotted as cumulative distance walked by an animal in a single session, with mean ± standard deviation (SD) of male and female mice in each group (ang-II-treated vs control).

3.4.3 Low-frequency Oscillations

An LLM was used to explore whether group (ang-II-treated vs saline-treated control), sex, or timepoint (T1 vs T2) had an effect on the power of LFOs in arterial HbT (0.06-0.2 Hz) while controlling for animal ID. The model revealed a significant interaction between group and sex (b =4294, SE = 1768, p = 0.0251). A post-hoc test revealed that male control mice exhibited higher LFO power than male ang-II-treated mice; additionally, male control mice exhibited higher LFO power than female mice (Table 5). No significant main effects of timepoint on LFO power in the artery were observed, as well as no other significant interactions (Figure 19).

Table 5 Simple Effects Group and Sex Interaction on LFO Power

	Contrast	estimate	p	t- ratio
Female	Ang-II - Control	826	0.4698	0.758

Male	Ang-II - Control	-3031	0.0106*	-3.080
Ang-II	Female - Male	133	0.8864	0.147
Control	Female - Male	-3724	0.0094*	-3.219

Note. significant terms are denoted with an asterisk.

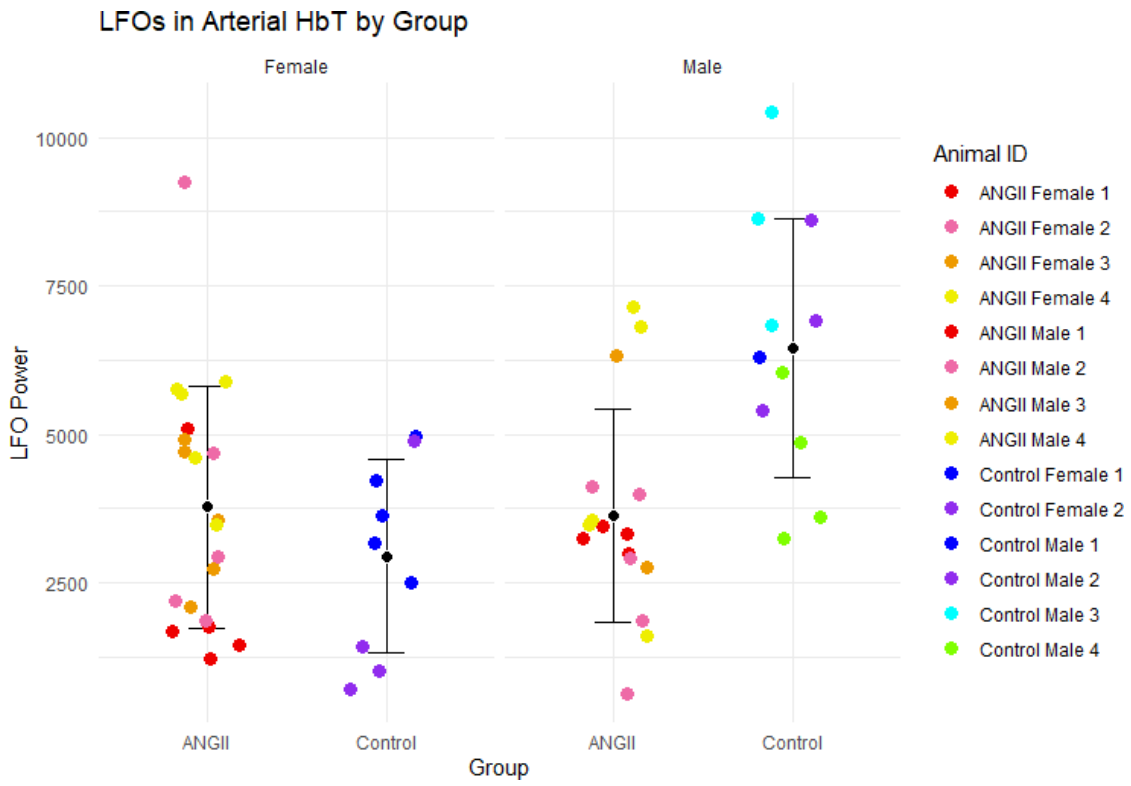

Fig 19. Power of LFOs in HbT by group. LFOs occurring in the arterial region of ang-II (n = 8) and control (n = 6) mice are plotted. Each data point represents the summation of power occurring between 0.06 - 0.2 Hz in a session, with mean ± standard deviation (SD) for each group.

3.4.4 Multi-unit activity

Analysis revealed that there were no significant main effects of group (p = 0.691), sex (p = 0.364), or inspired gas (p = 0.322) on peak MUA in response to a 2s stimulation in the oxygen-breathing condition (Figure 20), as well as no significant interactions. There were also no

significant main effects of group (p = 0.301), sex (p = 0.415), or inspired gas (p = 0.126) on AUC of MUA in response to a 2s stimulation in the air-breathing condition, as well as no significant interactions between group, sex, or inspired gas.

There was also no significant main effect of group (p = 0.890), sex (p = 0.968), or inspired gas (p = 0.359) on peak MUA in response to a 16s whisker stimulation in the oxygen-breathing condition, as well as no significant interactions between group, sex, or inspired gas. Additionally, in the air-breathing condition there was no significant main effect of group (p = 0.533), sex (p = 0.802), or inspired gas (p = 0.918) on AUC of MUA in response to a 16s whisker stimulation, as well as no significant interactions.

a.

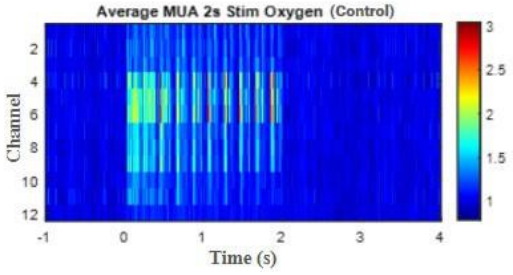

b.

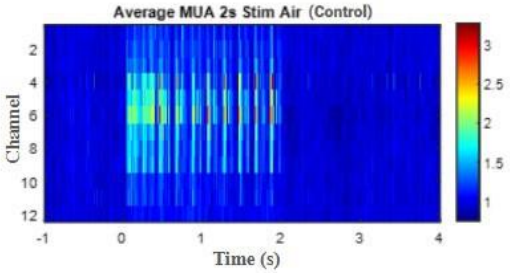

c.

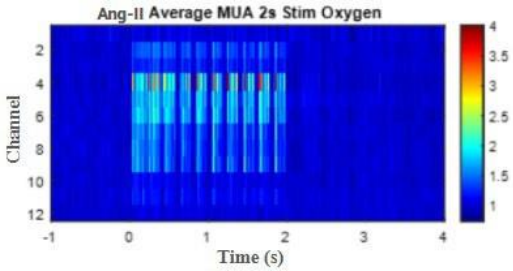

d.

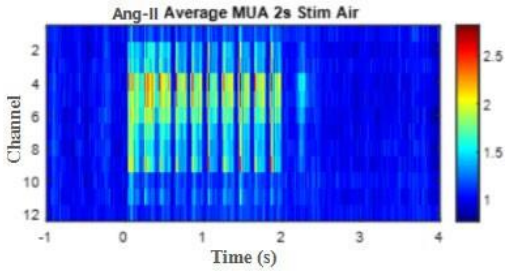

Fig 20. The average MUA response to a 2s mechanical whisker stimulation in saline-treated control mice (*N* = 14; *n* = 7 ang-II, *n* = 7 saline) when (a) inspired gas is 100% oxygen, and (b) when inspired gas is air. MUA responses to a 2s whisker stimulation in ang-II-treated mice are also shown in the (c) oxygen and (d) air-breathing conditions. Colour bar represents fractional change. Whisker stimulation occurs from 0-2s.

3.4.5 Novel Object Recognition Test

To obtain a measure of cognition, the NOR test was used. A t-test on preference index (%) by group (ang-II-treated vs saline-treated control) revealed that there were no significant differences between ang-II-treated mice and controls in terms of their short-term ($p = 0.6713$) and long-term ($p = 0.9325$) memory as determined using the NOR test (Figure 21).

a. b.

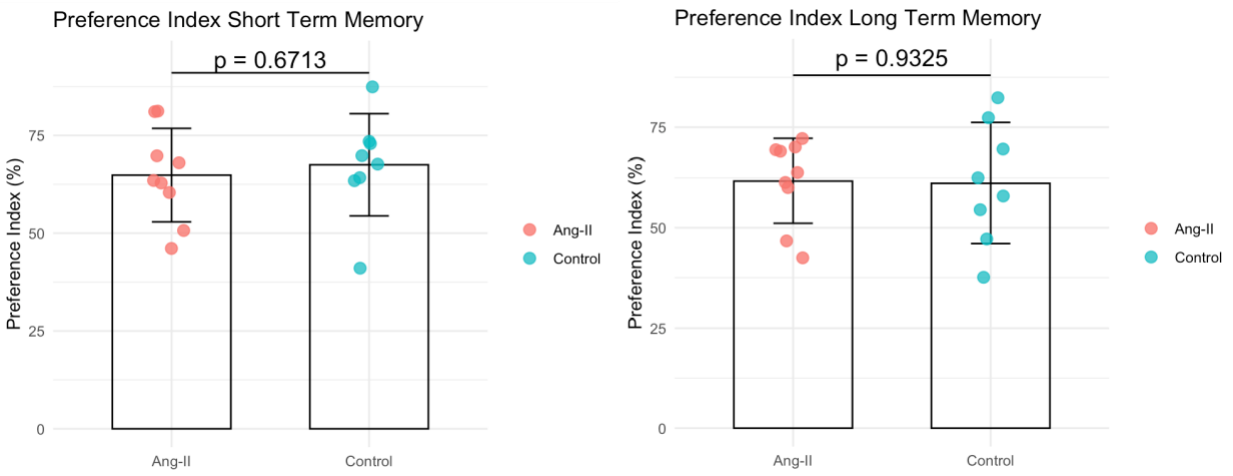

Fig 21. Shown above is the preference index (%) of ang-II-treated mice and saline-treated control mice to a novel object over a familiar one in (a) the short-term memory paradigm and (b) the long-term memory paradigm, with mean ± standard deviation (SD) for each group (ang-II-treated mice and control).

3.4.6 Immunohistochemistry

3.4.6.1 GFAP

GFAP staining was used to assess astrogliosis in the ang-II-treated and saline-treated control mice (Figure 22a, 22b). An ANOVA was used to investigate whether area coverage of GFAP staining or resting percentage differed between groups (ang-II vs control) or sex. Analysis revealed that there were no significant main effects of group [$F=(1,13) = 0.244$, $p = 0.629$, partial $\eta^2 = 0.02$] or sex [$F=(1,13) = 1.828$, $p = 0.199$, partial $\eta^2 = 0.12$] on GFAP area coverage (Figure

22c). There was also no significant interaction of group and sex on GFAP area coverage [F=(1,13) = 0.622, p = 0.444, partial η^2 = 0.05]. Analysis also revealed that there were no significant main effects of group [F=(1,13) = 2.906, p = 0.112, partial η^2 = 0.18] or sex [F=(1,13) = 0.063, p = 0.805, partial η^2 = 0.005] on GFAP resting percentage (Figure 22d), as well as no significant interaction of group and sex [F=(1,13) = 3.718, p = 0.076, partial η^2 = 0.22].

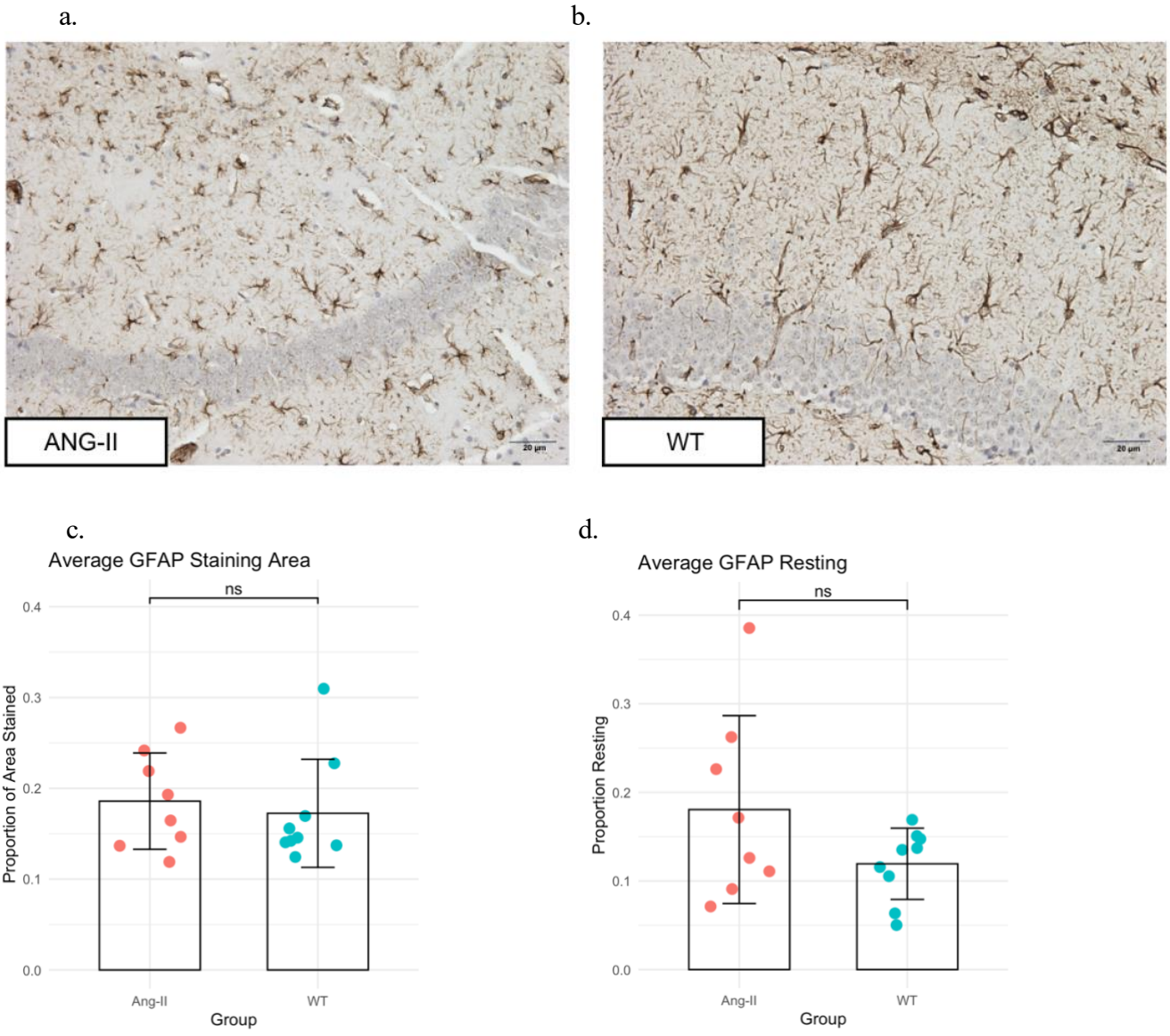

Fig 22. Depicted above is an example of a GFAP stain in an (a) ang-II-treated and (b) saline-treated control mouse coronal hippocampal slice. (c) Area and (d) resting percentage of GFAP are plotted for each group. Individual points represent a single animal with mean ± standard deviation (SD) for each group.

3.4.6.2 IBA1

Iba1 staining was used to assess microglia area coverage and activation in ang-II-treated and saline-treated control mice (Figure 23a, 23b). Analysis revealed that there were no significant main effects of group [$F=(1,14) = 1.106$, $p = 0.311$, partial $\eta^2 = 0.07$] or sex [$F=(1,14) = 0.106$, $p = 0.750$, partial $\eta^2 = 0.007$] on Iba1 area coverage (Figure 23c). There was also no significant interaction of group and sex on Iba1 area coverage [$F=(1,14) = 0.446$, $p = 0.515$, partial $\eta^2 = 0.03$]. Analysis also revealed no significant main effects of group [$F=(1,14) = 1.240$, $p = 0.284$, partial $\eta^2 = 0.08$] or sex [$F=(1,14) = 4.449$, $p = 0.0524$, partial $\eta^2 = 0.24$] (Figure 23d), as well as no significant interaction of group and sex on Iba1 resting percentage [$F=(1,14) = 2.028$, $p = 0.1763$, partial $\eta^2 = 0.13$].

a.

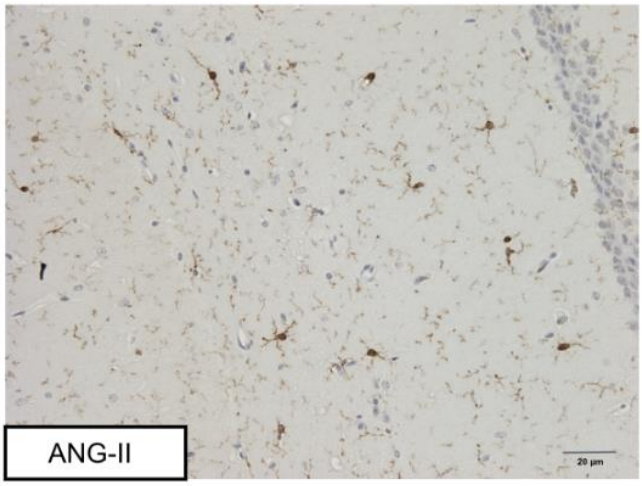

b.

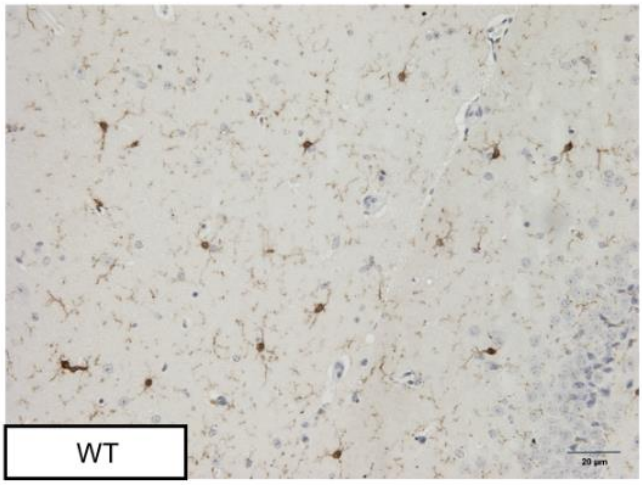

c.

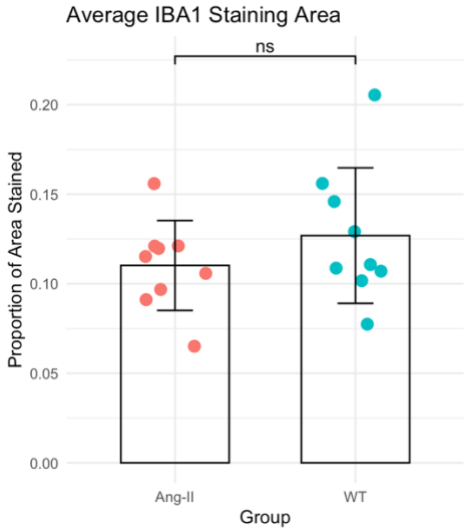

d.

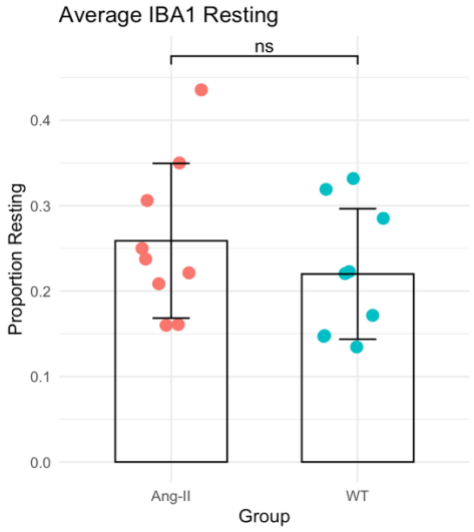

Fig 23. Shown above is an example of an Iba1 stain in an (a) ang-II-treated and (b) saline-treated control mouse coronal hippocampal slice. (c) Area coverage and (d) resting percentage of Iba1 are plotted for each group. Individual points represent a single animal with mean ± standard deviation (SD) for each group.

3.4.6.3 α-SMA

α-SMA staining was used to assess smooth muscle cells in ang-II-treated and saline-treated control mice (Figure 24a, 24b). Analysis revealed that there were no significant main effects of group [$F=(1,11) = 0.486$, $p = 0.500$, partial $\eta^2 = 0.04$] or sex [$F=(1,11) = 1.689$, $p = 0.220$, partial $\eta^2 = 0.13$] on α-SMA area coverage (Figure 24c). There was also no significant interaction of group and sex on α-SMA area coverage [$F=(1,11) = 0.331$, $p = 0.576$, partial $\eta^2 = 0.03$].

a.

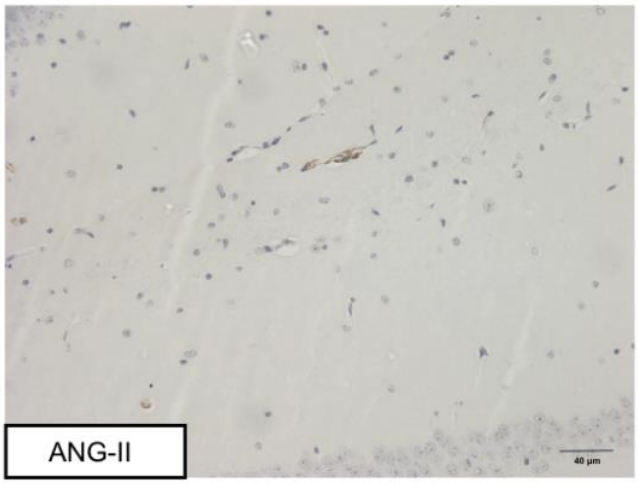
ANG-II

b.

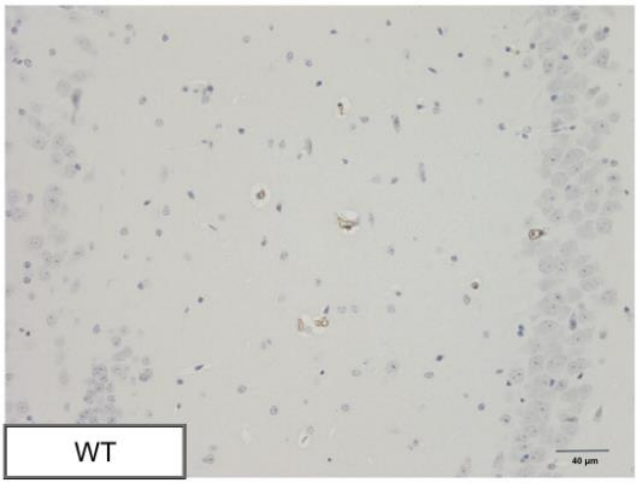
WT

c.

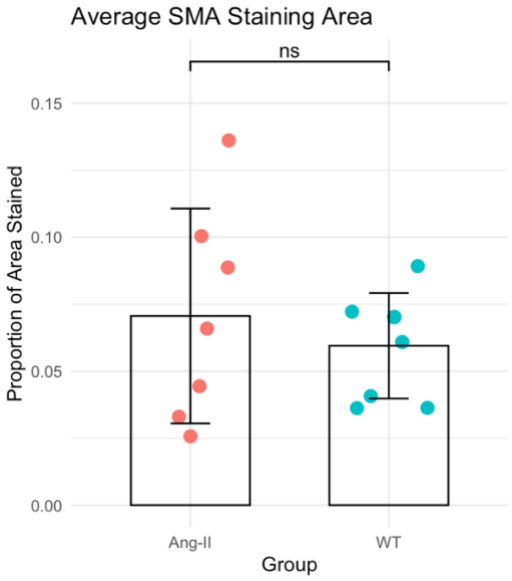
Average SMA Staining Area
ns
0.15
0.10
0.05
0.00
Proportion of Area Stained
Ang-II
WT
Group

Fig 24. Depicted above is an example of an α-SMA stain in an (a) ang-II-treated and (b) saline-treated control mouse coronal hippocampal slice. (c) Area coverage of α-SMA is plotted for each group. Individual points represent a single animal with mean ± standard deviation (SD) for each group.

3.5 Discussion

The aim of the current study was to assess the effects of a chronic ang-II-induced increase in blood pressure on brain vascular function. Sensory-evoked haemodynamic responses were assessed in awake ang-II-treated and control male and female mice, in addition to assessments of cognition, MUA, and histology. While overall haemodynamic responses typically did not differ significantly between ang-II-treated and control mice in the current study, we observed a notable difference in the time to onset of HbT responses to a 2s whisker stimulation in ang-II-treated mice compared to controls at early timepoints. The time to onset of the HbT response in the parenchyma ROI differed significantly between ang-II-treated mice and saline-treated controls at timepoint 1 of awake imaging (approximately days 5-8 of ang-II infusion), such that ang-II-treated mice exhibited a shorter time to onset of the evoked haemodynamic response than observed in controls. However, this effect was not observed in sessions in which a 16s stimulation occurred, or within the other ROIs (i.e., WBC, artery, vein). Further, no significant differences were observed between ang-II-treated mice and controls in terms of the peak or magnitude of MUA responses to whisker stimulation, suggesting intact NVC. Contrary to studies reporting attenuated haemodynamic responses in ang-II-treated mice (Boily et al., 2021; Capone et al., 2011; Kazama et al., 2003), the current study found limited treatment-dependent effects on HbT responses to mechanical whisker stimulation. Interestingly, using a dosage of ang-II similar to that of the current study (500ng/kg/min) Wiesmann et al. 2017, found decreased functional connectivity between several brain regions in ang-II-treated WT C57BL/6J mice, however, HTN-induced impairments in CBF were only observed in ang-II-treated APP-PSI mice (Wiesmann et al., 2017). However, attenuated CBF responses induced by whisker stimulation in ang-II-treated (600 ng/kg/min) C57BL/6L mice were observed by Capone et al., 2011, an effect that was observed before the elevation of arterial pressure as well as after HTN subsided (Capone et al., 2011).

The current study also found that sex emerged as a key variable influencing haemodynamic measures across groups. A significant main effect of sex was observed in the majority of parameters investigated in each ROI, suggesting a sex-dependent difference in the evoked haemodynamic responses of awake mice. Sex was found to significantly affect peak HbT response in all investigated ROIs, with female mice exhibiting a lower peak of HbT to a 2s whisker stimulation than that of male mice, regardless of treatment group. Additionally, sex was found to have a significant effect on the magnitude of the HbT response in the artery, WBC, and parenchyma ROIs, in that female mice exhibited a smaller AUC of the HbT response to a 2s whisker stimulation than that observed in male mice. Sex was also found to significantly affect the time to onset of the HbT response in the WBC following a 16s whisker stimulation, in that male mice exhibited a lower time to onset of HbT than female mice. A significant effect of timepoint on time to peak of the HbT response was also observed in the artery and WBC, in that time to peak of HbT was lower in T1 compared to T2 in response to a 16s whisker stimulation. There was also a significant interaction between sex and time point on the time to peak of the HbT response in the parenchyma. Female mice differed significantly in the time to peak of their HbT response in T1 compared to T2, specifically, the time to peak of this response was found to decrease from T1 to T2. Lastly, there was a significant effect of timepoint on time to peak of HbT in the artery and WBC, such that time to peak was lower in T1 compared to T2. Overall, while some impacts of timepoint were observed, the aforementioned findings suggest that cerebral haemodynamic responses as measured in the current study were primarily influenced by sex rather than treatment alone.

Interestingly, it was revealed that there were differences in locomotion, such that male mice were found to exhibit higher levels of locomotion during 2s whisker stimulation experiments than female mice during the awake imaging sessions. Locomotion has been found to alter the amplitude of evoked haemodynamic responses in awake mice (Eyre et al., 2022), thus, it could be possible that in the current study differential locomotor activity between male and female mice may partially contribute to the observed sex-dependent differences in haemodynamic responses. Further, others have reported that volitional whisker and body movements can enhance CBV in awake mice (Huo et al., 2014; Winder et al., 2017).

As vasomotion has been postulated to undergo changes in response to increases in blood

pressure, arterial LFOs were assessed. It was revealed that there was a significant interaction between group and sex on LFO power in the artery, in that male saline-treated control mice exhibited higher LFO power than ang-II-treated male mice, and further, male control mice were found to exhibit higher LFO power than female control mice. This effect was found to remain consistent over time, as there was no significant difference seen in LFO power between each group and sex from T1 to T2 of awake imaging. The finding of lower LFO power in ang-II-treated males compared to male controls aligns with studies that have observed alterations in vasomotion in hypertensive animal models (de Wit et al., 2003; Lefer et al., 1990; Liu et al., 2017). However, rather than enhancement of LFOs in HTN as reported by Lefer et al., 1990, the current study found LFO power to be lower in ang-II-treated males, aligning with the findings of Liu et al., 2017, who reported impaired vasomotion in spontaneously hypertensive rats (Liu et al., 2017). As lower LFO power in ang-II-treated males compared to controls was observed in the absence of major changes in NVC in the current study, these findings suggest that LFO deficits may represent an early pathophysiological event in HTN, occurring prior to overt changes in neurovascular coupling. In humans, some alterations in vasomotion have also been observed as a result of HTN. A study by Hollenberg & Sandor found significantly increased normalised power of vasomotion in patients with primary HTN, but found no significant differences in the frequency or cycle length of the oscillation between hypertensive and normotensive patients (Hollenberg & Sandor, 1984). The current study also found that male mice exhibited higher LFO power than female mice. As locomotion was found to differ between sexes in the current study, and it is known that locomotion affects haemodynamic responses (Eyre et al., 2022), it may be possible that locomotor behaviour contributed, at least partially, to the differences seen in LFOs in addition to haemodynamic responses. A study by Ahmadi et al., (2020), reported that a period of exercise was found to improve endothelial function of coronary arteries and thereby vascular vasomotion function (Ahmadi et al., 2020). Thus, while the current study cannot say for certain why LFO power was lower in female mice, differences in walking behaviour could possibly be a contributing factor. Further studies are needed to better characterise vasomotion in HTN as well as to examine potential differences in this process between sexes. As vasomotion may aid in the clearance of Aβ from the brain (Aldea et al., 2019; van Veluw et al., 2020), and HTN is one of the leading risk factors for AD, a better understanding of this process in the hypertensive state could be beneficial in finding therapeutic

targets for the prevention of AD.

The current study revealed that ang-II-treated mice and controls did not differ significantly in terms of their short-term or long-term memory, as determined by the NOR test; aligning with studies finding no difference in ang-II hypertensive mice and healthy mice in terms of cognitive performance (Cifuentes et al., 2015; Wiesmann et al., 2017). The negative findings in terms of changes in cognition might be related to the age of the mice in the current study, as some studies have found learning (Toth et al., 2013) and spatial memory (Csiszar et al., 2013) deficits in aged (24 month old) but not young (3 month old) mice after 4 weeks of angiotensin-II infusion. However, conversely, Duchemin et al. (2013) have found learning and spatial memory impairments in young (eight-week-old) mice after 21 days of angiotensin-II infusion at a rate of 1900 ng/kg/min (Duchemin et al., 2013). Although, this dosage of angiotensin-II was significantly higher than that used in the aforementioned studies (1000 ng/kg/min), as well as that used in the current study. Thus, another avenue for future research could be to further explore the effects of aging on HTN-related changes, as age may play a role in the development of HTN-mediated cognitive impairment; several studies have shown that mid-life HTN and elevated mid-life systolic blood pressure were associated with cognitive decline (Gottesman et al., 2014; Launer et al., 1995).

Contrary to previous studies, the current study also did not observe any significant differences at the cellular level between ang-II-treated mice and controls in terms of glial and vascular cells. This aligns with the findings of Milner et al. 2022, that found no differences in GFAP or Iba-1 in the middle prefrontal cortex of ang-II-treated mice, regardless of sex. However, in ang-II-treated male mice, an increase in the density of GFAP was observed in the subgranular hilus and a decrease in the density of Iba-1 in the CA1 region (Milner et al., 2022). In female ang-II-treated mice, an increase in the density of Iba-1 was observed in the dentate gyrus and the CA2/3a region (Milner et al., 2022). These results suggest sex and region-specific differences in glial activation as a result of ang-II treatment, and reveals the hippocampus as a particularly vulnerable brain region to ang-II treatment. In the current study, there were no significant differences in GFAP, Iba1, and SMA staining observed between groups or across sexes in the hippocampus or cortex.

While the current study did not observe significant differences in the markers associated with gliosis, inflammation, and vascular alterations that have been reported in ang-II treated mice after 4 weeks (Meissner et al., 2017), there does appear to be some inconsistency in the literature regarding detectable changes in these markers. Iulita et al., 2018, reported that after 14 days of infusion of a subpressor dose of ang-II (200 ng/kg/min), increased Iba-1 levels were observed but not an increase in GFAP (Iulita et al., 2018). Further, a study by Wiesmann et al., 2016, using a 500ng/kg/min dose of ang-II found no significant differences in the amount of activated microglia in mice as determined using Iba-1 staining (Wiesmann et al., 2017). Similarly, Cifuentes et al., 2014, also found no significant difference between ang-II-treated hypertensive mice (1000ng/kg/min) and control mice in terms of microglia activation (Iba-1) after 2.5 months of infusion (Cifuentes et al., 2015). However, in APP mice and ang-II-treated APP mice, higher levels of activated microglia were found, suggesting that microglia activation may be stimulated by the presence of Aβ, regardless of ang-II-induced HTN, as differences in microglia activation were not seen between ang-II-treated vs control mice (Cifuentes et al., 2015). Interestingly, Toth et al., 2013, found no significant hypertension-induced changes in microglia activation in young (3-month-old) ang-II treated mice (1000 ng/kg/min), but found an increase in microglia activation in aged ang-II treated mice (24-month-old) (Toth et al., 2013). Therefore, age may also play a role in levels of neuroinflammation in response to ang-II-induced HTN, possibly due to an impairment in the ability of the cerebral arteries of aged mice to functionally adapt to high levels of pressure, leading to disrupted autoregulation, BBB dysfunction, and neuroinflammation (Toth et al., 2013). As mice in the current study ranged from 6-8 months of age, it may be possible that clearer differences in some of the markers would have emerged at an older age. While differences in traditional markers of HTN-induced inflammatory and vascular changes were not consistently observed in the current study, early haemodynamic changes may point to potential sub-threshold alterations.

It may be possible that some effects were not detected due to limited statistical power when analysing subgroups by sex, therefore subtle changes may exist below the threshold of detection in the current design. Sex-specific physiological factors may also obscure typical ang-II effects. It is known that ang-II differentially affects female and male rodents and humans (Costa et al., 2016; Girouard et al., 2008; Sampson et al., 2008; Toering et al., 2015; Xue et al., 2005), with

males exhibiting greater sensitivity to the cardiovascular effects of ang-II. While the renin-angiotensin-aldosterone system (RAAS) intrinsically regulates cardiovascular function and blood pressure in both sexes, a shift in this system towards cardioprotective pathways is observed in females between puberty and menopause through modulation of vasodilator and vasoconstrictor pathways by sex hormones such as oestrogen (Colafella & Denton, 2018). The lack of confirmatory blood pressure data may also be a limitation of the current study. Ang-II-infusion is associated with a pressor response that is dependent on both the dose and length of time of infusion (Gomolak & Didion, 2014). Therefore, the timing of the assessments may not fully capture the full disease course. However, it has been reported that while lower doses of ang-II such as 200 ng/kg/min result in an increase in systolic pressure beginning at day 14 of infusion, a dose of 400 ng/kg/min was found to increase systolic pressure by day 7 (Gomolak & Didion, 2014), which would fall during timepoint 1 of imaging in the current study. Although, Capone et al. (2011), found no elevation in arterial pressure with a dose of 200 ng/kg/min, and an increase in arterial pressure by day 9 in C57BL/6 mice using a dose of 600 ng/kg/min (Capone et al., 2011), as used in the current study. As conflicting evidence exists regarding dose-specific timings of ang-II infusion on arterial pressure, measurements taken at the time of imaging experiments would aid in the interpretation and contextualisation of the current results. Future work may also benefit from additional markers to better characterise endothelial and inflammatory changes, for instance, assessing VCAM-1, ICAM-1, TNF-α or IL-1 using immunohistochemistry or transcriptomics. Comparing ang-II-induced effects with other hypertension models (e.g., DOCA-salt or genetically hypertensive mice such as BPH/2) could also help clarify if the modest changes observed here are model-specific and could additionally help further elucidate the effects of hypertension on brain vascular function.

3.5.1 Conclusion

In the current study we examined the effects of ang-II infusion on cerebrovascular function, low-frequency vascular oscillations, cognition, MUA, and glial/vascular cells. While ang-II is widely used to model HTN in rodents, our findings suggest that its effects may be more nuanced, particularly when examining early functional outcomes in the brain. Some treatment-specific effects were observed in the current study, notably, a shorter time to onset of the HbT response

to a 2s whisker stimulation was observed in ang-II-treated mice at an earlier imaging timepoint. Also, LFO power was found to be lower in ang-II-treated males compared to healthy male controls. These findings suggest that early or subtle cerebrovascular changes may precede overt changes in NVC responses, cognition, or widespread structural or inflammatory changes, in addition to suggesting important sex differences. Indeed, sex had significant effects on haemodynamic responses, LFOs, and locomotion in the current study, in that female mice exhibited lower peak and magnitude of HbT responses to stimulation, lower LFO power than male controls, and exhibited less locomotion during awake imaging sessions than male mice. These results could suggest that differential locomotor activity may have partially contributed to the observed sex-dependent haemodynamic differences. Therefore, our results highlight the importance of considering sex as a biological variable in preclinical HTN research, as the findings of the current study support the growing recognition that sex plays a critical role in the pathophysiological profile induced by ang-II.

3.6 References

Aldea, R., Weller, R. O., Wilcock, D. M., Carare, R. O., & Richardson, G. (2019). Cerebrovascular smooth muscle cells as the drivers of intramural periarterial drainage of the brain [Article]. *Frontiers in Aging Neuroscience*, *11*(JAN), Article 1. https://doi.org/10.3389/fnagi.2019.00001

Ameen-Ali KE, Simpson JE, Wharton SB, et al. The Time Course of Recognition Memory Impairment and Glial Pathology in the hAPP-J20 Mouse Model of Alzheimer's Disease (2019). *Journal of Alzheimer's Disease*, 68(2), 609-624. https://doi/10.3233/JAD-181238

Antonios, T. F., Singer, D. R., Markandu, N. D., Mortimer, P. S., & MacGregor, G. A. (1999). Structural skin capillary rarefaction in essential hypertension. *Hypertension*, *33*(4), 998-1001. https://doi.org/10.1161/01.hyp.33.4.998

Ahmadi, A., Roshan, V.D., Jalali, A. (2020). Coronary vasomotion and exercise-induced adaptations in coronary artery disease patients: A systematic review and meta-analysis. *J Res Med Sci*., 25:76. https://doi.org/10.4103/jrms.JRMS_580_18.

Bertuglia, S., Colantuoni, A., Coppini, G., & Intaglietta, M. (1991). Hypoxia- or hyperoxia-induced changes in arteriolar vasomotion in skeletal muscle microcirculation. *Am J Physiol*, *260*(2 Pt 2), H362-372. https://doi.org/10.1152/ajpheart.1991.260.2.H362

Boily, M., Li, L., Vallerand, D., & Girouard, H. (2021). Angiotensin II Disrupts Neurovascular Coupling by Potentiating Calcium Increases in Astrocytic Endfeet. *J Am Heart Assoc*, *10*(17), e020608. https://doi.org/10.1161/jaha.120.020608

Bruno, R. M., Masi, S., Taddei, M., Taddei, S., & Virdis, A. (2018). Essential Hypertension and Functional Microvascular Ageing. *High Blood Pressure & Cardiovascular Prevention*, *25*(1), 35-40. https://doi.org/10.1007/s40292-017-0245-9

Capone, C., Faraco, G., Park, L., Cao, X., Davisson, R. L., & Iadecola, C. (2011). The cerebrovascular dysfunction induced by slow pressor doses of angiotensin II precedes the development of hypertension. *Am J Physiol Heart Circ Physiol*, *300*(1), H397-407. https://doi.org/10.1152/ajpheart.00679.2010

Cifuentes, D., Poittevin, M., Dere, E., Broqueres-You, D., Bonnin, P., Benessiano, J., Pocard, M., Mariani, J., Kubis, N., Merkulova-Rainon, T., & Levy, B. I. (2015). Hypertension accelerates the progression of Alzheimer-like pathology in a mouse model of the disease. *Hypertension*, *65*(1), 218-224. https://doi.org/10.1161/HYPERTENSIONAHA.114.04139

Colafella, K. M. M., & Denton, K. M. (2018). Sex-specific differences in hypertension and associated cardiovascular disease. *Nature Reviews Nephrology*, *14*(3), 185-201. https://doi.org/10.1038/nrneph.2017.189

Colantuoni, A., Bertuglia, S., & Marchiafava, P. L. (2001). Phentolamine suppresses the increase in arteriolar vasomotion frequency due to systemic hypoxia in hamster skeletal muscle microcirculation. *Autonomic Neuroscience*, *90*(1), 148-151. https://doi.org/https://doi.org/10.1016/S1566-0702(01)00281-8

Costa, G., Garabito, M., Jiménez-Altayó, F., Onetti, Y., Sabate, M., Vila, E., & Dantas, A. P. (2016). Sex differences in angiotensin II responses contribute to a differential regulation of cox-mediated vascular dysfunction during aging. *Experimental Gerontology*, *85*, 71-80. https://doi.org/https://doi.org/10.1016/j.exger.2016.09.020

de Wit, C., Roos, F., Bolz, S.-S., & Pohl, U. (2003). Lack of vascular connexin 40 is associated with hypertension and irregular arteriolar vasomotion. *Physiological Genomics*, *13*(2), 169-177. https://doi.org/10.1152/physiolgenomics.00169.2002

Eyre, B., Shaw, K., Sharp, P., Boorman, L., Lee, L., Shabir, O., Berwick, J., & Howarth, C. (2022). The effects of locomotion on sensory-evoked haemodynamic responses in the cortex of awake mice. *Sci Rep*, *12*(1), 6236. https://doi.org/10.1038/s41598-022-10195-y

Fujii, K., Heistad, D. D., & Faraci, F. M. (1990). Vasomotion of basilar arteries in vivo. *American Journal of Physiology-Heart and Circulatory Physiology*, *258*(6), H1829-H1834. https://doi.org/10.1152/ajpheart.1990.258.6.H1829

Girouard, H., & Iadecola, C. (2006). Neurovascular coupling in the normal brain and in hypertension, stroke, and Alzheimer disease. *Journal of Applied Physiology*, *100*(1), 328-335. https://doi.org/10.1152/japplphysiol.00966.2005

Girouard, H., Lessard, A., Capone, C., Milner, T. A., & Iadecola, C. (2008). The neurovascular dysfunction induced by angiotensin II in the mouse neocortex is sexually dimorphic. *Am J Physiol Heart Circ Physiol*, *294*(1), H156-163. https://doi.org/10.1152/ajpheart.01137.2007

Gomolak, J. R., & Didion, S. P. (2014). Angiotensin II-induced endothelial dysfunction is temporally linked with increases in interleukin-6 and vascular macrophage accumulation. *Front Physiol*, *5*, 396. https://doi.org/10.3389/fphys.2014.00396

Gottesman, R. F., Schneider, A. L., Albert, M., Alonso, A., Bandeen-Roche, K., Coker, L., Coresh, J., Knopman, D., Power, M. C., Rawlings, A., Sharrett, A. R., Wruck, L. M., & Mosley, T. H. (2014). Midlife hypertension and 20-year cognitive change: the atherosclerosis risk in communities neurocognitive study. *JAMA Neurol*, *71*(10), 1218-1227. https://doi.org/10.1001/jamaneurol.2014.1646

Hock, C., Villringer, K., Müller-Spahn, F., Wenzel, R., Heekeren, H., Schuh-Hofer, S., Hofmann, M., Minoshima, S., Schwaiger, M., Dirnagl, U., & Villringer, A. (1997). Decrease in parietal cerebral hemoglobin oxygenation during performance of a verbal fluency task in patients with Alzheimer's disease monitored by means of near-infrared spectroscopy (NIRS) — correlation with simultaneous rCBF-PET measurements. *Brain Research*, *755*(2), 293-303. https://doi.org/https://doi.org/10.1016/S0006-8993(97)00122-4

Hollenberg, N. K., & Sandor, T. (1984). Vasomotion of renal blood flow in essential hypertension. Oscillations in xenon transit. *Hypertension*, *6*(4), 579-585. https://doi.org/10.1161/01.hyp.6.4.579

Huo, B.X., Smith, J.B., Drew, P.J. (2014). Neurovascular coupling and decoupling in the cortex during voluntary locomotion. J. Neurosci., 34, 10975–10981. https://doi.org/10.1523/JNEUROSCI.1369-14.2014.

Iadecola, C. (2010). The overlap between neurodegenerative and vascular factors in the pathogenesis of dementia. *Acta Neuropathol*, *120*(3), 287-296. https://doi.org/10.1007/s00401-010-0718-6

Intengan, H. D., & Schiffrin, E. L. (2001). Vascular Remodeling in Hypertension. *Hypertension*, *38*(3), 581-587. https://doi.org/doi:10.1161/hy09t1.096249

Iulita, M. F., Vallerand, D., Beauvillier, M., Haupert, N., C, A. U., Gagné, A., Vernoux, N., Duchemin, S., Boily, M., Tremblay, M., & Girouard, H. (2018). Differential effect of angiotensin II and blood pressure on hippocampal inflammation in mice. *J Neuroinflammation*, *15*(1), 62. https://doi.org/10.1186/s12974-018-1090-z

Jennings, J. R., Muldoon, M. F., Ryan, C., Price, J. C., Greer, P., Sutton-Tyrrell, K., van der Veen, F. M., & Meltzer, C. C. (2005). Reduced cerebral blood flow response and compensation among patients with untreated hypertension. *Neurology*, *64*(8), 1358-1365. https://doi.org/doi:10.1212/01.WNL.0000158283.28251.3C

Kazama, K., Wang, G., Frys, K., Anrather, J., & Iadecola, C. (2003). Angiotensin II attenuates functional hyperemia in the mouse somatosensory cortex. *Am J Physiol Heart Circ Physiol*, *285*(5), H1890-1899. https://doi.org/10.1152/ajpheart.00464.2003

Langford, D.J., Bailey, A.L., Chanda, M.L., Clarke, S.E., Drummond, T.E., Echols, S., Glick, S., Ingrao, J., Klassen-Ross, T., Lacroix-Fralish, M.L., Matsumiya, L., Sorge, R.E., Sotocinal, S.G., Tabaka, J.M., Wong, D., van den Maagdenberg, A.M., Ferrari, M.D., Craig, K.D., Mogil, J.S. (2010). Coding of facial expressions of pain in the laboratory mouse. *Nat Methods,* 7(6), 447-449. https://doi.org/10.1038/nmeth.1455. Epub 2010 May 9. PMID: 20453868.

Launer, L. J., Masaki, K., Petrovitch, H., Foley, D., & Havlik, R. J. (1995). The association between midlife blood pressure levels and late-life cognitive function. The Honolulu-Asia Aging Study. *Jama*, *274*(23), 1846-1851.

Laurent, S., & Boutouyrie, P. (2020). Arterial Stiffness and Hypertension in the Elderly [Review]. *Frontiers in Cardiovascular Medicine*, *Volume 7 - 2020*. https://doi.org/10.3389/fcvm.2020.544302

Lefer, D. J., Lynch, C. D., Lapinski, K. C., & Hutchins, P. M. (1990). Enhanced vasomotion of cerebral arterioles in spontaneously hypertensive rats. *Microvasc Res*, *39*(2), 129-139. https://doi.org/10.1016/0026-2862(90)90065-y

Liu, M., Zhang, X., Wang, B., Wu, Q., Li, B., Li, A., Zhang, H., & Xiu, R. (2017). Functional status of microvascular vasomotion is impaired in spontaneously hypertensive rat. *Sci Rep*, *7*(1), 17080. https://doi.org/10.1038/s41598-017-17013-w

Marques-Lopes, J., Van Kempen, T., Waters, E.M., Pickel, V.M., Iadecola, C., Milner, T.A. (2014). Slow-pressor angiotensin II hypertension and concomitant dendritic NMDA receptor trafficking in estrogen receptor β-containing neurons of the mouse hypothalamic paraventricular nucleus are sex and age dependent. *J Comp Neurol*., 522(13), 3075-3090. https://doi.org/10.1002/cne.23569.

Meissner, A., Minnerup, J., Soria, G., & Planas, A. M. (2017). Structural and functional brain alterations in a murine model of Angiotensin II-induced hypertension. *J Neurochem*, *140*(3), 509-521. https://doi.org/10.1111/jnc.13905

Milner, T. A., Chen, R. X., Welington, D., Rubin, B. R., Contoreggi, N. H., Johnson, M. A., Mazid, S., Marques-Lopes, J., Marongiu, R., & Glass, M. J. (2022). Angiotensin II differentially affects hippocampal glial inflammatory markers in young adult male and female mice. *Learn Mem*, *29*(9), 265-273. https://doi.org/10.1101/lm.053507.121

Nilsson, H., & Aalkjaer, C. (2003). Vasomotion: mechanisms and physiological importance. *Mol Interv*, *3*(2), 79-89, 51. https://doi.org/10.1124/mi.3.2.79

O'Brien, J. T., & Markus, H. S. (2014). Vascular risk factors and Alzheimer's disease. *BMC Med*, *12*, 218. https://doi.org/10.1186/s12916-014-0218-y

Park, L., Zhou, J., Koizumi, K., Wang, G., Anfray, A., Ahn, S. J., Seo, J., Zhou, P., Zhao, L., Paul, S., Anrather, J., & Iadecola, C. (2020). tPA Deficiency Underlies Neurovascular Coupling Dysfunction by Amyloid-β. *J Neurosci*, *40*(42), 8160-8173. https://doi.org/10.1523/jneurosci.1140-20.2020

Pascoal, I. F., Lindheimer, M. D., Nalbantian-Brandt, C., & Umans, J. G. (1998). Preeclampsia selectively impairs endothelium-dependent relaxation and leads to oscillatory activity in small omental arteries. *J Clin Invest*, *101*(2), 464-470. https://doi.org/10.1172/jci557

Salvi, P., Faini, A., Castiglioni, P., Brunacci, F., Montaguti, L., Severi, F., Gautier, S., Pretolani, E., Benetos, A., & Parati, G. (2018). Increase in slow-wave vasomotion by hypoxia and ischemia in lowlanders and highlanders. *J Appl Physiol (1985)*, *125*(3), 780-789. https://doi.org/10.1152/japplphysiol.00977.2017

Sampson, A. K., Moritz, K. M., Jones, E. S., Flower, R. L., Widdop, R. E., & Denton, K. M. (2008). Enhanced Angiotensin II Type 2 Receptor Mechanisms Mediate Decreases in Arterial Pressure Attributable to Chronic Low-Dose Angiotensin II in Female Rats. *Hypertension*, *52*(4), 666-671. https://doi.org/doi:10.1161/HYPERTENSIONAHA.108.114058

Tarantini, S., Fulop, G. A., Kiss, T., Farkas, E., Zölei-Szénási, D., Galvan, V., Toth, P., Csiszar, A., Ungvari, Z., & Yabluchanskiy, A. (2017). Demonstration of impaired neurovascular coupling responses in TG2576 mouse model of Alzheimer's disease using functional laser speckle contrast imaging. *Geroscience*, *39*(4), 465-473. https://doi.org/10.1007/s11357-017-9980-z

Tarantini, S., Tran, C. H. T., Gordon, G. R., Ungvari, Z., & Csiszar, A. (2017). Impaired neurovascular coupling in aging and Alzheimer's disease: Contribution of astrocyte dysfunction and endothelial impairment to cognitive decline. *Exp Gerontol*, *94*, 52-58. https://doi.org/10.1016/j.exger.2016.11.004

Toering, T. J., van der Graaf, A. M., Visser, F. W., Buikema, H., Navis, G., Faas, M. M., & Lely, A. T. (2015). Gender differences in response to acute and chronic angiotensin II infusion: a translational approach. *Physiological Reports*, *3*(7), e12434. https://doi.org/https://doi.org/10.14814/phy2.12434

Toth, P., Tucsek, Z., Sosnowska, D., Gautam, T., Mitschelen, M., Tarantini, S., Deak, F., Koller, A., Sonntag, W. E., Csiszar, A., & Ungvari, Z. (2013). Age-Related Autoregulatory Dysfunction and Cerebromicrovascular Injury in Mice with Angiotensin II-induced Hypertension. *Journal of Cerebral Blood Flow & Metabolism*, *33*(11), 1732-1742. https://doi.org/10.1038/jcbfm.2013.143

Toth, P., Tucsek, Z., Sosnowska, D., Gautam, T., Mitschelen, M., Tarantini, S., Deak, F., Koller, A., Sonntag, W. E., Csiszar, A., & Ungvari, Z. (2013). Age-related autoregulatory dysfunction and cerebromicrovascular injury in mice with angiotensin II-induced hypertension. *J Cereb Blood Flow Metab*, *33*(11), 1732-1742. https://doi.org/10.1038/jcbfm.2013.143

van Veluw, S. J., Hou, S. S., Calvo-Rodriguez, M., Arbel-Ornath, M., Snyder, A. C., Frosch, M. P., Greenberg, S. M., & Bacskai, B. J. (2020). Vasomotion as a Driving Force for Paravascular Clearance in the Awake Mouse Brain. *Neuron*, *105*(3), 549-561 e545. https://doi.org/10.1016/j.neuron.2019.10.033

Wiesmann, M., Roelofs, M., van der Lugt, R., Heerschap, A., Kiliaan, A. J., & Claassen, J. A. (2017). Angiotensin II, hypertension and angiotensin II receptor antagonism: Roles in the behavioural and brain pathology of a mouse model of Alzheimer's disease. *Journal of Cerebral Blood Flow & Metabolism*, *37*(7), 2396-2413. https://doi.org/10.1177/0271678x16667364

Wiesmann, M., Roelofs, M., van der Lugt, R., Heerschap, A., Kiliaan, A. J., & Claassen, J. A. (2017). Angiotensin II, hypertension and angiotensin II receptor antagonism: Roles in the behavioural and brain pathology of a mouse model of Alzheimer's disease. *J Cereb Blood Flow Metab*, *37*(7), 2396-2413. https://doi.org/10.1177/0271678x16667364

Winder, A.T., Echagarruga, C., Zhang, Q., Drew, P.J. (2017). Weak correlations between hemodynamic signals and ongoing neural activity during the resting state. Nat. Neurosci, 20, 1761–1769. https://doi.org/10.1038/s41593-017-0007-y.

Xue, B., Pamidimukkala, J., & Hay, M. (2005). Sex differences in the development of angiotensin II-induced hypertension in conscious mice. *American Journal of Physiology-Heart and Circulatory Physiology*, *288*(5), H2177-H2184. https://doi.org/10.1152/ajpheart.00969.2004

Youwakim, J., Vallerand, D., & Girouard, H. (2023). Neurovascular coupling in hypertension is impaired by IL-17A through oxidative stress. *International Journal of Molecular Sciences*, *24*(4), Article 3959. https://doi.org/10.3390/ijms24043959

Zhang, M., Mao, Y., Ramirez, S. H., Tuma, R. F., & Chabrashvili, T. (2010). Angiotensin II induced cerebral microvascular inflammation and increased blood-brain barrier permeability via oxidative stress. *Neuroscience*, *171*(3), 852-858. https://doi.org/10.1016/j.neuroscience.2010.09.029

Zimmerman, M.C., Lazartigues, E., Sharma, R.V., Davisson, R.L. (2004). Hypertension caused by angiotensin II infusion involves increased superoxide production in the central nervous system. *Circ Res*., 95(2), 210-216. https://doi.org/10.1161/01.RES.0000135483.12297.e4.

Zlokovic, B. V. (2011). Neurovascular pathways to neurodegeneration in Alzheimer's disease and other disorders. *Nat Rev Neurosci*, *12*(12), 723-738. https://doi.org/10.1038/nrn3114

Chapter 4 - Discussion and Conclusion

4 Discussion

The primary aim of this thesis was to investigate the impact of disease on cerebrovascular function. To investigate this, measures of neurovascular function obtained through in-vivo imaging of preclinical models of AD (J20-AD) and HTN (ang-II-induced) using 2D-OIS and electrophysiological techniques allowed for the exploration of the effects of disease (AD, HTN) on brain vascular function. As alterations in vasomotion have been observed in both AD (Kotliar et al., 2022; van Beek et al., 2012) and HTN (Hollenberg & Sandor, 1984; Pascoal et al., 1998), the thesis also aimed to investigate vasomotion in health and disease, and assess the feasibility of this process as a biomarker.

4.1 Overview of Findings

The first study included in the thesis (chapter 2), was a study investigating vasomotion in a preclinical model of AD. As vasomotion could be a biomarker of vascular dysfunction in AD, this study investigated LFOs (0.06 - 0.2 Hz) in HbT of anaesthetised J20-AD mice. The aim of this study was to assess whether there were differences in arterial LFOs between J20-AD and healthy mice, and further, to investigate the relationship of this signal to neural activity. An FFT was conducted on arterial HbT recorded using 2D-OIS, and powers within the 0-06 - 0.2 Hz range were summed and used as a measure of vasomotion for comparison within the groups. As some mice underwent 2D-OIS imaging and electrophysiology simultaneously, a kernel analysis was used to examine the relationship between LFOs and neural activity. The study found that LFOs increased when inspired breathing gas was switched from oxygen to air in all animals regardless of group, however, the power of LFOs did not differ significantly between J20-AD mice and healthy C57BL/6 mice. LFO power was found to only differ between the groups in our chronic preparation, in which an electrode implant had been inserted into the brain for electrophysiology. Interestingly, this study revealed a strong temporal relationship between the LFOs and MUA, suggesting that LFOs were being driven by underlying neuronal activity.

The second study included in the thesis (chapter 3), was a study investigating the effects of ang-II-induced HTN on cerebral haemodynamics and LFOs in awake mice. HTN has emerged as a leading risk factor for AD, through detrimental effects on the structure and functionality of cerebral vessels, ultimately leading to increased vascular resistance and impairments in CBF and NVC. However, the mechanisms underlying how HTN can lead to AD are incompletely understood. Therefore, the aim of this study was to further investigate the effects of HTN on brain vascular function. Mice were treated with ang-II (600ng/kg/min) delivered through an osmotic pump, or saline, for a 28-day period. Throughout the treatment period, mice underwent awake imaging of cerebral haemodynamics using 2D-OIS, the NOR test, and electrophysiological measurements. At the end of the 28 days, histology was performed on dissected brains. The current study found a faster time to onset of the HbT response to whisker stimulation in ang-II-treated mice, however, no other treatment-specific effects were observed on NVC. Additionally, locomotion was found to differ between male and female mice in terms of walking behaviour, in that male mice exhibited higher levels of locomotion than female mice. LFO power was also found to differ between the groups, in that male control mice exhibited significantly higher LFO power than ang-II-treated males. Interestingly, sex also emerged as a key variable affecting haemodynamic responses and LFOs, in that female mice exhibited a significantly lower peak and magnitude of their HbT response to whisker stimulation compared to males, as well as lower LFO power compared to male mice. No significant histological differences between ang-II-treated and saline-treated control mice were observed.

4.2 Vasomotion as a Biomarker for Disease

Despite the absence of disease-related differences in vasomotion observed in a preclinical model of AD, differences in LFO power were observed between ang-II-treated males and male controls, with ang-II-treated males exhibiting lower LFO powers. Contrary to initial hypotheses, the current work found no differences in LFOs between healthy C57BL/6 mice and J20-AD mice. This differs from several studies that have reported alterations in LFOs in AD (Bonnar et al.,

2023; Kotliar et al., 2022; Rivera-Rivera et al., 2020; van Beek et al., 2012). However, findings in this regard have also been quite conflicting, as both enhancements and impairments in vasomotion have been described. The current study found lower LFO power in ang-II-treated males than in male controls, aligning with studies finding alterations in vasomotion in HTN (Hollenberg & Sandor, 1984; Liu et al., 2017; Pascoal et al., 1998), specifically those that have reported deficits (Liu et al., 2017). The current study found impairments in vascular LFOs in ang-II-treated male mice that preceded any major detectable changes in NVC, cognitive function, and immunohistochemical profiles, suggesting that vasomotion deficits may represent an early pathophysiological event in HTN. It has been suggested that vasomotion might increase tissue perfusion (Nilsson & Aalkjaer, 2003), which could be why changes in the prevalence or amplitude of vasomotion might be expected to be observed in conditions like AD and HTN, which are both associated with compromised oxygen delivery (Foster et al., 2010; Liu et al., 2023). However, the current studies suggest that, under the conditions tested, vasomotion may lack sensitivity to early pathological changes in AD, particularly when neural activity is not controlled for or accounted for in analysis. It is possible that LFOs might become disrupted only at later stages of disease progression or under different physiological conditions (e.g., stress, hypoxia, aging).

4.3 Vasomotion and Neural Activity

One of the most notable findings of this work is discovery that vasomotion signals were primarily driven by neural activity. Thus, results of the current study may highlight inconsistencies with the use of the term “vasomotion” to describe LFOs in-vivo. It was found that LFOs within a range typically associated with vasomotion were in fact being driven by neuronal activity. Recently, the term “vasomotion” has been used to describe two separate phenomena: (1) LFOs that arise from intrinsic vascular mechanisms, i.e., vasomotion by its classic definition, and (2) LFOs that arise from a blend of neural-induced and neural-independent mechanisms, i.e., NVC. Several studies have reported coupling between cerebral LFOs and neuronal activity, in that LFOs can become entrained by neural activity in mice (Broggini et al., 2024; Mateo et al., 2017). Although, classically defined vasomotion has been found to occur

independently of neural activity (Hudetz et al., 1992; Mayhew et al., 1996). However, these findings have been in rat models, suggesting the possibility that vasomotion in-vivo might possibly differ between species in terms of its relationship to neural activity. Similar to the findings of LFOs in cerebral haemodynamics being driven by neural activity in mouse studies (Broggini et al., 2024; Mateo et al., 2017), LFOs in mice in the current study showed a similar relationship to MUA signals. These findings call for a more nuanced interpretation of vasomotion data in disease models and emphasise the need for experimental paradigms that can disentangle vascular versus neurogenic contributions to these LFOs. Future studies should further investigate the specific neural mechanisms that drive these oscillations and whether they differ across disease states or stages.

4.4 Hypertension and Neurovascular Coupling

Although global measures of NVC were largely preserved in ang-II-treated mice, a faster onset of the haemodynamic response (HbT) relative to control mice was observed. This is contrary to our expectations of delayed or blunted haemodynamic responses in ang-II-treated mice in the current study that have been reported by others (Capone et al., 2011; Kazama et al., 2003); which may reflect impairments in the signaling mechanisms that mediate the rapid coupling between neural activity and local vascular responses. Potential mechanisms could include altered endothelial function or early disruption of vascular responses due to factors such as hypertrophy or remodelling; both of which have been implicated in HTN (Iadecola & Davisson, 2008). In the current study, differences were observed in the timing of the HbT response in the parenchyma ROI compared to controls. The accelerated response in ang-II-treated mice could possibly indicate a state of enhanced or dysregulated vascular reactivity in the context of HTN. Alternatively, this could reflect a compensatory mechanism in response to the effects of ang-II aimed at preserving perfusion during neural activation. A large decline in parenchymal CBF has been observed in patients with high BP or with untreated or poorly controlled HTN compared to normotensive patients (Muller et al., 2012). Although, NVC responses to whisker stimulation were measured in mice in the current study, rCBF was not assessed. As the NVC response was found to differ slightly in ang-II-treated mice from controls, it would be of interest to see if rCBF

differed between the groups. However, several studies have reported attenuated NVC responses to sensory stimulation without changes in CBF (Capone et al., 2011; Kazama et al., 2003). Interestingly, the magnitude of the neurovascular response (i.e., peak and AUC) was not significantly different between the groups. The alteration in the timing of the response (time to onset specifically) found in the current study could suggest that temporal features of NVC may offer a more sensitive index of early vascular dysfunction than static amplitude-based metrics alone.

4.5 Sex Differences in Vascular and Behavioural Outcomes

Another notable outcome of this study was the identification of significant sex differences in both cerebrovascular and behavioural domains. The current study found that sex had a significant effect on both locomotor behaviour and haemodynamic function of the mice. Locomotion was found to differ significantly between males and females, specifically, male mice were found to walk more than female mice during the awake imaging sessions. Several rodent studies have revealed sex differences in physical activity levels, in that female mice and rats are often more active than males (Rosenfeld, 2017). Contrary to this, male mice were found to exhibit higher levels of locomotion than females. However, the effects of ang-II are known to differentially affect male and female mice (Costa et al., 2016; Girouard et al., 2008; Sampson et al., 2008; Toering et al., 2015; Xue et al., 2005), with greater cardiovascular effects on males. Thus, it may be possible that the cardiovascular effects introduced from ang-II infusion have additional effects on the walking behaviour of the mice.

In terms of cerebrovascular function, female mice exhibited a lower peak and smaller AUC of the HbT response compared to males. These differences were not observed across disease groups but were consistent within sex, suggesting intrinsic sex-based variability in vascular responsivity. Further, lower LFO power was observed in female control mice compared to males. As locomotion was found to differ between sexes in the current study, it could be possible that the differences observed in haemodynamic responses and LFOs in female mice compared to males could be contributed to, at least in part, by differential locomotor activity. These findings

align with growing literature highlighting the importance of sex as a biological variable in both cerebrovascular research and dementia risk (Brady et al., 2024; Girouard et al., 2008). The mechanisms underlying these differences, whether hormonal or metabolic, for instance, remain to be elucidated, but their presence underscores the need for sex-stratified analysis in future work.

4.6 Methodological Considerations and Limitations

A limitation of the current work is that specific changes in vessel diameter were not quantified when exploring vasomotion in-vivo. Thus, while OIS can be used to assess vasomotion in-vivo, more precise insights in terms of vessel diameter changes could be obtained with an imaging modality with a greater depth specificity and spatial resolution, such as two-photon microscopy. This could help provide additional insights into vasomotion in preclinical models of AD and HTN. Another limitation of the current studies is that the method used to acquire MUA data, i.e., electrode insertion into the WBC, is an invasive method that results in a CSD after insertion (Shabir et al., 2022; Shabir et al., 2020; Sharp et al., 2020), the effects of which subside over time. However, the timing of imaging experiments after electrode insertion should have allowed for sufficient time for haemodynamic recovery, at least in healthy mice (Shabir et al., 2022). In the study exploring LFOs in HbT in ang-II-treated mice, MUA data could not be collected simultaneously except for in the acute anaesthetised session, as the invasive procedure of electrode insertion into the barrel cortex cannot be performed in awake mice. Future work should consider the use of non-invasive techniques for the imaging of brain activity without the need for an electrode, such as GCaMP. This would additionally aid in avoiding the confounding effects of CSD when looking at MUA while also allowing for the recording of neural activity in awake mice. A benefit of exploring LFOs awake ang-II-treated mice as done in the current study, is that the confounds of anaesthetic use on LFOs could be avoided, as studies have reported that anaesthetic use impacts vasomotion in-vivo (Colantuoni et al., 1984; Hundley et al., 1988). As several studies have shown valuable insights into the effects of HTN on AD progression and pathology by using mixed-models (Cifuentes et al., 2015; Wiesmann et al., 2015), a useful avenue for future research that was not done in the current study would be to explore vascular

changes and LFOs in hypertensive AD mice, for instance, in J20-mice treated with ang-II. Further, as aging strongly influences vascular function, exploring this in different age ranges (i.e., in aged mice) could also be an important area of investigation.

4.7 Conclusion

This work contributes to the evolving understanding of neurovascular function in preclinical disease states. While no major changes in LFO power were observed in AD, the current study found lower LFO power in ang-II-treated males compared to healthy male controls. These deficits were found to occur before overt changes in NVC, cognition, or immunohistochemical markers between HTN and control mice, suggesting that changes in LFOs may represent an early pathophysiological event in the disease course of HTN. The current study also found that LFOs were driven by neuronal activity, providing important insights into the interpretation of vasomotion signals in-vivo, as what was previously interpreted as intrinsic vascular oscillations may instead reflect low-frequency NVC. Further, although NVC responses were found to be largely intact in HTN mice, the current study observed sex differences and timing alterations of HbT responses in HTN, as well as sex differences in LFOs. These findings highlight the complexity of vascular regulation in disease and reinforce the need for multifaceted, sex-aware approaches in future dementia research.

4.8 References

Aalkjaer, C., Boedtkjer, D., & Matchkov, V. (2011). Vasomotion - what is currently thought? *Acta Physiol (Oxf)*, *202*(3), 253-269. https://doi.org/10.1111/j.1748-1716.2011.02320.x

Aalkjaer, C., & Nilsson, H. (2005). Vasomotion: cellular background for the oscillator and for the synchronization of smooth muscle cells. *Br J Pharmacol*, *144*(5), 605-616. https://doi.org/10.1038/sj.bjp.0706084

Abell, J. G., Kivimäki, M., Dugravot, A., Tabak, A. G., Fayosse, A., Shipley, M., Sabia, S., & Singh-Manoux, A. (2018). Association between systolic blood pressure and dementia in the Whitehall II cohort study: role of age, duration, and threshold used to define hypertension. *European Heart Journal*, *39*(33), 3119-3125. https://doi.org/10.1093/eurheartj/ehy288

Ahmad, F., Mein, H., Jing, Y., Zhang, H., & Liu, P. (2021). Behavioural Functions and Cerebral Blood Flow in a P301S Tauopathy Mouse Model: A Time-Course Study. *Int J Mol Sci*, *22*(18). https://doi.org/10.3390/ijms22189727

Aldea, R., Weller, R. O., Wilcock, D. M., Carare, R. O., & Richardson, G. (2019). Cerebrovascular smooth muscle cells as the drivers of intramural periarterial drainage of the brain [Article]. *Frontiers in Aging Neuroscience*, *11*(JAN), Article 1. https://doi.org/10.3389/fnagi.2019.00001

Antonios, T. F., Singer, D. R., Markandu, N. D., Mortimer, P. S., & MacGregor, G. A. (1999). Structural skin capillary rarefaction in essential hypertension. *Hypertension*, *33*(4), 998-1001. https://doi.org/10.1161/01.hyp.33.4.998

Arvanitakis, Z., Capuano, A. W., Lamar, M., Shah, R. C., Barnes, L. L., Bennett, D. A., & Schneider, J. A. (2018). Late-life blood pressure association with cerebrovascular and Alzheimer disease pathology. *Neurology*, *91*(6), e517-e525. https://doi.org/10.1212/WNL.0000000000005951

Arvanitakis, Z., Shah, R. C., & Bennett, D. A. (2019). Diagnosis and Management of Dementia: Review. *Jama*, *322*(16), 1589-1599. https://doi.org/10.1001/jama.2019.4782

Attwell, D., Buchan, A. M., Charpak, S., Lauritzen, M., MacVicar, B. A., & Newman, E. A. (2010). Glial and neuronal control of brain blood flow. *Nature*, *468*(7321), 232-243. https://doi.org/10.1038/nature09613

Attwell, D., Mishra, A., Hall, C. N., O'Farrell, F. M., & Dalkara, T. (2016). What is a pericyte? *J Cereb Blood Flow Metab*, *36*(2), 451-455. https://doi.org/10.1177/0271678x15610340

Austin, S. A., Santhanam, A. V., & Katusic, Z. S. (2010). Endothelial nitric oxide modulates expression and processing of amyloid precursor protein. *Circ Res*, *107*(12), 1498-1502. https://doi.org/10.1161/circresaha.110.233080

Bader, M., & Ganten, D. (2008). Update on tissue renin–angiotensin systems. *Journal of Molecular Medicine*, *86*(6), 615-621. https://doi.org/10.1007/s00109-008-0336-0

Baumbach, G. L., Sigmund, C. D., & Faraci, F. M. (2003). Cerebral arteriolar structure in mice overexpressing human renin and angiotensinogen. *Hypertension*, *41*(1), 50-55. https://doi.org/10.1161/01.hyp.0000042427.05390.5c

Beason-Held, L. L., Moghekar, A., Zonderman, A. B., Kraut, M. A., & Resnick, S. M. (2007). Longitudinal changes in cerebral blood flow in the older hypertensive brain. *Stroke*, *38*(6), 1766-1773. https://doi.org/10.1161/STROKEAHA.106.477109

Benjamin, E. J., Larson, M. G., Keyes, M. J., Mitchell, G. F., Vasan, R. S., Keaney, J. F., Lehman, B. T., Fan, S., Osypiuk, E., & Vita, J. A. (2004). Clinical Correlates and Heritability of Flow-Mediated Dilation in the Community. *Circulation*, *109*(5), 613-619. https://doi.org/10.1161/01.CIR.0000112565.60887.1E

Benveniste, H., & Nedergaard, M. (2022). Cerebral small vessel disease: A glymphopathy? *Curr Opin Neurobiol*, *72*, 15-21. https://doi.org/10.1016/j.conb.2021.07.006

Berlau, D., J. , Corrada, M., M. , Head, E., & Kawas, C., H. . (2009). APOE ε2 is associated with intact cognition but increased Alzheimer pathology in the oldest old. *Neurology*, *72*(9), 829. https://doi.org/10.1212/01.wnl.0000343853.00346.a4

Bertuglia, S., Colantuoni, A., Coppini, G., & Intaglietta, M. (1991). Hypoxia- or hyperoxia-induced changes in arteriolar vasomotion in skeletal muscle microcirculation. *Am J Physiol*, *260*(2 Pt 2), H362-372. https://doi.org/10.1152/ajpheart.1991.260.2.H362

Berwick, J., Johnston, D., Jones, M., Martindale, J., Redgrave, P., McLoughlin, N., Schiessl, I., & Mayhew, J. E. W. (2005). Neurovascular coupling investigated with two-dimensional optical imaging spectroscopy in rat whisker barrel cortex. *European Journal of Neuroscience*, *22*(7), 1655-1666. https://doi.org/https://doi.org/10.1111/j.1460-9568.2005.04347.x

Boegehold, M. A. (1993). Enhanced arteriolar vasomotion in rats with chronic salt-induced hypertension. *Microvasc Res*, *45*(1), 83-94. https://doi.org/10.1006/mvre.1993.1008

Bolivar, J. J. (2013). Essential hypertension: an approach to its etiology and neurogenic pathophysiology. *Int J Hypertens*, *2013*, 547809. https://doi.org/10.1155/2013/547809

Bonder, D. E., & McCarthy, K. D. (2014). Astrocytic Gq-GPCR-linked IP3R-dependent Ca2+ signaling does not mediate neurovascular coupling in mouse visual cortex in vivo. *J Neurosci*, *34*(39), 13139-13150. https://doi.org/10.1523/jneurosci.2591-14.2014

Bonnar, O., Shaw, K., Anderle, S., Grijseels, D. M., Clarke, D., Bell, L., King, S. L., & Hall, C. N. (2023). APOE4 expression confers a mild, persistent reduction in neurovascular function in the visual cortex and hippocampus of awake mice. *J Cereb Blood Flow Metab*, *43*(11), 1826-1841. https://doi.org/10.1177/0271678x231172842

Bonnar, O., Shaw, K., Grijseels, D. M., Clarke, D., Bell, L., Anderle, S., King, S. L., & Hall, C. N. (2022). https://doi.org/10.1101/2021.05.26.445731

Boonen, H. C., & De Mey, J. G. (1990). Increased calcium sensitivity in isolated resistance arteries from spontaneously hypertensive rats: effects of dihydropyridines. *Eur J Pharmacol*, *179*(3), 403-412. https://doi.org/10.1016/0014-2999(90)90181-5

Bosch, A. J., Harazny, J. M., Kistner, I., Friedrich, S., Wojtkiewicz, J., & Schmieder, R. E. (2017). Retinal capillary rarefaction in patients with untreated mild-moderate hypertension. *BMC Cardiovasc Disord*, *17*(1), 300. https://doi.org/10.1186/s12872-017-0732-x

Brady, B., Zheng, L., Kootar, S., Anstey, K.J. (2024). Sex and gender differences in risk scores for dementia and Alzheimer's disease among cisgender, transgender, and non-binary adults. *Alzheimer's Dement*., 20, 5–15. https://doi.org/10.1002/alz.13317

Broggini, T., Duckworth, J., Ji, X., Liu, R., Xia, X., Mächler, P., Shaked, I., Munting, L. P., Iyengar, S., Kotlikoff, M., van Veluw, S. J., Vergassola, M., Mishne, G., & Kleinfeld, D. (2024). Long-wavelength traveling waves of vasomotion modulate the perfusion of cortex. *Neuron*, *112*(14), 2349-2367.e2348. https://doi.org/https://doi.org/10.1016/j.neuron.2024.04.034

Brown, R., Benveniste, H., Black, S. E., Charpak, S., Dichgans, M., Joutel, A., Nedergaard, M., Smith, K. J., Zlokovic, B. V., & Wardlaw, J. M. (2018). Understanding the role of the perivascular space in cerebral small vessel disease. *Cardiovasc Res*, *114*(11), 1462-1473. https://doi.org/10.1093/cvr/cvy113

Canavan, M., & O'Donnell, M. J. (2022). Hypertension and Cognitive Impairment: A Review of Mechanisms and Key Concepts [Mini Review]. *Frontiers in Neurology*, *Volume 13 - 2022*. https://www.frontiersin.org/journals/neurology/articles/10.3389/fneur.2022.821135

Cao, X., Peterson, J. R., Wang, G., Anrather, J., Young, C. N., Guruju, M. R., Burmeister, M. A., Iadecola, C., & Davisson, R. L. (2012). Angiotensin II–Dependent Hypertension Requires Cyclooxygenase

1–Derived Prostaglandin E2 and EP1 Receptor Signaling in the Subfornical Organ of the Brain. *Hypertension*, *59*(4), 869-876. https://doi.org/10.1161/HYPERTENSIONAHA.111.182071

Capone, C., Faraco, G., Park, L., Cao, X., Davisson, R. L., & Iadecola, C. (2011). The cerebrovascular dysfunction induced by slow pressor doses of angiotensin II precedes the development of hypertension. *Am J Physiol Heart Circ Physiol*, *300*(1), H397-407. https://doi.org/10.1152/ajpheart.00679.2010

Capone, C., Faraco, G., Peterson, J. R., Coleman, C., Anrather, J., Milner, T. A., Pickel, V. M., Davisson, R. L., & Iadecola, C. (2012). Central cardiovascular circuits contribute to the neurovascular dysfunction in angiotensin II hypertension. *J Neurosci*, *32*(14), 4878-4886. https://doi.org/10.1523/JNEUROSCI.6262-11.2012

Carlson, S. H., Oparil, S., Chen, Y. F., & Wyss, J. M. (2002). Blood pressure and NaCl-sensitive hypertension are influenced by angiotensin-converting enzyme gene expression in transgenic mice. *Hypertension*, *39*(2), 214-218. https://doi.org/10.1161/hy0202.104267

Cates, M. J., Steed, P. W., Abdala, A. P., Langton, P. D., & Paton, J. F. (2011). Elevated vertebrobasilar artery resistance in neonatal spontaneously hypertensive rats. *J Appl Physiol (1985)*, *111*(1), 149-156. https://doi.org/10.1152/japplphysiol.00220.2011

Chavez-Gutierrez, L., & Szaruga, M. (2020). Mechanisms of neurodegeneration - Insights from familial Alzheimer's disease. *Semin Cell Dev Biol*, *105*, 75-85. https://doi.org/10.1016/j.semcdb.2020.03.005

Cheignon, C., Tomas, M., Bonnefont-Rousselot, D., Faller, P., Hureau, C., & Collin, F. (2018). Oxidative stress and the amyloid beta peptide in Alzheimer's disease. *Redox Biol*, *14*, 450-464. https://doi.org/10.1016/j.redox.2017.10.014

Chen, J. X., Xue, K. Y., Xin, J. J., Yan, X., Li, R. L., Wang, X. X., Wang, X. L., Tong, M. M., Gan, L., Li, H., Lan, J., Li, X., Zhuo, C. L., Li, L. Y., Deng, Z. J., Zhang, H. Y., & Jiang, W. (2019). 5-Lipoxagenase deficiency attenuates L-NAME-induced hypertension and vascular remodeling.

Biochim Biophys Acta Mol Basis Dis, *1865*(9), 2379-2392. https://doi.org/10.1016/j.bbadis.2019.05.021

Cifuentes, D., Poittevin, M., Dere, E., Broqueres-You, D., Bonnin, P., Benessiano, J., Pocard, M., Mariani, J., Kubis, N., Merkulova-Rainon, T., & Levy, B. I. (2015). Hypertension accelerates the progression of Alzheimer-like pathology in a mouse model of the disease. *Hypertension*, *65*(1), 218-224. https://doi.org/10.1161/HYPERTENSIONAHA.114.04139

Colantuoni, A., Bertuglia, S., & Intaglietta, M. (1984). Quantitation of rhythmic diameter changes in arterial microcirculation. *American Journal of Physiology-Heart and Circulatory Physiology*, *246*(4), H508-H517. https://doi.org/10.1152/ajpheart.1984.246.4.H508

Colonna, M., & Butovsky, O. (2017). Microglia Function in the Central Nervous System During Health and Neurodegeneration. *Annu Rev Immunol*, *35*, 441-468. https://doi.org/10.1146/annurev-immunol-051116-052358

Coomans, E. M., Tomassen, J., Ossenkoppele, R., Tijms, B. M., Lorenzini, L., ten Kate, M., Collij, L. E., Heeman, F., Rikken, R. M., van der Landen, S. M., den Hollander, M. E., Golla, S. S. V., Yaqub, M., Windhorst, A. D., Barkhof, F., Scheltens, P., de Geus, E. J. C., Visser, P. J., van Berckel, B. N. M., & den Braber, A. (2023). Genetically identical twin-pair difference models support the amyloid cascade hypothesis. *Brain*, *146*(9), 3735-3746. https://doi.org/10.1093/brain/awad077

Corrada, M. M., Hayden, K. M., Paganini-Hill, A., Bullain, S. S., DeMoss, J., Aguirre, C., Brookmeyer, R., & Kawas, C. H. (2017). Age of onset of hypertension and risk of dementia in the oldest-old: The 90+ Study. *Alzheimers Dement*, *13*(2), 103-110. https://doi.org/10.1016/j.jalz.2016.09.007

Crous-Bou, M., Minguillon, C., Gramunt, N., & Molinuevo, J. L. (2017). Alzheimer's disease prevention: from risk factors to early intervention. *Alzheimers Res Ther*, *9*(1), 71. https://doi.org/10.1186/s13195-017-0297-z

Csiszar, A., Tucsek, Z., Toth, P., Sosnowska, D., Gautam, T., Koller, A., Deak, F., Sonntag, W. E., & Ungvari, Z. (2013). Synergistic effects of hypertension and aging on cognitive function and

hippocampal expression of genes involved in beta-amyloid generation and Alzheimer's disease. *Am J Physiol Heart Circ Physiol*, *305*(8), H1120-1130. https://doi.org/10.1152/ajpheart.00288.2013

Cunningham, E. L., Todd, S. A., Passmore, P., Bullock, R., & McGuinness, B. (2021). Pharmacological treatment of hypertension in people without prior cerebrovascular disease for the prevention of cognitive impairment and dementia. *Cochrane Database of Systematic Reviews*(5). https://doi.org/10.1002/14651858.CD004034.pub4

Dai, W., Lopez, O. L., Carmichael, O. T., Becker, J. T., Kuller, L. H., & Gach, H. M. (2008). Abnormal regional cerebral blood flow in cognitively normal elderly subjects with hypertension. *Stroke*, *39*(2), 349-354. https://doi.org/10.1161/STROKEAHA.107.495457

Dalkara, T., Gursoy-Ozdemir, Y., & Yemisci, M. (2011). Brain microvascular pericytes in health and disease. *Acta Neuropathologica*, *122*(1), 1-9. https://doi.org/10.1007/s00401-011-0847-6

Daneman, R., & Prat, A. (2015). The blood-brain barrier. *Cold Spring Harb Perspect Biol*, *7*(1), a020412. https://doi.org/10.1101/cshperspect.a020412

de Montgolfier, O., Pinçon, A., Pouliot, P., Gillis, M. A., Bishop, J., Sled, J. G., Villeneuve, L., Ferland, G., Lévy, B. I., Lesage, F., Thorin-Trescases, N., & Thorin, É. (2019). High Systolic Blood Pressure Induces Cerebral Microvascular Endothelial Dysfunction, Neurovascular Unit Damage, and Cognitive Decline in Mice. *Hypertension*, *73*(1), 217-228. https://doi.org/10.1161/hypertensionaha.118.12048

Delacroix, S., & Chokka, R. G. (2014). Hypertension: Pathophysiology and Treatment. *Journal of Neurology & Neurophysiology*, *05*(06). https://doi.org/10.4172/2155-9562.1000250

Di Marco, L. Y., Farkas, E., Martin, C., Venneri, A., & Frangi, A. F. (2015). Is Vasomotion in Cerebral Arteries Impaired in Alzheimer's Disease? *J Alzheimers Dis*, *46*(1), 35-53. https://doi.org/10.3233/JAD-142976

Diem, A. K., Sharp, M. M., Gatherer, M., Bressloff, N. W., Carare, R. O., & Richardson, G. (2017). Arterial pulsations cannot drive intramural periarterial drainage: Significance for Aβ drainage [Article]. *Frontiers in Neuroscience*, *11*(AUG), Article 475. https://doi.org/10.3389/fnins.2017.00475

Ding, J., Davis-Plourde, K. L., Sedaghat, S., Tully, P. J., Wang, W., Phillips, C., Pase, M. P., Himali, J. J., Gwen Windham, B., Griswold, M., Gottesman, R., Mosley, T. H., White, L., Guðnason, V., Debette, S., Beiser, A. S., Seshadri, S., Ikram, M. A., Meirelles, O., . . . Launer, L. J. (2020). Antihypertensive medications and risk for incident dementia and Alzheimer's disease: a meta-analysis of individual participant data from prospective cohort studies. *The Lancet Neurology*, *19*(1), 61-70. https://doi.org/10.1016/S1474-4422(19)30393-X

Dirnagl, U., Kaplan, B., Jacewicz, M., & Pulsinelli, W. (1989). Continuous Measurement of Cerebral Cortical Blood Flow by Laser—Doppler Flowmetry in a Rat Stroke Model. *Journal of Cerebral Blood Flow & Metabolism*, *9*(5), 589-596. https://doi.org/10.1038/jcbfm.1989.84

Dohi, Y., Thiel, M. A., Bühler, F. R., & Lüscher, T. F. (1990). Activation of endothelial L-arginine pathway in resistance arteries. Effect of age and hypertension. *Hypertension*, *16*(2), 170-179. https://doi.org/10.1161/01.HYP.16.2.170

Donato, A. J., Machin, D. R., & Lesniewski, L. A. (2018). Mechanisms of Dysfunction in the Aging Vasculature and Role in Age-Related Disease. *Circ Res*, *123*(7), 825-848. https://doi.org/10.1161/CIRCRESAHA.118.312563

Dubois, B., Feldman, H. H., Jacova, C., Hampel, H., Molinuevo, J. L., Blennow, K., DeKosky, S. T., Gauthier, S., Selkoe, D., Bateman, R., Cappa, S., Crutch, S., Engelborghs, S., Frisoni, G. B., Fox, N. C., Galasko, D., Habert, M.-O., Jicha, G. A., Nordberg, A., . . . Cummings, J. L. (2014). Advancing research diagnostic criteria for Alzheimer's disease: the IWG-2 criteria. *The Lancet Neurology*, *13*(6), 614-629. https://doi.org/https://doi.org/10.1016/S1474-4422(14)70090-0

Duchemin, S., Belanger, E., Wu, R., Ferland, G., & Girouard, H. (2013). Chronic perfusion of angiotensin II causes cognitive dysfunctions and anxiety in mice. *Physiol Behav*, *109*, 63-68. https://doi.org/10.1016/j.physbeh.2012.10.005

Elahi, F. M., Alladi, S., Black, S. E., Claassen, J., DeCarli, C., Hughes, T. M., Moonen, J., Pajewski, N. M., Price, B. R., Satizabal, C., Shaaban, C. E., Silva, N., Snyder, H. M., Sveikata, L., Williamson, J. D., Wolters, F. J., & Hainsworth, A. H. (2023). Clinical trials in vascular cognitive impairment following SPRINT-MIND: An international perspective. *Cell Rep Med*, *4*(6), 101089. https://doi.org/10.1016/j.xcrm.2023.101089

Escartin, C., Galea, E., Lakatos, A., O'Callaghan, J. P., Petzold, G. C., Serrano-Pozo, A., Steinhäuser, C., Volterra, A., Carmignoto, G., Agarwal, A., Allen, N. J., Araque, A., Barbeito, L., Barzilai, A., Bergles, D. E., Bonvento, G., Butt, A. M., Chen, W.-T., Cohen-Salmon, M., . . . Verkhratsky, A. (2021). Reactive astrocyte nomenclature, definitions, and future directions. *Nature Neuroscience*, *24*(3), 312-325. https://doi.org/10.1038/s41593-020-00783-4

Eyre, B., Shaw, K., Sharp, P., Boorman, L., Lee, L., Shabir, O., Berwick, J., & Howarth, C. (2022). The effects of locomotion on sensory-evoked haemodynamic responses in the cortex of awake mice. *Sci Rep*, *12*(1), 6236. https://doi.org/10.1038/s41598-022-10195-y

Fang, J., Zhang, P., Zhou, Y., Chiang, C. W., Tan, J., Hou, Y., Stauffer, S., Li, L., Pieper, A. A., Cummings, J., & Cheng, F. (2021). Endophenotype-based in silico network medicine discovery combined with insurance record data mining identifies sildenafil as a candidate drug for Alzheimer's disease. *Nat Aging*, *1*(12), 1175-1188. https://doi.org/10.1038/s43587-021-00138-z

Faraci, F. M., & Heistad, D. D. (1998). Regulation of the cerebral circulation: role of endothelium and potassium channels. *Physiol Rev*, *78*(1), 53-97. https://doi.org/10.1152/physrev.1998.78.1.53

Faraco, G., Park, L., Zhou, P., Luo, W., Paul, S.M., Anrather, J., Iadecola, C. (2016). Hypertension enhances Aβ-induced neurovascular dysfunction, promotes β-secretase activity, and leads to amyloidogenic processing of APP. *J Cereb Blood Flow Metab.*, 36(1), 241-52. https://doi.org/10.1038/jcbfm.2015.79.

Ferrario, C. M., & Strawn, W. B. (2006). Role of the Renin-Angiotensin-Aldosterone System and Proinflammatory Mediators in Cardiovascular Disease. *The American Journal of Cardiology*, *98*(1), 121-128. https://doi.org/https://doi.org/10.1016/j.amjcard.2006.01.059

Foster, G. E., Hanly, P. J., Ahmed, S. B., Beaudin, A. E., Pialoux, V., & Poulin, M. J. (2010). Intermittent Hypoxia Increases Arterial Blood Pressure in Humans Through a Renin-Angiotensin System-Dependent Mechanism. *Hypertension*, *56*(3), 369-377. https://doi.org/doi:10.1161/HYPERTENSIONAHA.110.152108

Foulquier, S., Namsolleck, P., Van Hagen, B. T., Milanova, I., Post, M. J., Blankesteijn, W. M., Rutten, B. P., Prickaerts, J., Van Oostenbrugge, R. J., & Unger, T. (2018). Hypertension-induced cognitive impairment: insights from prolonged angiotensin II infusion in mice. *Hypertens Res*, *41*(10), 817-827. https://doi.org/10.1038/s41440-018-0090-9

Fournier, D., Luft, F. C., Bader, M., Ganten, D., & Andrade-Navarro, M. A. (2012). Emergence and evolution of the renin–angiotensin–aldosterone system. *Journal of Molecular Medicine*, *90*(5), 495-508. https://doi.org/10.1007/s00109-012-0894-z

Fu, H., Li, J., Zhang, C., Du, P., Gao, G., Ge, Q., Guan, X., & Cui, D. (2024). Aβ-Aggregation-Generated Blue Autofluorescence Illuminates Senile Plaques as well as Complex Blood and Vascular Pathologies in Alzheimer's Disease. *Neuroscience Bulletin*, *40*(8), 1115-1126. https://doi.org/10.1007/s12264-023-01175-x

Fuchs, F. D., & Whelton, P. K. (2020). High Blood Pressure and Cardiovascular Disease. *Hypertension*, *75*(2), 285-292. https://doi.org/10.1161/HYPERTENSIONAHA.119.14240

Fujii, K., Heistad, D. D., & Faraci, F. M. (1990). Vasomotion of basilar arteries in vivo. *American Journal of Physiology-Heart and Circulatory Physiology*, *258*(6), H1829-H1834. https://doi.org/10.1152/ajpheart.1990.258.6.H1829

Fujishima, M., Ibayashi, S., Fujii, K., & Mori, S. (1995). Cerebral blood flow and brain function in hypertension. *Hypertens Res*, *18*(2), 111-117. https://doi.org/10.1291/hypres.18.111

Galley, H. F., & Webster, N. R. (2004). Physiology of the endothelium. *BJA: British Journal of Anaesthesia*, *93*(1), 105-113. https://doi.org/10.1093/bja/aeh163

Gallo, G., Volpe, M., & Savoia, C. (2021). Endothelial Dysfunction in Hypertension: Current Concepts and Clinical Implications. *Front Med (Lausanne)*, *8*, 798958. https://doi.org/10.3389/fmed.2021.798958

Gao, C., Jiang, J., Tan, Y., & Chen, S. (2023). Microglia in neurodegenerative diseases: mechanism and potential therapeutic targets. *Signal Transduction and Targeted Therapy*, *8*(1), 359. https://doi.org/10.1038/s41392-023-01588-0

Gao, N., Wang, H., Xu, X., Yang, Z., & Zhang, T. (2021). Angiotensin II induces cognitive decline and anxiety-like behavior via disturbing pattern of theta-gamma oscillations. *Brain Res Bull*, *174*, 84-91. https://doi.org/10.1016/j.brainresbull.2021.06.002

Gentile, M. T., Poulet, R., Pardo, A. D., Cifelli, G., Maffei, A., Vecchione, C., Passarelli, F., Landolfi, A., Carullo, P., & Lembo, G. (2009). β-Amyloid deposition in brain is enhanced in mouse models of arterial hypertension [Article]. *Neurobiology of Aging*, *30*(2), 222-228. https://doi.org/10.1016/j.neurobiolaging.2007.06.005

Girouard, H., & Iadecola, C. (2006). Neurovascular coupling in the normal brain and in hypertension, stroke, and Alzheimer disease. *Journal of Applied Physiology*, *100*(1), 328-335. https://doi.org/10.1152/japplphysiol.00966.2005

Girouard, H., Lessard, A., Capone, C., Milner, T. A., & Iadecola, C. (2008). The neurovascular dysfunction induced by angiotensin II in the mouse neocortex is sexually dimorphic. *Am J Physiol Heart Circ Physiol*, *294*(1), H156-163. https://doi.org/10.1152/ajpheart.01137.2007

Goate, A., Chartier-Harlin, M.-C., Mullan, M., Brown, J., Crawford, F., Fidani, L., Giuffra, L., Haynes, A., Irving, N., James, L., Mant, R., Newton, P., Rooke, K., Roques, P., Talbot, C., Pericak-Vance, M., Roses, A., Williamson, R., Rossor, M., . . . Hardy, J. (1991). Segregation of a missense mutation in the amyloid precursor protein gene with familial Alzheimer's disease. *Nature*, *349*(6311), 704-706. https://doi.org/10.1038/349704a0

Gokina, N. I., Bevan, R. D., Walters, C. L., & Bevan, J. A. (1996). Electrical activity underlying rhythmic contraction in human pial arteries. *Circ Res*, *78*(1), 148-153. https://doi.org/10.1161/01.res.78.1.148

Gomolak, J. R., & Didion, S. P. (2014). Angiotensin II-induced endothelial dysfunction is temporally linked with increases in interleukin-6 and vascular macrophage accumulation. *Front Physiol*, *5*, 396. https://doi.org/10.3389/fphys.2014.00396

Gonzalez-Villalobos, R. A., Seth, D. M., Satou, R., Horton, H., Ohashi, N., Miyata, K., Katsurada, A., Tran, D. V., Kobori, H., & Navar, L. G. (2008). Intrarenal angiotensin II and angiotensinogen augmentation in chronic angiotensin II-infused mice. *Am J Physiol Renal Physiol*, *295*(3), F772-779. https://doi.org/10.1152/ajprenal.00019.2008

Gottesman, R. F., Albert, M. S., Alonso, A., Coker, L. H., Coresh, J., Davis, S. M., Deal, J. A., McKhann, G. M., Mosley, T. H., Sharrett, A. R., Schneider, A. L. C., Windham, B. G., Wruck, L. M., & Knopman, D. S. (2017). Associations Between Midlife Vascular Risk Factors and 25-Year Incident Dementia in the Atherosclerosis Risk in Communities (ARIC) Cohort. *JAMA Neurology*, *74*(10), 1246-1254. https://doi.org/10.1001/jamaneurol.2017.1658

Gottesman, R. F., Schneider, A. L., Albert, M., Alonso, A., Bandeen-Roche, K., Coker, L., Coresh, J., Knopman, D., Power, M. C., Rawlings, A., Sharrett, A. R., Wruck, L. M., & Mosley, T. H. (2014). Midlife hypertension and 20-year cognitive change: the atherosclerosis risk in communities neurocognitive study. *JAMA Neurol*, *71*(10), 1218-1227. https://doi.org/10.1001/jamaneurol.2014.1646

Gouveia-Freitas, K., & Bastos-Leite, A. J. (2021). Perivascular spaces and brain waste clearance systems: relevance for neurodegenerative and cerebrovascular pathology. *Neuroradiology*, *63*(10), 1581-1597. https://doi.org/10.1007/s00234-021-02718-7

Govindpani, K., McNamara, L. G., Smith, N. R., Vinnakota, C., Waldvogel, H. J., Faull, R. L., & Kwakowsky, A. (2019). Vascular Dysfunction in Alzheimer's Disease: A Prelude to the Pathological Process or a Consequence of It? *J Clin Med*, *8*(5). https://doi.org/10.3390/jcm8050651

Grant, R. I., Hartmann, D. A., Underly, R. G., Berthiaume, A.-A., Bhat, N. R., & Shih, A. Y. (2019). Organizational hierarchy and structural diversity of microvascular pericytes in adult mouse cortex. *Journal of Cerebral Blood Flow & Metabolism*, *39*(3), 411-425. https://doi.org/10.1177/0271678x17732229

Griffith, T. M., & Edwards, D. H. (1993). Mechanisms underlying chaotic vasomotion in isolated resistance arteries: roles of calcium and EDRF. *Biorheology*, *30*(5-6), 333-347. https://doi.org/10.3233/bir-1993-305-605

Griffith, T. M., & Edwards, D. H. (1994). Fractal analysis of role of smooth muscle Ca2+ fluxes in genesis of chaotic arterial pressure oscillations. *Am J Physiol*, *266*(5 Pt 2), H1801-1811. https://doi.org/10.1152/ajpheart.1994.266.5.H1801

Grootaert, M. O. J., & Bennett, M. R. (2021). Vascular smooth muscle cells in atherosclerosis: time for a re-assessment. *Cardiovasc Res*, *117*(11), 2326-2339. https://doi.org/10.1093/cvr/cvab046

Gros, R., Van Wert, R., You, X., Thorin, E., & Husain, M. (2002). Effects of age, gender, and blood pressure on myogenic responses of mesenteric arteries from C57BL/6 mice. *Am J Physiol Heart Circ Physiol*, *282*(1), H380-388. https://doi.org/10.1152/ajpheart.2002.282.1.H380

Gustafsson, H., Mulvany, M. J., & Nilsson, H. (1993). Rhythmic contractions of isolated small arteries from rat: influence of the endothelium. *Acta Physiol Scand*, *148*(2), 153-163. https://doi.org/10.1111/j.1748-1716.1993.tb09545.x

Hadaczek, P., Yamashita, Y., Mirek, H., Tamas, L., Bohn, M. C., Noble, C., Park, J. W., & Bankiewicz, K. (2006). The "perivascular pump" driven by arterial pulsation is a powerful mechanism for the distribution of therapeutic molecules within the brain. *Mol Ther*, *14*(1), 69-78. https://doi.org/10.1016/j.ymthe.2006.02.018

Halabi, C. M., Beyer, A. M., de Lange, W. J., Keen, H. L., Baumbach, G. L., Faraci, F. M., & Sigmund, C. D. (2008). Interference with PPAR gamma function in smooth muscle causes vascular dysfunction and hypertension. *Cell Metab*, *7*(3), 215-226. https://doi.org/10.1016/j.cmet.2007.12.008

Hardy, J., & Selkoe, D. J. (2002). The amyloid hypothesis of Alzheimer's disease: progress and problems on the road to therapeutics. *Science*, *297*(5580), 353-356. https://doi.org/10.1126/science.1072994

Harrison, I. F., Ismail, O., Machhada, A., Colgan, N., Ohene, Y., Nahavandi, P., Ahmed, Z., Fisher, A., Meftah, S., Murray, T. K., Ottersen, O. P., Nagelhus, E. A., O'Neill, M. J., Wells, J. A., & Lythgoe, M. F. (2020). Impaired glymphatic function and clearance of tau in an Alzheimer's disease model. *Brain*, *143*(8), 2576-2593. https://doi.org/10.1093/brain/awaa179

Helm, P. J., Ottersen, O. P., & Nase, G. (2009). Analysis of optical properties of the mouse cranium--implications for in vivo multi photon laser scanning microscopy. *J Neurosci Methods*, *178*(2), 316-322. https://doi.org/10.1016/j.jneumeth.2008.12.032

Hermann, M., Flammer, A., & Lüscher, T. F. (2006). Nitric Oxide in Hypertension. *The Journal of Clinical Hypertension*, *8*(s12), 17-29. https://doi.org/https://doi.org/10.1111/j.1524-6175.2006.06032.x

Hickman, S., Izzy, S., Sen, P., Morsett, L., & El Khoury, J. (2018). Microglia in neurodegeneration. *Nat Neurosci*, *21*(10), 1359-1369. https://doi.org/10.1038/s41593-018-0242-x

Higashi, Y., Kihara, Y., & Noma, K. (2012). Endothelial dysfunction and hypertension in aging. *Hypertension Research*, *35*(11), 1039-1047. https://doi.org/10.1038/hr.2012.138

Hock, C., Villringer, K., Müller-Spahn, F., Wenzel, R., Heekeren, H., Schuh-Hofer, S., Hofmann, M., Minoshima, S., Schwaiger, M., Dirnagl, U., & Villringer, A. (1997). Decrease in parietal cerebral hemoglobin oxygenation during performance of a verbal fluency task in patients with Alzheimer's disease monitored by means of near-infrared spectroscopy (NIRS) — correlation with simultaneous rCBF-PET measurements. *Brain Research*, *755*(2), 293-303. https://doi.org/https://doi.org/10.1016/S0006-8993(97)00122-4

Hollenberg, N. K., & Sandor, T. (1984). Vasomotion of renal blood flow in essential hypertension. Oscillations in xenon transit. *Hypertension*, *6*(4), 579-585. https://doi.org/10.1161/01.hyp.6.4.579

Holloway, E. T., & Bohr, D. F. (1973). Reactivity of vascular smooth muscle in hypertensive rats. *Circ Res*, *33*(6), 678-685. https://doi.org/10.1161/01.res.33.6.678

Hsia, A. Y., Masliah, E., McConlogue, L., Yu, G.-Q., Tatsuno, G., Hu, K., Kholodenko, D., Malenka, R. C., Nicoll, R. A., & Mucke, L. (1999). Plaque-independent disruption of neural circuits in Alzheimer's disease mouse models. *Proceedings of the National Academy of Sciences*, *96*(6), 3228-3233. https://doi.org/10.1073/pnas.96.6.3228

Hübel, N., Hosseini-Zare, M. S., Žiburkus, J., & Ullah, G. (2017). The role of glutamate in neuronal ion homeostasis: A case study of spreading depolarization. *PLoS Comput Biol*, *13*(10), e1005804. https://doi.org/10.1371/journal.pcbi.1005804

Hudetz, A. G., Roman, R. J., & Harder, D. R. (1992). Spontaneous flow oscillations in the cerebral cortex during acute changes in mean arterial pressure. *J Cereb Blood Flow Metab*, *12*(3), 491-499. https://doi.org/10.1038/jcbfm.1992.67

Hughes, D., Judge, C., Murphy, R., Loughlin, E., Costello, M., Whiteley, W., Bosch, J., O'Donnell, M. J., & Canavan, M. (2020). Association of Blood Pressure Lowering With Incident Dementia or Cognitive Impairment: A Systematic Review and Meta-analysis. *Jama*, *323*(19), 1934-1944. https://doi.org/10.1001/jama.2020.4249

Hundley, W. G., Renaldo, G. J., Levasseur, J. E., & Kontos, H. A. (1988). Vasomotion in cerebral microcirculation of awake rabbits. *American Journal of Physiology-Heart and Circulatory Physiology*, *254*(1), H67-H71. https://doi.org/10.1152/ajpheart.1988.254.1.H67

Hussain, M., & Awan, F. R. (2018). Hypertension regulating angiotensin peptides in the pathobiology of cardiovascular disease. *Clinical and Experimental Hypertension*, *40*(4), 344-352. https://doi.org/10.1080/10641963.2017.1377218

Iadecola, C. (2013). The pathobiology of vascular dementia. *Neuron*, *80*(4), 844-866. https://doi.org/10.1016/j.neuron.2013.10.008

Iadecola, C., & Davisson, R. L. (2008). Hypertension and cerebrovascular dysfunction. *Cell Metab*, *7*(6), 476-484. https://doi.org/10.1016/j.cmet.2008.03.010

Iadecola, C., & Gottesman, R. F. (2019). Neurovascular and Cognitive Dysfunction in Hypertension. *Circ Res*, *124*(7), 1025-1044. https://doi.org/10.1161/CIRCRESAHA.118.313260

Iadecola, C., Yaffe, K., Biller, J., Bratzke, L. C., Faraci, F. M., Gorelick, P. B., Gulati, M., Kamel, H., Knopman, D. S., Launer, L. J., Saczynski, J. S., Seshadri, S., & Hazzouri, A. Z. A. (2016). Impact of Hypertension on Cognitive Function: A Scientific Statement From the American Heart Association. *Hypertension*, *68*(6), e67-e94. https://doi.org/doi:10.1161/HYP.0000000000000053

Iliff, J. J., Wang, M., Zeppenfeld, D. M., Venkataraman, A., Plog, B. A., Liao, Y., Deane, R., & Nedergaard, M. (2013). Cerebral arterial pulsation drives paravascular CSF-interstitial fluid exchange in the murine brain. *J Neurosci*, *33*(46), 18190-18199. https://doi.org/10.1523/JNEUROSCI.1592-13.2013

Institoris, A., Vandal, M., Peringod, G., Catalano, C., Tran, C. H., Yu, X., Visser, F., Breiteneder, C., Molina, L., Khakh, B. S., Nguyen, M. D., Thompson, R. J., & Gordon, G. R. (2022). Astrocytes amplify neurovascular coupling to sustained activation of neocortex in awake mice. *Nature Communications*, *13*(1), 7872. https://doi.org/10.1038/s41467-022-35383-2

Intaglietta, M. (1990). Vasomotion and flowmotion: physiological mechanisms and clinical evidence. *Vascular Medicine Review*, *vmr-1*(2), 101-112. https://doi.org/10.1177/1358836x9000100202

Intaglietta, M. (1991). Arteriolar vasomotion: implications for tissue ischemia. *Blood Vessels*, *28 Suppl 1*, 1-7. https://doi.org/10.1159/000158912

Ito, D., Imai, Y., Ohsawa, K., Nakajima, K., Fukuuchi, Y., & Kohsaka, S. (1998). Microglia-specific localisation of a novel calcium binding protein, Iba1. *Molecular Brain Research*, *57*(1), 1-9. https://doi.org/https://doi.org/10.1016/S0169-328X(98)00040-0

Iturria-Medina, Y., Sotero, R. C., Toussaint, P. J., Mateos-Pérez, J. M., Evans, A. C., Weiner, M. W., Aisen, P., Petersen, R., Jack, C. R., Jagust, W., Trojanowki, J. Q., Toga, A. W., Beckett, L., Green, R. C., Saykin, A. J., Morris, J., Shaw, L. M., Khachaturian, Z., Sorensen, G., . . . The Alzheimer's Disease Neuroimaging, I. (2016). Early role of vascular dysregulation on late-onset Alzheimer's disease based on multifactorial data-driven analysis. *Nature Communications*, *7*(1), 11934. https://doi.org/10.1038/ncomms11934

Jack, C. R., Jr., & Holtzman, D. M. (2013). Biomarker modeling of Alzheimer's disease. *Neuron*, *80*(6), 1347-1358. https://doi.org/10.1016/j.neuron.2013.12.003

Jagtiani, E., Yeolekar, M., Naik, S., & Patravale, V. (2022). In vitro blood brain barrier models: An overview. *J Control Release*, *343*, 13-30. https://doi.org/10.1016/j.jconrel.2022.01.011

Jama, H. A., Muralitharan, R. R., Xu, C., O'Donnell, J. A., Bertagnolli, M., Broughton, B. R. S., Head, G. A., & Marques, F. Z. (2022). Rodent models of hypertension. *Br J Pharmacol*, *179*(5), 918-937. https://doi.org/10.1111/bph.15650

Jennings, J. R., Muldoon, M. F., & Sved, A. F. (2020). Is the Brain an Early or Late Component of Essential Hypertension? *Am J Hypertens*, *33*(6), 482-490. https://doi.org/10.1093/ajh/hpaa038

Jessen, N. A., Munk, A. S., Lundgaard, I., & Nedergaard, M. (2015). The Glymphatic System: A Beginner's Guide. *Neurochem Res*, *40*(12), 2583-2599. https://doi.org/10.1007/s11064-015-1581-6

Karran, E., & De Strooper, B. (2022). The amyloid hypothesis in Alzheimer disease: new insights from new therapeutics. *Nature Reviews Drug Discovery*, *21*(4), 306-318. https://doi.org/10.1038/s41573-022-00391-w

Kaur, J., Fahmy, L. M., Davoodi-Bojd, E., Zhang, L., Ding, G., Hu, J., Zhang, Z., Chopp, M., & Jiang, Q. (2021). Waste Clearance in the Brain. *Front Neuroanat*, *15*, 665803. https://doi.org/10.3389/fnana.2021.665803

Kawada, N., Imai, E., Karber, A., Welch, W. J., & Wilcox, C. S. (2002). A mouse model of angiotensin II slow pressor response: role of oxidative stress. *J Am Soc Nephrol*, *13*(12), 2860-2868. https://doi.org/10.1097/01.asn.0000035087.11758.ed

Kawasaki, K., Seki, K., & Hosoda, S. (1981). Spontaneous rhythmic contractions in isolated human coronary arteries. *Experientia*, *37*(12), 1291-1292. https://doi.org/10.1007/bf01948367

Kazama, K., Anrather, J., Zhou, P., Girouard, H., Frys, K., Milner, T. A., & Iadecola, C. (2004). Angiotensin II impairs neurovascular coupling in neocortex through NADPH oxidase-derived radicals. *Circ Res*, *95*(10), 1019-1026. https://doi.org/10.1161/01.RES.0000148637.85595.c5

Kazama, K., Wang, G., Frys, K., Anrather, J., & Iadecola, C. (2003). Angiotensin II attenuates functional hyperemia in the mouse somatosensory cortex. *Am J Physiol Heart Circ Physiol*, *285*(5), H1890-1899. https://doi.org/10.1152/ajpheart.00464.2003

Kennerley, A. J., Berwick, J., Martindale, J., Johnston, D., Papadakis, N., & Mayhew, J. E. (2005). Concurrent fMRI and optical measures for the investigation of the hemodynamic response function. *Magnetic Resonance in Medicine*, *54*(2), 354-365. https://doi.org/https://doi.org/10.1002/mrm.20511

Kennerley, A. J., Harris, S., Bruyns-Haylett, M., Boorman, L., Zheng, Y., Jones, M., & Berwick, J. (2012). Early and late stimulus-evoked cortical hemodynamic responses provide insight into the neurogenic nature of neurovascular coupling. *Journal of Cerebral Blood Flow and Metabolism*, *32*(3), 468-480. https://doi.org/10.1038/jcbfm.2011.163

Kettenmann, H., Hanisch, U. K., Noda, M., & Verkhratsky, A. (2011). Physiology of microglia. *Physiol Rev*, *91*(2), 461-553. https://doi.org/10.1152/physrev.00011.2010

Kim, B.H., Kim, S., Nam, Y., Park, Y.H., Shin, S.M., & Moon, M. (2025). Second-generation anti-amyloid monoclonal antibodies for Alzheimer's disease: current landscape and future perspectives. *Transl Neurodegener.,*14, 6. https://doi.org/10.1186/s40035-025-00465-w

Kim, J., & Jeong, Y. (2013). Augmentation of sensory-evoked hemodynamic response in an early Alzheimer's disease mouse model. *J Alzheimers Dis*, *37*(4), 857-868. https://doi.org/10.3233/jad-121900

Kimbrough, I. F., Robel, S., Roberson, E. D., & Sontheimer, H. (2015). Vascular amyloidosis impairs the gliovascular unit in a mouse model of Alzheimer's disease. *Brain*, *138*(Pt 12), 3716-3733. https://doi.org/10.1093/brain/awv327

Kisler, K., Nelson, A. R., Rege, S. V., Ramanathan, A., Wang, Y., Ahuja, A., Lazic, D., Tsai, P. S., Zhao, Z., Zhou, Y., Boas, D. A., Sakadžić, S., & Zlokovic, B. V. (2017). Pericyte degeneration leads to neurovascular uncoupling and limits oxygen supply to brain. *Nat Neurosci*, *20*(3), 406-416. https://doi.org/10.1038/nn.4489

Klohs, J., Rudin, M., Shimshek, D. R., & Beckmann, N. (2014). Imaging of cerebrovascular pathology in animal models of Alzheimer's disease. *Front Aging Neurosci*, *6*, 32. https://doi.org/10.3389/fnagi.2014.00032

Knox, E. G., Aburto, M. R., Clarke, G., Cryan, J. F., & O'Driscoll, C. M. (2022). The blood-brain barrier in aging and neurodegeneration. *Mol Psychiatry*, *27*(6), 2659-2673. https://doi.org/10.1038/s41380-022-01511-z

Kotliar, K., Ortner, M., Conradi, A., Hacker, P., Hauser, C., Günthner, R., Moser, M., Muggenthaler, C., Diehl-Schmid, J., Priller, J., Schmaderer, C., & Grimmer, T. (2022). Altered retinal cerebral vessel oscillation frequencies in Alzheimer's disease compatible with impaired amyloid clearance. *Neurobiol Aging*, *120*, 117-127. https://doi.org/10.1016/j.neurobiolaging.2022.08.012

Kruyer, A., Soplop, N., Strickland, S., & Norris, E. H. (2015). Chronic Hypertension Leads to Neurodegeneration in the TgSwDI Mouse Model of Alzheimer's Disease. *Hypertension*, *66*(1), 175-182. https://doi.org/10.1161/HYPERTENSIONAHA.115.05524

Küng, C. F., Moreau, P., Takase, H., & Lüscher, T. F. (1995). L-NAME hypertension alters endothelial and smooth muscle function in rat aorta. Prevention by trandolapril and verapamil. *Hypertension*, *26*(5), 744-751. https://doi.org/10.1161/01.hyp.26.5.744

Lacoste, B., Tong, X. K., Lahjouji, K., Couture, R., & Hamel, E. (2013). Cognitive and cerebrovascular improvements following kinin B1 receptor blockade in Alzheimer's disease mice. *J Neuroinflammation*, *10*, 57. https://doi.org/10.1186/1742-2094-10-57

Lamb, F. S., Myers, J. H., Hamlin, M. N., & Webb, R. C. (1985). Oscillatory contractions in tail arteries from genetically hypertensive rats. *Hypertension*, *7*(3 Pt 2), I25-30. https://doi.org/10.1161/01.hyp.7.3_pt_2.i25

Launer, L. J., Masaki, K., Petrovitch, H., Foley, D., & Havlik, R. J. (1995). The association between midlife blood pressure levels and late-life cognitive function. The Honolulu-Asia Aging Study. *Jama*, *274*(23), 1846-1851.

Launer, L. J., Petrovitch, H., Ross, G. W., Markesbery, W., & White, L. R. (2008). AD brain pathology: Vascular origins?: Results from the HAAS autopsy study. *Neurobiology of Aging*, *29*(10), 1587-1590. https://doi.org/https://doi.org/10.1016/j.neurobiolaging.2007.03.008

Lecrux, C., & Hamel, E. (2011). The neurovascular unit in brain function and disease. *Acta Physiol (Oxf)*, *203*(1), 47-59. https://doi.org/10.1111/j.1748-1716.2011.02256.x

Lefer, D. J., Lynch, C. D., Lapinski, K. C., & Hutchins, P. M. (1990). Enhanced vasomotion of cerebral arterioles in spontaneously hypertensive rats. *Microvasc Res*, *39*(2), 129-139. https://doi.org/10.1016/0026-2862(90)90065-y

Lerman, L. O., Kurtz, T. W., Touyz, R. M., Ellison, D. H., Chade, A. R., Crowley, S. D., Mattson, D. L., Mullins, J. J., Osborn, J., Eirin, A., Reckelhoff, J. F., Iadecola, C., & Coffman, T. M. (2019). Animal Models of Hypertension: A Scientific Statement From the American Heart Association. *Hypertension*, *73*(6), e87-e120. https://doi.org/10.1161/HYP.0000000000000090

Li, L., Tong, X. K., Hosseini Kahnouei, M., Vallerand, D., Hamel, E., & Girouard, H. (2021). Impaired Hippocampal Neurovascular Coupling in a Mouse Model of Alzheimer's Disease. *Front Physiol*, *12*, 715446. https://doi.org/10.3389/fphys.2021.715446

Ling, W. C., Mustafa, M. R., Vanhoutte, P. M., & Murugan, D. D. (2018). Chronic administration of sodium nitrite prevents hypertension and protects arterial endothelial function by reducing oxidative stress in angiotensin II-infused mice. *Vascul Pharmacol*, *102*, 11-20. https://doi.org/10.1016/j.vph.2017.05.003

Liu, G., Yang, C., Wang, X., Chen, X., Wang, Y., & Le, W. (2023). Oxygen metabolism abnormality and Alzheimer's disease: An update. *Redox Biology*, *68*, 102955. https://doi.org/https://doi.org/10.1016/j.redox.2023.102955

Liu, M., Zhang, X., Wang, B., Wu, Q., Li, B., Li, A., Zhang, H., & Xiu, R. (2017). Functional status of microvascular vasomotion is impaired in spontaneously hypertensive rat. *Sci Rep*, *7*(1), 17080. https://doi.org/10.1038/s41598-017-17013-w

Liu, Y. Z., Chen, J. K., Li, Z. P., Zhao, T., Ni, M., Li, D. J., Jiang, C. L., & Shen, F. M. (2014). High-salt diet enhances hippocampal oxidative stress and cognitive impairment in mice. *Neurobiol Learn Mem*, *114*, 10-15. https://doi.org/10.1016/j.nlm.2014.04.010

Ma, T. K., Kam, K. K., Yan, B. P., & Lam, Y. Y. (2010). Renin-angiotensin-aldosterone system blockade for cardiovascular diseases: current status. *Br J Pharmacol*, *160*(6), 1273-1292. https://doi.org/10.1111/j.1476-5381.2010.00750.x

Machado, M. F., Muela, H. C. S., Costa-Hong, V. A., Yassuda, M. S., Moraes, N. C., Memória, C. M., Bor-Seng-Shu, E., Massaro, A. R., Nitrini, R., Bortolotto, L. A., & Nogueira, R. d. C. (2020).

Evaluation of cerebral autoregulation performance in patients with arterial hypertension on drug treatment. *The Journal of Clinical Hypertension*, *22*(11), 2114-2120. https://doi.org/https://doi.org/10.1111/jch.14052

Malonek, D., & Grinvald, A. (1996). Interactions Between Electrical Activity and Cortical Microcirculation Revealed by Imaging Spectroscopy: Implications for Functional Brain Mapping. *Science*, *272*(5261), 551-554. https://doi.org/10.1126/science.272.5261.551

Mateo, C., Knutsen, P. M., Tsai, P. S., Shih, A. Y., & Kleinfeld, D. (2017). Entrainment of Arteriole Vasomotor Fluctuations by Neural Activity Is a Basis of Blood-Oxygenation-Level-Dependent "Resting-State" Connectivity. *Neuron*, *96*(4), 936-948.e933. https://doi.org/10.1016/j.neuron.2017.10.012

Mawuenyega, K. G., Sigurdson, W., Ovod, V., Munsell, L., Kasten, T., Morris, J. C., Yarasheski, K. E., & Bateman, R. J. (2010). Decreased clearance of CNS beta-amyloid in Alzheimer's disease. *Science*, *330*(6012), 1774. https://doi.org/10.1126/science.1197623

Mayhew, J. E., Askew, S., Zheng, Y., Porrill, J., Westby, G. W., Redgrave, P., Rector, D. M., & Harper, R. M. (1996). Cerebral vasomotion: a 0.1-Hz oscillation in reflected light imaging of neural activity. *Neuroimage*, *4*(3 Pt 1), 183-193. https://doi.org/10.1006/nimg.1996.0069

Meissner, A., Minnerup, J., Soria, G., & Planas, A. M. (2017). Structural and functional brain alterations in a murine model of Angiotensin II-induced hypertension. *J Neurochem*, *140*(3), 509-521. https://doi.org/10.1111/jnc.13905

Mendez, M. F. (2019). Early-onset Alzheimer Disease and Its Variants. *Continuum (Minneap Minn)*, *25*(1), 34-51. https://doi.org/10.1212/CON.0000000000000687

Mestre, H., Du, T., Sweeney, A. M., Liu, G., Samson, A. J., Peng, W., Mortensen, K. N., Stæger, F. F., Bork, P. A. R., Bashford, L., Toro, E. R., Tithof, J., Kelley, D. H., Thomas, J. H., Hjorth, P. G., Martens, E. A., Mehta, R. I., Solis, O., Blinder, P., . . . Nedergaard, M. (2020). Cerebrospinal fluid

influx drives acute ischemic tissue swelling. *Science*, *367*(6483). https://doi.org/10.1126/science.aax7171

Mestre, H., Kostrikov, S., Mehta, R. I., & Nedergaard, M. (2017). Perivascular spaces, glymphatic dysfunction, and small vessel disease. *Clin Sci (Lond)*, *131*(17), 2257-2274. https://doi.org/10.1042/CS20160381

Meyer, M. F., Rose, C. J., Hulsmann, J. O., Schatz, H., & Pfohl, M. (2003). Impaired 0.1-Hz vasomotion assessed by laser Doppler anemometry as an early index of peripheral sympathetic neuropathy in diabetes. *Microvasc Res*, *65*(2), 88-95. https://doi.org/10.1016/s0026-2862(02)00015-8

Mills, E., Kuhn, C. M., Feinglos, M. N., & Surwit, R. (1993). Hypertension in CB57BL/6J mouse model of non-insulin-dependent diabetes mellitus. *Am J Physiol*, *264*(1 Pt 2), R73-78. https://doi.org/10.1152/ajpregu.1993.264.1.R73

Mills, K. T., Stefanescu, A., & He, J. (2020). The global epidemiology of hypertension. *Nature Reviews Nephrology*, *16*(4), 223-237. https://doi.org/10.1038/s41581-019-0244-2

Moltzer, E., Verkuil, A. V., van Veghel, R., Danser, A. H., & van Esch, J. H. (2010). Effects of angiotensin metabolites in the coronary vascular bed of the spontaneously hypertensive rat: loss of angiotensin II type 2 receptor-mediated vasodilation. *Hypertension*, *55*(2), 516-522. https://doi.org/10.1161/HYPERTENSIONAHA.109.145037

Monassier, L., Combe, R., & Fertak, L. E. (2006). Mouse models of hypertension. *Drug Discovery Today: Disease Models*, *3*(3), 273-281. https://doi.org/10.1016/j.ddmod.2006.10.008

Montagne, A., Zhao, Z., & Zlokovic, B. V. (2017). Alzheimer's disease: A matter of blood-brain barrier dysfunction? *J Exp Med*, *214*(11), 3151-3169. https://doi.org/10.1084/jem.20171406

Muhl, L., Mocci, G., Pietilä, R., Liu, J., He, L., Genové, G., Leptidis, S., Gustafsson, S., Buyandelger, B., Raschperger, E., Hansson, E. M., Björkegren, J. L. M., Vanlandewijck, M., Lendahl, U., &

Betsholtz, C. (2022). A single-cell transcriptomic inventory of murine smooth muscle cells. *Developmental Cell*, *57*(20), 2426-2443.e2426. https://doi.org/10.1016/j.devcel.2022.09.015

Muller, M., van der Graaf, Y., Visseren, F. L., Mali, W. P., Geerlings, M. I., & Group, S. S. (2012). Hypertension and longitudinal changes in cerebral blood flow: the SMART-MR study. *Ann Neurol*, *71*(6), 825-833. https://doi.org/10.1002/ana.23554

Munting, L. P., Derieppe, M., Suidgeest, E., Hirschler, L., van Osch, M. J., Denis de Senneville, B., & van der Weerd, L. (2021). Cerebral blood flow and cerebrovascular reactivity are preserved in a mouse model of cerebral microvascular amyloidosis. *Elife*, *10*. https://doi.org/10.7554/eLife.61279

Nakaji, K., Ihara, M., Takahashi, C., Itohara, S., Noda, M., Takahashi, R., & Tomimoto, H. (2006). Matrix metalloproteinase-2 plays a critical role in the pathogenesis of white matter lesions after chronic cerebral hypoperfusion in rodents. *Stroke*, *37*(11), 2816-2823. https://doi.org/10.1161/01.STR.0000244808.17972.55

Nation, D. A., Sweeney, M. D., Montagne, A., Sagare, A. P., D'Orazio, L. M., Pachicano, M., Sepehrband, F., Nelson, A. R., Buennagel, D. P., Harrington, M. G., Benzinger, T. L. S., Fagan, A. M., Ringman, J. M., Schneider, L. S., Morris, J. C., Chui, H. C., Law, M., Toga, A. W., & Zlokovic, B. V. (2019). Blood–brain barrier breakdown is an early biomarker of human cognitive dysfunction. *Nature Medicine*, *25*(2), 270-276. https://doi.org/10.1038/s41591-018-0297-y

Nelson, A. R., Sweeney, M. D., Sagare, A. P., & Zlokovic, B. V. (2016). Neurovascular dysfunction and neurodegeneration in dementia and Alzheimer's disease. *Biochimica Et Biophysica Acta-Molecular Basis of Disease*, *1862*(5), 887-900. https://doi.org/10.1016/j.bbadis.2015.12.016

Nemoto, M., Nomura, Y., Tamura, M., Sato, C., Houkin, K., & Abe, H. (1997). Optical imaging and measuring of local hemoglobin concentration and oxygenation changes during somatosensory stimulation in rat cerebral cortex. *Adv Exp Med Biol*, *428*, 521-531. https://doi.org/10.1007/978-1-4615-5399-1_74

Nilsson, H., & Aalkjaer, C. (2003). Vasomotion: mechanisms and physiological importance. *Mol Interv*, *3*(2), 79-89, 51. https://doi.org/10.1124/mi.3.2.79

Niwa, K., Porter, V. A., Kazama, K. E. N., Cornfield, D., Carlson, G. A., & Iadecola, C. (2001). Aβ-peptides enhance vasoconstriction in cerebral circulation [Article]. *American Journal of Physiology - Heart and Circulatory Physiology*, *281*(6 50-6), H2417-H2424. https://doi.org/10.1152/ajpheart.2001.281.6.h2417

Nizar, K., Uhlirova, H., Tian, P., Saisan, P. A., Cheng, Q., Reznichenko, L., Weldy, K. L., Steed, T. C., Sridhar, V. B., MacDonald, C. L., Cui, J., Gratiy, S. L., Sakadzić, S., Boas, D. A., Beka, T. I., Einevoll, G. T., Chen, J., Masliah, E., Dale, A. M., . . . Devor, A. (2013). In vivo stimulus-induced vasodilation occurs without IP3 receptor activation and may precede astrocytic calcium increase. *J Neurosci*, *33*(19), 8411-8422. https://doi.org/10.1523/jneurosci.3285-12.2013

Omote, M., Kajimoto, N., & Mizusawa, H. (1993). The ionic mechanism of phenylephrine-induced rhythmic contractions in rabbit mesenteric arteries treated with ryanodine. *Acta Physiol Scand*, *147*(1), 9-13. https://doi.org/10.1111/j.1748-1716.1993.tb09467.x

Pacholko, A., & Iadecola, C. (2024). Hypertension, Neurodegeneration, and Cognitive Decline. *Hypertension*, *81*(5), 991-1007. https://doi.org/doi:10.1161/HYPERTENSIONAHA.123.21356

Pacurari, M., Kafoury, R., Tchounwou, P. B., & Ndebele, K. (2014). The Renin-Angiotensin-aldosterone system in vascular inflammation and remodeling. *Int J Inflam*, *2014*, 689360. https://doi.org/10.1155/2014/689360

Panza, J. A., Quyyumi, A. A., Callahan, T. S., & Epstein, S. E. (1993). Effect of antihypertensive treatment on endothelium-dependent vascular relaxation in patients with essential hypertension. *Journal of the American College of Cardiology*, *21*(5), 1145-1151. https://doi.org/https://doi.org/10.1016/0735-1097(93)90238-V

Park, J. B., Charbonneau, F., & Schiffrin, E. L. (2001). Correlation of endothelial function in large and small arteries in human essential hypertension. *Journal of Hypertension*, *19*(3).

https://journals.lww.com/jhypertension/fulltext/2001/03000/correlation_of_endothelial_function_in_large_and.9.aspx

Park, L., Hochrainer, K., Hattori, Y., Ahn, S. J., Anfray, A., Wang, G., Uekawa, K., Seo, J., Palfini, V., Blanco, I., Acosta, D., Eliezer, D., Zhou, P., Anrather, J., & Iadecola, C. (2020). Tau induces PSD95–neuronal NOS uncoupling and neurovascular dysfunction independent of neurodegeneration [Article]. *Nature Neuroscience*, *23*(9), 1079-1089. https://doi.org/10.1038/s41593-020-0686-7

Pascoal, I. F., Lindheimer, M. D., Nalbantian-Brandt, C., & Umans, J. G. (1998). Preeclampsia selectively impairs endothelium-dependent relaxation and leads to oscillatory activity in small omental arteries. *J Clin Invest*, *101*(2), 464-470. https://doi.org/10.1172/jci557

Peppiatt, C. M., Howarth, C., Mobbs, P., & Attwell, D. (2006). Bidirectional control of CNS capillary diameter by pericytes. *Nature*, *443*(7112), 700-704. https://doi.org/10.1038/nature05193

Phillips, A. A., Chan, F. H., Zheng, M. M. Z., Krassioukov, A. V., & Ainslie, P. N. (2016). Neurovascular coupling in humans: Physiology, methodological advances and clinical implications. *Journal of Cerebral Blood Flow & Metabolism*, *36*(4), 647-664. https://doi.org/10.1177/0271678x15617954

Plog, B. A., & Nedergaard, M. (2018). The Glymphatic System in Central Nervous System Health and Disease: Past, Present, and Future. *Annu Rev Pathol*, *13*, 379-394. https://doi.org/10.1146/annurev-pathol-051217-111018

Pradhan, R. K., & Chakravarthy, V. S. (2011). Informational dynamics of vasomotion in microvascular networks: a review. *Acta Physiol (Oxf)*, *201*(2), 193-218. https://doi.org/10.1111/j.1748-1716.2010.02198.x

Presa, J. L., Saravia, F., Bagi, Z., & Filosa, J. A. (2020). Vasculo-Neuronal Coupling and Neurovascular Coupling at the Neurovascular Unit: Impact of Hypertension. *Front Physiol*, *11*, 584135. https://doi.org/10.3389/fphys.2020.584135

Qiu, C., Winblad, B., & Fratiglioni, L. (2009). Low diastolic pressure and risk of dementia in very old people: a longitudinal study. *Dement Geriatr Cogn Disord*, *28*(3), 213-219. https://doi.org/10.1159/000236913

Rajeev, V., Fann, D. Y., Dinh, Q. N., Kim, H. A., De Silva, T. M., Lai, M. K. P., Chen, C. L., Drummond, G. R., Sobey, C. G., & Arumugam, T. V. (2022). Pathophysiology of blood brain barrier dysfunction during chronic cerebral hypoperfusion in vascular cognitive impairment. *Theranostics*, *12*(4), 1639-1658. https://doi.org/10.7150/thno.68304

Reeves, B. C., Karimy, J. K., Kundishora, A. J., Mestre, H., Cerci, H. M., Matouk, C., Alper, S. L., Lundgaard, I., Nedergaard, M., & Kahle, K. T. (2020). Glymphatic System Impairment in Alzheimer's Disease and Idiopathic Normal Pressure Hydrocephalus. *Trends Mol Med*, *26*(3), 285-295. https://doi.org/10.1016/j.molmed.2019.11.008

Renna, N. F., de Las Heras, N., & Miatello, R. M. (2013). Pathophysiology of vascular remodeling in hypertension. *Int J Hypertens*, *2013*, 808353. https://doi.org/10.1155/2013/808353

Ribeiro, M. O., Antunes, E., de Nucci, G., Lovisolo, S. M., & Zatz, R. (1992). Chronic inhibition of nitric oxide synthesis. A new model of arterial hypertension. *Hypertension*, *20*(3), 298-303. https://doi.org/10.1161/01.hyp.20.3.298

Rivadulla, C., de Labra, C., Grieve, K. L., & Cudeiro, J. (2011). Vasomotion and neurovascular coupling in the visual thalamus in vivo. *PLoS One*, *6*(12), e28746. https://doi.org/10.1371/journal.pone.0028746

Rivera-Rivera, L. A., Cody, K. A., Rutkowski, D., Cary, P., Eisenmenger, L., Rowley, H. A., Carlsson, C. M., Johnson, S. C., & Johnson, K. M. (2020). Intracranial vascular flow oscillations in Alzheimer's disease from 4D flow MRI. *Neuroimage Clin*, *28*, 102379. https://doi.org/10.1016/j.nicl.2020.102379

Rizzoni, D., Porteri, E., Castellano, M., Bettoni, G., Muiesan, M. L., Muiesan, P., Giulini, S. M., & Agabiti-Rosei, E. (1996). Vascular hypertrophy and remodeling in secondary hypertension. *Hypertension*, *28*(5), 785-790. https://doi.org/10.1161/01.hyp.28.5.785

Roberts, J., Kahle, M. P., & Bix, G. J. (2012). Perlecan and the blood-brain barrier: beneficial proteolysis? *Front Pharmacol*, *3*, 155. https://doi.org/10.3389/fphar.2012.00155

Rogaev, E. I., Sherrington, R., Rogaeva, E. A., Levesque, G., Ikeda, M., Liang, Y., Chi, H., Lin, C., Holman, K., Tsuda, T., Mar, L., Sorbi, S., Nacmias, B., Piacentini, S., Amaducci, L., Chumakov, I., Cohen, D., Lannfelt, L., Fraser, P. E., . . . George-Hyslop, P. H. S. (1995). Familial Alzheimer's disease in kindreds with missense mutations in a gene on chromosome 1 related to the Alzheimer's disease type 3 gene. *Nature*, *376*(6543), 775-778. https://doi.org/10.1038/376775a0

Rosenberg, G. A. (2012). Neurological Diseases in Relation to the Blood–Brain Barrier. *Journal of Cerebral Blood Flow & Metabolism*, *32*(7), 1139-1151. https://doi.org/10.1038/jcbfm.2011.197

Rosenfeld, C. S. (2017). Sex-dependent differences in voluntary physical activity. *J Neurosci Res*, *95*(1-2), 279-290. https://doi.org/10.1002/jnr.23896

Royea, J., Zhang, L., Tong, X. K., & Hamel, E. (2017). Angiotensin IV Receptors Mediate the Cognitive and Cerebrovascular Benefits of Losartan in a Mouse Model of Alzheimer's Disease. *J Neurosci*, *37*(22), 5562-5573. https://doi.org/10.1523/jneurosci.0329-17.2017

Sada, T., Koike, H., Ikeda, M., Sato, K., Ozaki, H., & Karaki, H. (1990). Cytosolic free calcium of aorta in hypertensive rats. Chronic inhibition of angiotensin converting enzyme. *Hypertension*, *16*(3), 245-251. https://doi.org/10.1161/01.hyp.16.3.245

Sakurai, T., & Terui, N. (2006). Effects of sympathetically induced vasomotion on tissue-capillary fluid exchange. *American Journal of Physiology-Heart and Circulatory Physiology*, *291*(4), H1761-H1767. https://doi.org/10.1152/ajpheart.00280.2006

Salvi, P., Faini, A., Castiglioni, P., Brunacci, F., Montaguti, L., Severi, F., Gautier, S., Pretolani, E., Benetos, A., & Parati, G. (2018). Increase in slow-wave vasomotion by hypoxia and ischemia in lowlanders and highlanders. *J Appl Physiol (1985)*, *125*(3), 780-789. https://doi.org/10.1152/japplphysiol.00977.2017

Scheffer, S., Hermkens, D. M. A., Van Der Weerd, L., De Vries, H. E., & Daemen, M. J. A. P. (2021). Vascular Hypothesis of Alzheimer Disease: Topical Review of Mouse Models [Article]. *Arteriosclerosis, Thrombosis, and Vascular Biology*, *41*(4), 1265-1283. https://doi.org/10.1161/ATVBAHA.120.311911

Scheuner, D., Eckman, C., Jensen, M., Song, X., Citron, M., Suzuki, N., Bird, T. D., Hardy, J., Hutton, M., Kukull, W., Larson, E., Levy-Lahad, E., Viitanen, M., Peskind, E., Poorkaj, P., Schellenberg, G., Tanzi, R., Wasco, W., Lannfelt, L., . . . Younkin, S. (1996). Secreted amyloid beta-protein similar to that in the senile plaques of Alzheimer's disease is increased in vivo by the presenilin 1 and 2 and APP mutations linked to familial Alzheimer's disease. *Nat Med*, *2*(8), 864-870. https://doi.org/10.1038/nm0896-864

Schiffrin, E. L. (2020). How Structure, Mechanics, and Function of the Vasculature Contribute to Blood Pressure Elevation in Hypertension. *Can J Cardiol*, *36*(5), 648-658. https://doi.org/10.1016/j.cjca.2020.02.003

Schiffrin, E. L., Park, J. B., Intengan, H. D., & Touyz, R. M. (2000). Correction of Arterial Structure and Endothelial Dysfunction in Human Essential Hypertension by the Angiotensin Receptor Antagonist Losartan. *Circulation*, *101*(14), 1653-1659. https://doi.org/doi:10.1161/01.CIR.101.14.1653

Schiweck, J., Eickholt, B. J., & Murk, K. (2018). Important Shapeshifter: Mechanisms Allowing Astrocytes to Respond to the Changing Nervous System During Development, Injury and Disease [Review]. *Frontiers in Cellular Neuroscience*, *Volume 12 - 2018*. https://doi.org/10.3389/fncel.2018.00261

Schmidt-Lucke, C., Borgström, P., & Schmidt-Lucke, J. A. (2002). Low frequency flowmotion/(vasomotion) during patho-physiological conditions. *Life Sci*, *71*(23), 2713-2728. https://doi.org/10.1016/s0024-3205(02)02110-0

Schneider, J. A., Arvanitakis, Z., Leurgans, S. E., & Bennett, D. A. (2009). The neuropathology of probable Alzheimer disease and mild cognitive impairment. *Annals of Neurology*, *66*(2), 200-208. https://doi.org/https://doi.org/10.1002/ana.21706

Schreiber, S., Drukarch, B., Garz, C., Niklass, S., Stanaszek, L., Kropf, S., Bueche, C., Held, F., Vielhaber, S., Attems, J., Reymann, K.G., Heinze, H.J., Carare, R.O., Wilhelmus, M.M. (2014). Interplay between age, cerebral small vessel disease, parenchymal amyloid-β, and tau pathology: Longitudinal studies in hypertensive stroke-prone rats. *Journal of Alzheimer's Disease*, 42(3), S205-S215. https://doi.org/10.3233/JAD-132618.

Scott, J. H., Menouar, M. A., & Dunn, R. J. (2023). Physiology, Aldosterone. In *StatPearls*. StatPearls Publishing

Shabir, O., Pendry, B., Lee, L., Eyre, B., Sharp, P. S., Rebollar, M. A., Drew, D., Howarth, C., Heath, P. R., Wharton, S. B., Francis, S. E., & Berwick, J. (2022). Assessment of neurovascular coupling and cortical spreading depression in mixed mouse models of atherosclerosis and Alzheimer's disease. *Elife*, *11*. https://doi.org/10.7554/eLife.68242

Shabir, O., Sharp, P., Rebollar, M. A., Boorman, L., Howarth, C., Wharton, S. B., Francis, S. E., & Berwick, J. (2020a). Enhanced Cerebral Blood Volume under Normobaric Hyperoxia in the J20-hAPP Mouse Model of Alzheimer's Disease. *Sci Rep*, *10*(1), 7518. https://doi.org/10.1038/s41598-020-64334-4

Shabir, O., Sharp, P., Rebollar, M. A., Boorman, L., Howarth, C., Wharton, S. B., Francis, S. E., & Berwick, J. (2020). Enhanced Cerebral Blood Volume under Normobaric Hyperoxia in the J20-hAPP Mouse Model of Alzheimer's Disease. *Scientific Reports*, *10*(1), 7518. https://doi.org/10.1038/s41598-020-64334-4

Shabir, O., Sharp, P., Rebollar, M. A., Boorman, L., Howarth, C., Wharton, S. B., Francis, S. E., & Berwick, J. (2020b). Enhanced Cerebral Blood Volume under Normobaric Hyperoxia in the J20-

hAPP Mouse Model of Alzheimer's Disease [Article]. *Scientific Reports*, *10*(1), Article 7518. https://doi.org/10.1038/s41598-020-64334-4

Sharp, P. S., Ameen-Ali, K. E., Boorman, L., Harris, S., Wharton, S., Howarth, C., Shabir, O., Redgrave, P., & Berwick, J. (2020). Neurovascular coupling preserved in a chronic mouse model of Alzheimer's disease: Methodology is critical. *J Cereb Blood Flow Metab*, *40*(11), 2289-2303. https://doi.org/10.1177/0271678x19890830

Sharp, P. S., Shaw, K., Boorman, L., Harris, S., Kennerley, A. J., Azzouz, M., & Berwick, J. (2015). Comparison of stimulus-evoked cerebral hemodynamics in the awake mouse and under a novel anesthetic regime. *Sci Rep*, *5*, 12621. https://doi.org/10.1038/srep12621

Shen, M., Quertermous, T., Fischbein, M. P., & Wu, J. C. (2021). Generation of Vascular Smooth Muscle Cells From Induced Pluripotent Stem Cells: Methods, Applications, and Considerations. *Circ Res*, *128*(5), 670-686. https://doi.org/10.1161/CIRCRESAHA.120.318049

Sherrington, R., Rogaev, E. I., Liang, Y., Rogaeva, E. A., Levesque, G., Ikeda, M., Chi, H., Lin, C., Li, G., Holman, K., Tsuda, T., Mar, L., Foncin, J. F., Bruni, A. C., Montesi, M. P., Sorbi, S., Rainero, I., Pinessi, L., Nee, L., . . . St George-Hyslop, P. H. (1995). Cloning of a gene bearing missense mutations in early-onset familial Alzheimer's disease. *Nature*, *375*(6534), 754-760. https://doi.org/10.1038/375754a0

Shibata, M., Ohtani, R., Ihara, M., & Tomimoto, H. (2004). White matter lesions and glial activation in a novel mouse model of chronic cerebral hypoperfusion. *Stroke*, *35*(11), 2598-2603. https://doi.org/10.1161/01.STR.0000143725.19053.60

Siekmann, A. F. (2023). Biology of vascular mural cells. *Development*, *150*(16). https://doi.org/10.1242/dev.200271

Skoog, I., Nilsson, L., Persson, G., Lernfelt, B., Landahl, S., Palmertz, B., Andreasson, L. A., Odén, A., & Svanborg, A. (1996). 15-year longitudinal study of blood pressure and dementia. *The Lancet*, *347*(9009), 1141-1145. https://doi.org/https://doi.org/10.1016/S0140-6736(96)90608-X

Sofroniew, M. V., & Vinters, H. V. (2010). Astrocytes: biology and pathology. *Acta Neuropathol*, *119*(1), 7-35. https://doi.org/10.1007/s00401-009-0619-8

Stelzner, J. A., Krogsgaard, A., Kulkoviene, G., Sperling, L., & Lind, B. L. (2024). Astrocyte Contribution to Brain State-Dependent Neurovascular Coupling. bioRxiv, 2024.2004.2016.589720. https://doi.org/10.1101/2024.04.16.589720

Strandgaard, S., & Paulson, O. B. (1989). Cerebral blood flow and its pathophysiology in hypertension. *Am J Hypertens*, *2*(6 Pt 1), 486-492. https://doi.org/10.1093/ajh/2.6.486

Swan, G. E., DeCarli, C., Miller, B. L., Reed, T., Wolf, P. A., Jack, L. M., & Carmelli, D. (1998). Association of midlife blood pressure to late-life cognitive decline and brain morphology. *Neurology*, *51*(4), 986-993. https://doi.org/10.1212/wnl.51.4.986

Sweeney, M. D., Kisler, K., Montagne, A., Toga, A. W., & Zlokovic, B. V. (2018). The role of brain vasculature in neurodegenerative disorders. *Nat Neurosci*, *21*(10), 1318-1331. https://doi.org/10.1038/s41593-018-0234-x

Swerdlow, R. H., Burns, J. M., & Khan, S. M. (2014). The Alzheimer's disease mitochondrial cascade hypothesis: Progress and perspectives. *Biochimica et Biophysica Acta (BBA) - Molecular Basis of Disease*, *1842*(8), 1219-1231. https://doi.org/https://doi.org/10.1016/j.bbadis.2013.09.010

Tao, B., Gong, W., Xu, C., Ma, Z., Mei, J., Chen, M. (2024). The relationship between hypoxia and Alzheimer’s disease: an updated review. Front. Aging Neurosci.,16. https://doi.org/https://doi.org/10.3389/fnagi.2024.1402774

Tarantini, S., Hertelendy, P., Tucsek, Z., Valcarcel-Ares, M. N., Smith, N., Menyhart, A., Farkas, E., Hodges, E. L., Towner, R., Deak, F., Sonntag, W. E., Csiszar, A., Ungvari, Z., & Toth, P. (2015). Pharmacologically-induced neurovascular uncoupling is associated with cognitive impairment in mice. *J Cereb Blood Flow Metab*, *35*(11), 1871-1881. https://doi.org/10.1038/jcbfm.2015.162

Tarantini, S., Tucsek, Z., Valcarcel-Ares, M. N., Toth, P., Gautam, T., Giles, C. B., Ballabh, P., Wei, J. Y., Wren, J. D., Ashpole, N. M., Sonntag, W. E., Ungvari, Z., & Csiszar, A. (2016). Circulating IGF-1 deficiency exacerbates hypertension-induced microvascular rarefaction in the mouse hippocampus and retrosplenial cortex: implications for cerebromicrovascular and brain aging [Article]. *Age*, *38*(4), 273-289. https://doi.org/10.1007/s11357-016-9931-0

Te Riet, L., van Esch, J. H., Roks, A. J., van den Meiracker, A. H., & Danser, A. H. (2015). Hypertension: renin-angiotensin-aldosterone system alterations. *Circ Res*, *116*(6), 960-975. https://doi.org/10.1161/circresaha.116.303587

Toh, C. H., & Siow, T. Y. (2021). Glymphatic Dysfunction in Patients With Ischemic Stroke. *Front Aging Neurosci*, *13*, 756249. https://doi.org/10.3389/fnagi.2021.756249

Toth, P., Tucsek, Z., Sosnowska, D., Gautam, T., Mitschelen, M., Tarantini, S., Deak, F., Koller, A., Sonntag, W. E., Csiszar, A., & Ungvari, Z. (2013). Age-related autoregulatory dysfunction and cerebromicrovascular injury in mice with angiotensin II-induced hypertension. *J Cereb Blood Flow Metab*, *33*(11), 1732-1742. https://doi.org/10.1038/jcbfm.2013.143

Uchida, K. (2022). Waste Clearance in the Brain and Neuroinflammation: A Novel Perspective on Biomarker and Drug Target Discovery in Alzheimer's Disease. *Cells*, *11*(5). https://doi.org/10.3390/cells11050919

Ungvari, Z., Toth, P., Tarantini, S., Prodan, C. I., Sorond, F., Merkely, B., & Csiszar, A. (2021). Hypertension-induced cognitive impairment: from pathophysiology to public health. *Nat Rev Nephrol*, *17*(10), 639-654. https://doi.org/10.1038/s41581-021-00430-6

van Beek, A. H., Lagro, J., Olde-Rikkert, M. G., Zhang, R., & Claassen, J. A. (2012). Oscillations in cerebral blood flow and cortical oxygenation in Alzheimer's disease. *Neurobiol Aging*, *33*(2), 428.e421-431. https://doi.org/10.1016/j.neurobiolaging.2010.11.016

van Dijk, S. E., Drenth, N., Hafkemeijer, A., Labadie, G., Witjes-Ané, M. W., Blauw, G. J., Rombouts, S. A., van der Grond, J., & van Rooden, S. (2024). Neurovascular coupling in early stage dementia - A case-control study. *J Cereb Blood Flow Metab*, *44*(6), 1013-1023. https://doi.org/10.1177/0271678x231214102

van Dyck, C.H., Swanson, C.J., Aisen, P., Bateman, R.J., Chen, C., Gee, M., Kanekiyo, M., Li, D., Reyderman, L., Cohen, S., Froelich, L., Katayama, S., Sabbagh, M., Vellas, B., Watson, D., Dhadda, S., Irizarry, M., Kramer, L.D., Iwatsubo, T. (2022). Lecanemab in Early Alzheimer's Disease. N Engl J Med., 388(1), 9-21. https://doi.org/10.1056/NEJMoa2212948.

van Veluw, S. J., Hou, S. S., Calvo-Rodriguez, M., Arbel-Ornath, M., Snyder, A. C., Frosch, M. P., Greenberg, S. M., & Bacskai, B. J. (2020). Vasomotion as a Driving Force for Paravascular Clearance in the Awake Mouse Brain. *Neuron*, *105*(3), 549-561 e545. https://doi.org/10.1016/j.neuron.2019.10.033

Vanhoutte, P. M., Shimokawa, H., Feletou, M., & Tang, E. H. (2017). Endothelial dysfunction and vascular disease - a 30th anniversary update. *Acta Physiol (Oxf)*, *219*(1), 22-96. https://doi.org/10.1111/apha.12646

Volianskis, A., Køstner, R., Mølgaard, M., Hass, S., & Jensen, M. S. (2010). Episodic memory deficits are not related to altered glutamatergic synaptic transmission and plasticity in the CA1 hippocampus of the APPswe/PS1δE9-deleted transgenic mice model of ß-amyloidosis. *Neurobiol Aging*, *31*(7), 1173-1187. https://doi.org/10.1016/j.neurobiolaging.2008.08.005

Volterra, A., & Meldolesi, J. (2005). Astrocytes, from brain glue to communication elements: the revolution continues. *Nature Reviews Neuroscience*, *6*(8), 626-640. https://doi.org/10.1038/nrn1722

Wang, B., Zhang, G., Wang, X., Yu, C., Li, Q., Lu, W., Wang, F., & Shao, Y. (2024). Abnormal changes of cerebral blood flow in hypertension with different risk levels. *Med Discoverie*s, 3(6): 1163.

Watts, S. W., Traub, O., & Webb, R. C. (1994). Effects of ramipril on contractile oscillations in arteries from genetically hypertensive rats. *Clin Exp Hypertens*, *16*(6), 881-898. https://doi.org/10.3109/10641969409078032

Weber, M. A., Schiffrin, E. L., White, W. B., Mann, S., Lindholm, L. H., Kenerson, J. G., Flack, J. M., Carter, B. L., Materson, B. J., Ram, C. V. S., Cohen, D. L., Cadet, J.-C., Jean-Charles, R. R., Taler, S., Kountz, D., Townsend, R. R., Chalmers, J., Ramirez, A. J., Bakris, G. L., . . . Harrap, S. B. (2014). Clinical Practice Guidelines for the Management of Hypertension in the Community. *The Journal of Clinical Hypertension*, *16*(1), 14-26. https://doi.org/https://doi.org/10.1111/jch.12237

Weisbrod, R. M., Shiang, T., Al Sayah, L., Fry, J. L., Bajpai, S., Reinhart-King, C. A., Lob, H. E., Santhanam, L., Mitchell, G., Cohen, R. A., & Seta, F. (2013). Arterial stiffening precedes systolic hypertension in diet-induced obesity. *Hypertension*, *62*(6), 1105-1110. https://doi.org/10.1161/HYPERTENSIONAHA.113.01744

Wiesmann, M., Capone, C., Zerbi, V., Mellendijk, L., Heerschap, A., Claassen, J. A. H. R., & Kiliaana, A. J. (2015). Hypertension impairs cerebral blood flow in a mouse model for alzheimer's disease [Article]. *Current Alzheimer Research*, *12*(10), 914-922. https://doi.org/10.2174/1567205012666151027130135

Xue, Y., Liu, N., Zhang, M., Ren, X., Tang, J., & Fu, J. (2020). Concomitant enlargement of perivascular spaces and decrease in glymphatic transport in an animal model of cerebral small vessel disease. *Brain Res Bull*, *161*, 78-83. https://doi.org/10.1016/j.brainresbull.2020.04.008

Yoshizaki, K., Adachi, K., Kataoka, S., Watanabe, A., Tabira, T., Takahashi, K., & Wakita, H. (2008). Chronic cerebral hypoperfusion induced by right unilateral common carotid artery occlusion causes delayed white matter lesions and cognitive impairment in adult mice. *Exp Neurol*, *210*(2), 585-591. https://doi.org/10.1016/j.expneurol.2007.12.005

You, D., Loufrani, L., Baron, C., Levy, B. I., Widdop, R. E., & Henrion, D. (2005). High blood pressure reduction reverses angiotensin II type 2 receptor-mediated vasoconstriction into vasodilation in

spontaneously hypertensive rats. *Circulation*, *111*(8), 1006-1011. https://doi.org/10.1161/01.CIR.0000156503.62815.48

Youwakim, J., Vallerand, D., & Girouard, H. (2023). Neurovascular Coupling in Hypertension Is Impaired by IL-17A through Oxidative Stress [Article]. *International Journal of Molecular Sciences*, *24*(4), Article 3959. https://doi.org/10.3390/ijms24043959

Yu, Q., Larson, D. F., Slayback, D., Lundeen, T. F., Baxter, J. H., & Watson, R. R. (2004). Characterization of high-salt and high-fat diets on cardiac and vascular function in mice. *Cardiovasc Toxicol*, *4*(1), 37-46. https://doi.org/10.1385/ct:4:1:37

Zain, M., & Awan, F. R. (2014). Renin Angiotensin Aldosterone System (RAAS): its biology and drug targets for treating diabetic nephropathy. *Pak J Pharm Sci*, *27*(5), 1379-1391.

Zhang, H., Jin, B., & Faber, J. E. (2019). Mouse models of Alzheimer's disease cause rarefaction of pial collaterals and increased severity of ischemic stroke. *Angiogenesis*, *22*(2), 263-279. https://doi.org/10.1007/s10456-018-9655-0

Zhang, K., Kan, H., Mao, A., Geng, L., & Ma, X. (2021). Single-cell analysis of salt-induced hypertensive mouse aortae reveals cellular heterogeneity and state changes. *Exp Mol Med*, *53*(12), 1866-1876. https://doi.org/10.1038/s12276-021-00704-w

Zhang, X., & Le, W. (2010). Pathological role of hypoxia in Alzheimer's disease. *Exp Neurol*, *223*(2), 299-303. https://doi.org/10.1016/j.expneurol.2009.07.033

Zhang, Y., Chen, H., Li, R., Sterling, K., Song, W. (2023). Amyloid β-based therapy for Alzheimer's disease: challenges, successes and future. Signal Transduct Target Ther., 8(1), 248. https://doi.org/10.1038/s41392-023-01484-7.

Zhao, Y., & Gong, C. X. (2015). From chronic cerebral hypoperfusion to Alzheimer-like brain pathology and neurodegeneration. *Cell Mol Neurobiol*, *35*(1), 101-110. https://doi.org/10.1007/s10571-014-0127-9

Zhao, Y., Gu, J. H., Dai, C. L., Liu, Q., Iqbal, K., Liu, F., & Gong, C. X. (2014). Chronic cerebral hypoperfusion causes decrease of O-GlcNAcylation, hyperphosphorylation of tau and behavioral deficits in mice. *Front Aging Neurosci*, *6*, 10. https://doi.org/10.3389/fnagi.2014.00010

Zizek, B., Poredos, P., & Videcnik, V. (2001). Endothelial dysfunction in hypertensive patients and in normotensive offspring of subjects with essential hypertension. *Heart*, *85*(2), 215-217. https://doi.org/10.1136/heart.85.2.215

Zlokovic, B. V. (2011). Neurovascular pathways to neurodegeneration in Alzheimer's disease and other disorders. *Nat Rev Neurosci*, *12*(12), 723-738. https://doi.org/10.1038/nrn3114

Zonta, M., Angulo, M. C., Gobbo, S., Rosengarten, B., Hossmann, K. A., Pozzan, T., & Carmignoto, G. (2003). Neuron-to-astrocyte signaling is central to the dynamic control of brain microcirculation. *Nat Neurosci*, *6*(1), 43-50. https://doi.org/10.1038/nn980

Zuloaga, K. L., Zhang, W., Yeiser, L. A., Stewart, B., Kukino, A., Nie, X., Roese, N. E., Grafe, M. R., Pike, M. M., Raber, J., & Alkayed, N. J. (2015). Neurobehavioral and imaging correlates of hippocampal atrophy in a mouse model of vascular cognitive impairment. *Transl Stroke Res*, *6*(5), 390-398. https://doi.org/10.1007/s12975-015-0412-z